

S082B Data Analysis Guide

Table of Contents

by Irene
Packer

- 1.0 Introduction
- 2.0 The Apollo Telescope Mount
 - 2.1 The Solar Instruments
 - 2.2 Supporting Instrumentation
- 3.0 The S082B Instrument
 - 3.1 General Description
 - 3.2 The Telescope and Pointing
 - 3.3 Astigmatism, Spectral Resolution, and Stray Light
 - 3.4 Optical Coatings
 - 3.5 Thermal Control System
 - 3.6 Film and Film Camera
 - 3.7 Instrument Performance
- 4.0 Film History
 - 4.1 Batches
 - 4.2 Film Sequence Log
 - 4.3 Mounting
 - 4.4 Processing the Film
 - 4.5 Loss of D_{\max} and Contrast
 - 4.6 Fog
- 5.0 Calibration and Absolute Spectrophotometry
 - 5.1 CALROC Intensity Calibration
 - 5.2 ATM Calibration
 - 5.3 Photometry of S082B Spectra
 - 5.3.1 Characteristic Curves
 - 5.3.2 Conversion to Absolute Intensity
 - 5.3.3 Curvature of Spectra
 - 5.4 References
- 6.0 NSSDC Copies of the Data
 - 6.1 Photographic Procedures
 - 6.2 Transfer Curves
 - 6.3 Image Degradation
 - 6.4 Film Catalog
- 7.0 Observing Programs
 - 7.1 The Joint Observing Program
 - 7.2 The Calibration Rocket Program - CALROC
 - 7.3 Solar Forecast Services
 - 7.4 Skylab Associated Solar Programs

Table of Contents

- 8.0 Spectral Atlas
- 8.1 References

Appendices

- A. Skylab Documentation
- B. Catalog of Exposures (micro-fiche)
- C. Film Sequence Log
- D. Bibliography
- E. Line Lists for S082B Data
 - E.1 The Short Wavelength Spectra
 - E.2 The Long Wavelength Spectra
 - E.3 Forbidden Lines
- F. Wavelength Scale for NSSDC Copies of S082B Spectra

1.0 INTRODUCTION*

The sun's radiation from the atmospheric cutoff near 3000 Å to 1000 Å in the extreme ultraviolet (XUV) is of great interest in solar physics because it can be of assistance in explaining the physical processes by which the sun's energy is transmitted through its outer atmosphere against a steep temperature gradient. This is the region of the atmosphere where the temperature reaches its minimum value, 4400 K, between the photosphere and the chromosphere, then rises extremely rapidly as the million degree corona is approached. The spectrum from 3000 to 2100 Å comes from the layers lower down than the temperature minimum, and is the usual continuum with Fraunhofer lines. From about 1535 to 1000 Å the radiation originates in the chromosphere and transition region, $T \approx 20,000$ K, and its spectrum is one of intense emission lines above a weak continuum. But from 1535 to 2100 Å the spectrum is an extremely complex combination of absorption lines, emission lines and continuum; this represents a mixture of radiation from layers between the temperature minimum and the chromosphere, with a number of lines from the transition region. Scattered over the entire range, 3000 to 1000 Å, are the forbidden lines from the corona.

The Apollo Telescope Mount (ATM), the manned solar observatory on Skylab, provided a unique opportunity for large scale observations of the sun from above the earth's atmosphere. Supported by a coordinated program of ground-based observations, the joint observing program of its six advanced telescopes brought to bear the greatest possible observational and analytic power on fundamental problems in solar physics.

The ATM took advantage of all that had been learned from over 25 years of solar space research conducted by means of sounding rockets, Orbiting Solar Observatories (OSO's) and monitoring satellites such as SOLRAD. Each of these programs had excelled in its own particular way: rockets, for development of specialized instruments having extremely great observing power, but which were always severely limited in observing time and wavelength span, or spatial resolution or spectral resolution; OSO's not limited in observing time, but constrained in information acquisition rate, as well as in spatial and spectral resolution; SOLRAD, having excellent time resolution, but limited to broad-band detectors.

* Material for this section has been extracted from a paper in Applied Optics, 16, 879, 1977, by J. D-F. Bartoe, G. E. Brueckner, J. D. Purcell and R. Tousey, Extreme Ultraviolet Spectrograph ATM Experiment S082B.

These programs had established the need for continuous solar observation combining the specialized observing powers that each type of small instrument had provided. ATM came close to realizing this ideal. It provided almost continuous observation of the solar atmosphere for a period instrument was enormous. In addition, by fostering the simultaneous operation of the newest and most powerful ground-based observational techniques, the total resulting program represented a massive attack on the problems in solar physics, resembling that mounted during the IGY for geophysics.

This Guide has been prepared to assist collaboration in the analysis of SO82B data, especially from copies of the data supplied through the National Space Science Data Center through the National Space Science Data Center at NASA/GSFC. We have found, however; that by gathering the most useful data into one source, it is of benefit to any researchers who may be familiar with the general experiment but not with the specific details required in making a study of the data. Therefore, a brief description of the experiment, the instrument, and supporting features of ATM and the Skylab program have been included in addition to specific details of the calibration of film and instrument.

An extensive bibliography of papers by the NRL ATM analysis team is given in the Appendix indicating fruitful directions of research provided by the data and those staff members knowledgeable in specific areas.

A list of documentation references, the catalog of exposures (on microfiche), a wavelength scale, and line lists to assist in identification of lines are also included.

Requests for information about collaborating with NRL may be directed to specific members of the data reduction team whose names appear on related publications listed in the Bibliography. Access to original flight data and supporting material may be arranged by contacting Dr. Richard Tousey, Principal Investigator.

2.0 THE APOLLO TELESCOPE MOUNT*

Skylab consisted of four principal parts. Largest was the Saturn Workshop (SWS), which provided living and working quarters for the three-man crews. It contained also most of the experiments other than the ATM. The hydrogen tank of a Saturn IVB booster (second stage of Saturn IB) that was converted to become the SWS was a cylinder 15 m long and 6.7 m in diameter.

The second major section was the Multiple Docking Adapter (MDA), center of the space complex, 5.2 m long and 3.2 m in diameter. This was attached to the SWS through an airlock module (AM) and contained the control and display panel for the ATM. It had two docking ports: the first port, located on the long axis extending through the AWS, was for docking the CSM when on each visitation it came up with its crew of three; the second port, 90 away, was an alternate dock for a rescue mission, should it be required. Opposite the latter port was the ATM. The third part was the CSM itself, much the same as the Apollo Spacecraft developed for the lunar landings.

The ATM and its solar instruments are shown in Fig. 2.1. It consisted of two concentric elements: the outer framework, or rack, an octagonal structure 3.4 m across and 4.4 m in length, and inside the rack a cylinder or canister, 2.1 m in diameter and 3 m in length. The canister housed the solar instruments. It was attached to the rack through a pair of large gimbal rings carried on a large ring bearing, which allowed rotation of the entire canister around its axis. A stiff cruciform structure divided the space into four quadrants and formed the optical bench to which the ATM instruments were attached.

The ATM was designed to keep the instruments within the canister aimed steadily and precisely at the desired point on the sun regardless of disturbances such as those caused by crew movement, within ± 2.5 arc sec in yaw and pitch and 5 arc min in roll. These specifications were actually exceeded in flight. Short-time (minutes) yaw and pitch stability was ± 0.5 arc sec, and short-time roll stability was excellent. Part of the success in stability control was derived from the 3 arc min stability of the entire Skylab, accomplished by an orthogonal system of control moment gyros (CMG).

Fine pointing of the ATM was accomplished with a solar pointing control system (PCS), which sensed the Sun's center to a few tenths of an arc sec and sent error signals

* Material for this section has been extracted from a paper in Applied Optics, 16, 825, 1977 by R. Tousey, Apollo Telescope Mount of Skylab: An Overview

into the torque motors that controlled the rotational positions of the ATM canister gimbals. Offset pointing of the ATM in yaw or in pitch by steps of 1.25 arc sec up to 24 arc min could be introduced by counter-rotating a pair of quartz wedges placed in the solar beam incident on either the pitch or the yaw solar sensors. Rotation of the prisms was accomplished by a crewman with his panel "joystick". Digital indicators read out yaw and pitch to 1 arc sec, and roll to 1 arc min.

A most important subsystem was the digital computer. It enabled the crewman to initiate complex commands simply. The computer could also be operated by ground command, while the crew was sleeping, or in case of emergency. Thus many experiments were operated while the crew were asleep, and also during the unmanned periods between missions.

A problem in the design of the ATM was the great thermal stability required to preserve the focus of the ultrahigh resolution optical instruments. Passive thermal stabilization alone was not sufficient to meet the requirements and was augmented by an active fluid-cooling system for the ATM canister. The refrigerator consisted of a loop, located inside the skin of the canister, through which water and methanol was circulated to radiators on the outside of the canister, facing space. This system maintained the temperature of the canister wall to $50 \pm 5^\circ \text{ F}$ with cyclic variations of $\pm 3^\circ \text{ F}$. In addition, several experiments had their own thermal-control heater systems, designed to maintain the temperature at all locations to within 2.5° F of the design and calibration temperature and to limit the rate of change to no greater than 0.05° F per 5 minutes.

2.1 The Solar Instruments

Table 2.1 summarizes the major solar experiments and instrumentation mounted in the ATM. Brief sketches of these are given below.

S052: White light Coronagraph

The white light coronagraph on Skylab was designed by the High Altitude Observatory of the National Center for Atmospheric Research. The scientific goal of the S052 instrument was the observation of the outer corona from about 0.5 solar radius (R_\odot) to $5R_\odot$ above the solar limb, with high spatial and temporal resolution, and from these data to deduce the 3-D form of the corona and its evolution and rapid change. These photographs from Skylab form a nearly continuous record of the corona for 9 months that is of the character observed for only a few minutes once each year or two at natural eclipse. More than 35,000 useful photographs were secured, including coverage of more than 100 transient eruptions in the corona.

SO54: X-Ray Spectrographic Telescope

The American Science and Engineering Corporation (AS&E) and the Goddard Space Flight Center (GSFC) jointly pioneered the use of the Wolter lens, grazing-incidence telescope for imaging the sun in X-rays.

The instrument flown in ATM by AS&E employed a Wolter lens and was equipped with six filters, each with a different transmittance curve. It was also possible to introduce a 1440-lines/mm transmission grating into the beam and thus obtain low resolution spectra of small bright features such as flares. Limited operation was carried on in the unattended and unmanned modes. A total of 31,785 exposures were made, with times ranging from 1/64 sec to 256 sec. Soft X-ray images from this telescope show in a most spectacular fashion the coronal holes, where the high speed solar wind streams originate.

SO56: X-Ray Telescope

The GSFC also utilized a Wolter lens-type telescopic camera for ATM. In dimensions and general characteristics SO56 and SO54 were much alike. The principal difference between them was that SO56 had some three times less light gathering area, but was equipped with a different series of filters, which enabled it to record somewhat harder X-rays. Although the instrument was operated only in the manned mode, 27,972 excellent X-ray images were secured. It was particularly successful in recording images of high spatial resolution, which showed the growth phase of flares in detail.

SO55: Ultraviolet Spectrometer-Spectroheliometer

The Harvard College Observatory spectrometer and spectroheliometer was designed to secure calibrated EUV spectra and images of selected portions of the solar disk in the light of a number of strong emission lines. The lines were chosen to sample a broad range of solar temperatures, from the middle chromosphere to the low corona. Detection was entirely photoelectric using seven, independent, open-channel, electron multipliers in a variety of ways. Four modes of operation were available: (1) the spectrum of a selected 5 x 5-sec arc solar area could be scanned in 3.8 min with a resolution of 1.6 Å; (2) the readings from the seven multipliers, set at seven important wavelengths ranging from 280 Å to 1350 Å, could be read out as functions of time with 40-msec time resolution; (3) the sun could be recorded at seven wavelengths but with the instrument scanning a line 5 sec of arc wide and 5 min of arc long once in 5 sec, or; (4) a 5 x 5-min of arc area could be scanned with 5 x 5-sec of arc spatial resolution in 5 min at seven wavelengths. The instrument

was operated in both unattended and unmanned modes, but without the capability of fine pointing except when manned and with a crewman in charge. Excellent results were obtained with intensity data covering a wide dynamic range with high precision.

S082A: Extreme Ultraviolet Spectroheliograph

The XUV spectroheliograph of the Naval Research Laboratory was an objective grating instrument which produced simultaneous, monochromatic images of the entire sun over a broad range of the XUV. Over the 171-630-A range a spectrum of solar images each 18.6 mm in diameter was recorded. The instrument produced results of extreme interest and acquired a total of 1032 useful exposures.

S082B: Ultraviolet Spectrograph

A type of solar observation considered of great importance was the recording of the XUV spectrum at great spectral and spatial resolution for different kinds of solar regions, for example, filaments, active regions, the limb, flares, and so on. The large NRL spectrograph was designed for this purpose. Being a photographic instrument, it had tremendous information-gathering ability. The short wavelength range covered the XUV from 970 A to 1970 A with a spectral resolution of 0.06 A, which was sufficient to obtain useful line profiles. The long wavelength range extended from 1940 A to 3940 A with 0.12 A spectral resolution. Photoelectric servo-control of the primary mirror was provided to enable the 2-sec of arc wide slit to be stepped across the limb at intervals of 1 sec of arc. The slit was also equipped with an imaging system which allowed the crewman to see exactly where the sun's limb fell on the slit plate relative to the slit in order to calibrate the automatic image-positioning device. The instrument suffered principally from having too long a slit to isolate sufficiently the smallest solar features, but it performed very well, and 6400 spectra were obtained.

The NRL photographic and HCO photoelectric instruments complemented each other in many ways. The spectral range covered by HCO, nominally 280-1350 A, overlapped generously NRL's S082A range, 171-630 A, and S082B's range, 970-3940 A. The advantages of photoelectric over photographic recording are the increased precision of the intensity measurements and the wider dynamic range covered. Photographic recording, on the other hand, is capable of gathering information far more rapidly than photoelectric, but to cover a large dynamic range requires making a series of exposures covering a wide range of times. In temporal resolution photoelectric recording is superior;

photographic excels in spatial and spectral resolution. To the greatest extent practicable SO55, SO82A and B were operated together.

2.2 Supporting Instrumentation

Each group of ATM experimenters recognized the need for supporting instrumentation of various kinds in order to make optimum use of the six major solar instruments. The supporting instruments fall into several classes as follows:

(1) Instruments to enable the crewman to point the ATM at a pre-selected solar position with pre-selected roll, with coordinate values displayed on-board, and telemetered to ground.

(2) Instruments to present solar images to the crewman in various wavelength bands, to enable him to point the ATM at features of interest that he could see.

(3) Instruments to alert the crew to the occurrence of a solar flare so that they could initiate observing programs, and also instruments to assist in anticipating the occurrence of a solar flare.

The H-Alpha Telescopes

The two H- α telescopes were the most useful devices for showing the crewmen the precise pointing of the ATM relative to features on the solar disk and for recording this position. A spectral resolution of 0.7 Å was achieved with Fabry-Perot-type filters. This assured maximum visibility of solar flares and the chromospheric network. Zoom lenses were arranged to provide optical telescopic systems which could be used at low or high magnification, with a resolution of 1 to 2 arc sec at the high setting. The ATM control and display (C+D) panel was equipped with two identical cathode ray tube monitors of six inches diameter, each with an electronic reticle. The images produced by the two H- α telescopes could be presented on either of these scopes, and any other TV-type image such as the XUV monitor image could also be presented. It was thus also possible to view at the same time a highly magnified image of a small part of the sun and an image of the entire sun.

H- α #1 was equipped with a camera for recording photographically on 35 mm film the H- α solar image as projected on the SO55 slit with 1 arc sec spatial resolution. A mechanically-movable reticle system adjusted to the relative co-alignment between SO55 and SO82B then made it possible to record the precise positions of both SO82B and SO55.

H- α #2 was not equipped with photographic recording, and was used mainly to present for study by the crewman a high quality H- α image of the entire sun. Like H- α #1 it was equipped with a movable reticle that was visible in the image of the CRT, and could be zoomed to high magnification. Therefore it also could be used for pointing.

White Light Solar Pointing Devices

There were several instruments that imaged the sun in white light and could be used for establishing and recording solar pointing coordinates. The principal device was the optical pointing control system (PCS), described earlier. This was designed to point the entire ATM at any desired angles in pitch and yaw relative to the solar center with an accuracy of 1.25 arc sec. The pointing coordinates were displayed on the C&D panel and were also transmitted by telemetry for recording on the ground. In addition, they were recorded on the ends of the film strips of S082A and B by photography of a photodiode matrix built into each of these instruments. Additional pointing information was given by the special white light pointing error sensor built into S052 for the purpose of aligning the external and internal occulters and the entire instrument.

Roll, however, could not be established as easily and accurately as yaw and pitch. Several methods were available. One utilized the Skylab rate-gyro system which operated together with the CMG's to stabilize the entire Skylab. A possible but little used method was to observe a sunspot in the white light image projected on the S082B slit and displayed on one of the CRTs of the C&D panel. The most precise information was given by a star tracker mounted on the ATM. The star tracker measured the angle between Canopus or certain other stars and the ATM yaw and pitch directions.

The XUV Monitor

The XUV monitor of NRL was a device which showed the crew in real time a visible image of the sun produced by its emission in the extreme ultraviolet band 171-500 Å, approximately. This band included radiation from the corona and transition layer, with a contribution of about 20% from the chromosphere. The monitor was equipped with a reticle circle and cross that permitted it to be used for pointing with a spatial resolution of 15-20 arc sec. The pattern of features and their intensities on this monitor were more nearly like those of the radiation studied by the solar instruments than was the pattern of emission shown by the H- α telescopes. The XUV images were transmitted by TV to the ground several times a day for use by the ATM PI's in planning the observing programs. A file

of the ground pictures plus polaroid exposures of the on-board monitor is available for study at NRL. The XUV monitor was extremely valuable for predicting and locating the occurrence of a solar flare and was also found most useful for locating boundaries of coronal holes and bright points in both active regions and the network.

X-Ray Detectors

As part of MSFC's SO56 there was included a device known as the X-ray Event Analyzer (XREA). Its purpose was to measure the total X-ray flux emitted in the band 2.5-20 A, or 5-20 A and 27-33 A. The detecting system made use of two proportional counters with pulse-height analyzers and data processing for display to the crewman and for telemetry to the ground.

Another device somewhat similar to the XREA was the Photomultiplier Exposure Counter (PMEC), constructed by AS&E for use with SO54. This used a photo-multiplier to count the scintillations produced by X-rays in a NaI: Tl crystal that viewed the entire solar flux. It was equipped with filters that restricted its sensitivity to the hard X-ray spectrum. A range of five decades of intensity was converted by compression into a decimal range of 0-1000 counts per sec.

Still another X-ray detector was the X-ray imaging system constructed by AS&E. This consisted of a small Wolter lens which imaged the sun in X-rays onto a thin scintillator crystal. The visible light scintillations emitted by this crystal were detected by an image dissector tube which scanned the image and displayed the X-ray sun on a separate small CRT on the C&D panel. This image allowed the crewman to determine which active region was flaring. The principal use made of this system, however, was for display of the X-ray count level being detected by the IDT.

All three systems were used to record the solar X-ray flux and to alert the crew to an increase in flux level of magnitude sufficient to suggest that a flare might be expected or that a flare was in progress. The data collected by the XREA and by the PMEC were of great value to the principal investigator teams in connection with planning during the mission and are also useful in the interpretation of results. They supplement X-ray flux measurements made by other systems, such as the NRL SOLRAD 9 and 10 solar monitoring satellites.

The Radio Noise Burst Monitor

The solar radio noise burst monitor provided monitoring of the radio bursts emitted by the whole sun in the 6 cm band. These radio bursts are sometimes precursors of flares. The monitor consisted of a receiver and display that showed on a meter above the C&D panel the level of noise in units of solar radio flux. This device could also be used to activate an audible alarm system to the crew when the flux exceeded a certain threshold value.

Figure Captions

Fig. 2.1 A sketch of the Apollo Telescope Mount. Three of the instruments can be seen attached to the central cruciform supporting structure.

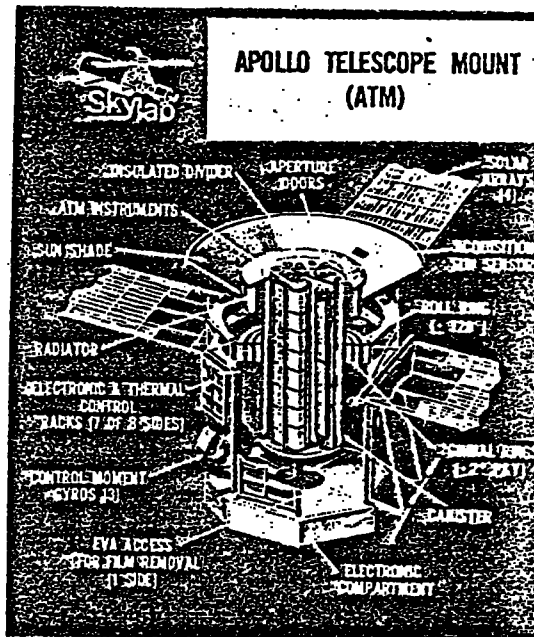


Fig. 2.1 A sketch of the Apollo Telescope Mount. Three of the instruments can be seen attached to the central cruciform supporting structure.

Table 2.1

Table X. Summary of ATM Instruments

Name and number	Institution P.I. (mission)	Wavelength range	Wavelength resolution	Spatial resolution	Field of view	Temporal resolution	Recording	Manned (M) unmanned (UM) unattended (UA)
White light coronagraph S052	HAO R. M. MacQueen	3700-7000 Å	—	8.2"	1.5-6 R	> 40 sec	Photographic, TV & TM	M, UM, UA
UV spectrograph S082B	NRL R. Tousey	3940-1940 Å 1970-970 Å	0.12 Å 0.06 Å	2" x 60" 2" x 60"	Anywhere within ±24' of sun ctr.	> 0.15 sec	Photographic	M
EUV spectrometer- spectroheliometer S055	HCO E. M. Reeves	1350-280 Å	1.6 Å	5" x 5"	5' x 5' 5' x 5' 5" x 5"	5 m 5 sec 40 msec	Photoelectric and TM	M, UM, UA
XUV spectrohelio- graph S082A	NRL R. Tousey	630-171 Å	0.025 Å	2.5" x 2.5"	57' x ~60'	> 2.0 sec	Photographic	M, UA
X-ray spectrographic telescope S054 S054	AS&E G. Vaiana	60-3.5 Å	Bands grating: 0.15 Å at 7 Å	~2"	48' diam	2.5 sec	Photographic	M, UM, UA
X-ray telescope S056	MSFC J. E. Milligan	53-3 Å	Bands	~2"	38' diam	> 3.5 sec	Photographic	M, UA
H-α #1	HCO E. M. Reeves	6563 ± 0.35 Å	—	~1"	16-4.4'	1/30 sec	Photographic TV & TM	M, UM, UA
H-α #2	MSFC P. Hassler, Jr.	6563 ± 0.35 Å	—	~1"	35-7'	1/30 sec	TV & TM	M
XUV monitor	NRL R. Tousey	171-500 Å	None	15" x 15"	56' diam	1/30 sec to 4 sec	TV & TM	M
X-ray scope	AS&E G. Vaiana	2-10 Å 0-8 Å	None	1'	48' diam	~1 sec	TV & digital	M
PMEC	AS&E G. Vaiana	0-8 Å	Pulse height	None	Full sun	Continuous	Digital & TM	M, UM, UA
XREA	MSFC J. E. Milligan	2.5-33 Å	Pulse height	None	Full sun	Continuous	Digital & TM	M, UA
RNBM	MSFC O. K. Garriott	6 cm		None	Full sun	Continuous	Meter	M

3.0 THE SO82B INSTRUMENT*

The large NRL spectrograph used for Experiment SO82B was a photographic instrument similar to those flown in rockets by NRL from 1960 to 1966. The short wavelength range covered the XUV from 970 to 1970 Å with a spectral resolution of 0.06 Å, which was sufficient to obtain useful line profiles. The long wavelength range extended from 1940 to 3940 Å with 0.12 Å spectral resolution. Double dispersion was used to reduce the focused stray-light from the long wavelength part of the solar spectrum, which at 5000 Å is 10^4 more intense than at 1500 Å.

To obtain sufficiently high spatial resolution a primary mirror was used to image the sun on the spectrograph slit. In this way a solar element 2 arc sec wide and 60 arc sec long was resolved. The mirror added a third reflecting surface, however, which greatly reduced the speed of the system at wavelengths less than 1100 Å, the short wavelength end of the range where high reflectance coatings are available. To compensate for this and to increase the speed generally, the instrumental astigmatism and therefore the lengths of the spectral lines were reduced.

Photoelectric servo-control of the primary mirror was provided to enable the 2 arc sec wide slit to be stepped across the limb at intervals of 1 arc sec. The slit was also equipped with an imaging system which allowed the crewman to see exactly where the sun's limb fell on the slit plate relative to the slit in order to calibrate the automatic image-positioning device. The instrument suffered principally from having too long a slit to isolate sufficiently the smallest solar features.

Temporal resolution achievable was approximately 1 min, sufficient to follow the change in the spectrum during the flash phase of a flare, or to search for oscillations of a 5 minute period in the low chromosphere.

3.1 General Description

The overall optical system of the XUV solar spectrograph is shown in perspective in Fig. 3.1. It consisted of a single mirror telescope and a double grating spectrograph.

The spectrograph directed the light passing through the slit to one of two interchangeable predisperser gratings, which selected the short or long wavelength band reaching the main grating through the waveband aperture.

* Material for this section has been extracted from a paper in Applied Optics, 16, 879, 1977, by J.-D. F. Bartoe, G. E. Brueckner, J. D. Purcell and R. Tousey. Extreme Ultraviolet Spectrograph ATM Experiment SO82B.

The main grating was concave with 2000 mm radius of curvature, 600 lines per mm, and 76 x 152 mm clear aperture. The second order of this grating was used to cover the spectral range 970-1970 Å. This was selected by means of a 500 mm radius predisperser grating having 300 lines per mm. When used in the first order the range 1940-3940 Å was selected by a predisperser ruled with 150 lines per mm. Each predisperser was ruled in 10 parts, for each of which the spacing was changed slightly to introduce a change in sagittal focus just sufficient to compensate for the astigmatism of the main grating.

The dispersion of the spectrograph was 8.3 Å/mm and 4.2 Å/mm in the long and short wavelength modes, respectively. The spectral resolution was ≈ 0.05 Å at 1500 Å and ≈ 0.10 Å at 3000 Å. The spatial resolution, determined by the slit and mirror, was 2 x 60 arc sec.

Photographic films used were Eastman Kodak Schumann-emulsions, mainly type 104, but with some of the more sensitive type 201. A camera magazine held 201 film strips, each of which could be moved to 8 positions, permitting the exposure of 1608 spectra per camera. A small chip of fast, red sensitive film was placed at the end of each film strip for recording essential exposure data displayed in binary code on a diode array flasher.

3.2 The Telescope and Pointing

The telescope mirror was an off-axis paraboloid, of 1 m focal length and 54 x 121 mm clear aperture. The mirror formed on the entrance slit of the spectrograph a solar image of 9.3 mm diameter, with a resolution of approximately 1 arc sec, close to diffraction limited as measured with visible light.

Figure 3.2 shows the telescope and the pointing reference system. The telescope mirror was mounted on a one axis pivot system which permitted it to be rotated by a servo motor about an axis parallel to the slit. This motion allowed the sun's limb to be aligned more precisely with respect to the spectrograph slit, and provided greater pointing stability in one axis than was achievable with the ATM pointing system alone.

The stability in one axis was thereby increased to $\leq + 1$ arc sec with a jitter $\leq + 1$ arc sec per sec. In laboratory tests the servo system was able to maintain this pointing accuracy when exposed to drift rates as high as 14 arc sec per sec. In addition, the pointing reference system could position the solar limb at any angle with respect to the spectrograph slit over a range of ± 70 arc sec with an accuracy of 1 arc sec.

The servo loop was controlled by an image dissector tube (IDT), which received an image of the sun reflected by the slit plate. The slit plate itself was a thin film of nickel over copper with a 10 micron by 300 micron slit etched through it. In addition, fiducial marks were etched into the nickel layer only. These fiducial marks were used by the pointing reference system electronics to determine the position of the solar limb with respect to the slit. The slit plate and its slit were designed to conduct away the heat produced by the solar image.

In the "limb pointing" mode, the system was under servo control. The "boresight" mode was used for manual pointing of the spectrograph, for checking coalignment with the other ATM instruments and especially the ATM pointing control system (PCS), and for locating sunspots. In the latter mode, the IDT output from the whitelight solar image on the slit plate was displayed on one of the CRT's at the C&D panel.

Researchers who need to know the location on the sun of a particular exposure must refer to supplementary documentation listed in Appendix A. The most directly useful of these is the Harvard ATM H-Alpha Atlas and Atlas Guide (#11), which gives a print of the sun exposed in $H\alpha$ as projected on the SO55 slit, with the position of the SO82B slit indicated. The appropriate orientation coordinates are also given. In addition to the selected Atlas prints made for each ATM pointing change, all $H\alpha$ exposures made from Skylab are available separately on 35 mm film. See also a description of the H-alpha telescopes in Section 2.2.

3.3 Astigmatism, Spectral Resolution, and Stray Light

By the introduction of the telescope mirror to the spectrograph design, small regions of the sun could be studied quantitatively, an advantage over earlier rocket instruments. In the former instruments the predisperser gratings served to form a very small image of the sun on the slit, and were also slightly deformed to neutralize the astigmatism of the main grating. By ruling a special type of predisperser for SO82B, instrumental astigmatism was reduced and speed was increased to offset the loss incurred by the third reflection of the telescope.

Figure 3.3 illustrates the astigmatism acquired by use of the Rowland mounting for a grating. With the rulings of the grating perpendicular to the plane of the paper, the tangential focus of the diffracted slit image from A lies on the Rowland circle at B, where the slit width is in focus. The sagittal focus, or focus of the slit length, lies on a line perpendicular to the grating normal and tangent to the Rowland circle as at point C.

This is known as Sirk's position. A converse arrangement with the tangential focus at point B and the sagittal focus at point C should produce a stigmatic image at point A. The predispersers of the ATM spectrograph were designed to approximate this special condition. The idea was to make use of the change in sagittal focus of a concave spherical grating, secured by continuously changing the grating spacing in the proper way during ruling. This property of a grating has been known for some years in connection with grating errors; it had never been made use of in spectrograph design. To rule such a grating would have required development of a device by means of which the grating spacing could be changed continuously and precisely. It was possible, however, to approximate the continuous change with a multipartite grating, ruled in ten 40 mm long and 3.6-mm wide segments, each having a slightly different ruling spacing. In the reduction of the astigmatism the spectrum was narrowed, and an increase in speed of the instrument was obtained.

Figure 3.4 illustrates the effect of the segmented predisperser. Diffracted rays from each segment come to a tangential focus on the Rowland circle of the predisperser grating, as in a conventional Rowland mount. However, the ray bundles from different panels cross each other at point C before they reach the Rowland circle of the predisperser. Thus a pseudotangential focus is formed at point C. The sagittal focus of each panel still occurs along the predisperser's sagittal focal plane in the vicinity of point B. Therefore the slit width is in focus at point B, while the slit length is in pseudofocus at point C, the Sirk's position for the main grating.

The size of the clear aperture of the telescope mirror allowed only the central eight segments to be illuminated. As shown in Fig. 3.5, the diffracted beam from these eight predisperser panels considerably overfilled the main grating. For any particular wavelength, only five adjacent predisperser panels, or four plus a half panel at each end, illuminated the main grating. This permitted the optimization to be made over a greater range of wavelengths because different segments were used at, say, 1200 Å than at 1800 Å. The ruling spacing of each predisperser segment was chosen to optimize the distance between points C and B for the different parts of the wavelength range. Figure 3.6 shows the astigmatism at the film plane for both uniformly ruled and segmented predispersers as a function of wavelength. The spectrum height for the case of the segmented predisperser on the average is one-fourth that for the uniformly ruled predisperser. Thus the instrument speed was increased by about a factor of 4. Without this increase in speed, the long exposure times necessary to obtain the weaker lines and continua of the solar XUV spectra, particularly for recording spectra above the solar limb, would have been too long for practical application on Skylab.

Although the segmented predisperser increased the instrument speed, it degraded slightly the spectral resolution at the film plane. This was caused by the off-plane aberrations of the Rowland mounting. As Fig. 3.7(a) illustrates, the beam incident on the main grating was not parallel to the plane of the main grating's Rowland circle, and the departure was a function of wavelength. Point B is the sagittal focus of the predisperser; it is also the point at which the main grating Rowland circle intercepts the plane of the figure. The line at point B defining the extent of the beam diverging from C is not centered with the Rowland circle plane, and the beam incident on the main grating is inclined with respect to this plane.

Thus the main grating is used off-plane. Figure 3.7 (b) illustrates a conventional Rowland mounting with an off-plane slit source; Fig. 3.7(c) shows the curved and tilted line image of the slit that is produced. The aberrations are exaggerated and not to scale. When the segmented predisperser is used, each segment illuminates the main grating at a slightly different angle in such a way that the final image is compressed; however, the compressed portions are not in precise registration in the lateral direction, as illustrated in Fig. 3.7(d). Hence, the spectral resolution is degraded.

Figure 3.8 shows the spectral resolution at the film plane as measured from laboratory spectra. The upper and lower curves apply, respectively, to the short and long wavelength ranges of the instrument. Photometrically determined full widths at half maximum were used to obtain the measured points. For comparison, the theoretically attainable resolution, as derived from a 3-D ray tracing computer program, is indicated by the solid line. For the most part, the spectral resolution is 30,000, but is decreased to 20,000 at the short wavelength end because of the off-plane aberrations. The spectral resolution of the instrument achieved during flight agreed well with the preflight laboratory measurements.

A shortcoming in this design of a double-dispersion, dual predisperser spectrograph lay in the use of the second order of the main grating in combination with the first order of the 300-l/mm predisperser. The focused stray light from the predisperser that included all wavelengths came to a vertical linear focus on the waveband aperture; this aperture allowed a significant fraction to pass through and onto the main grating. The main grating, in turn, brought the long wavelength portion of the stray light to focus in its first order. Therefore, the desired spectrum, 977-1970 Å, was overlaid with a broad, faint spectrum of 1954-3940 Å wavelength, whose height was determined by the waveband aperture. This unwanted spectrum was

of greater intensity relative to the XUV for spectra of regions on the sun's disk than for positions close to or above the limb. It became insignificant at wavelengths shorter than 1500 Å. The predisperser grating was ruled in a way that minimized the focused stray light.

3.4 Optical Coatings

The optical surfaces were coated to provide the maximum reflectance possible for the short wavelength band and to reduce the speed in the long wavelength band where the solar intensity is so great. Figure 3.9 lists the coatings on each element and shows the total instrument reflectance, including the efficiencies of the gratings.

In order to obtain the maximum possible efficiency at the short wavelengths where the solar spectrum is weakest, the 300-l/mm predisperser and the main grating were blazed at 1200 Å. The peak in the instrument reflectance at about 1300 Å shows the effect of the blaze. The sudden decrease in reflectance below 1200 Å was caused mainly by the decreasing reflectance of the magnesium fluoride; it was especially prominent because the beam was reflected by three such surfaces. The minimum at 2900 Å is a characteristic of the multilayer Al-ZnS coating.

3.5 Thermal Control System

In order to maintain good focus and to avoid smearing the image, the over-all temperature of the spectrograph was maintained between 20.9° C and 21.2° C, and the local thermal differences were held to less than 0.2° C, although the temperature of the ATM canister ranged from 10° C to 27° C and that of the ATM spar from 16° C to 21° C. Prior to installation in the ATM, the instrument was focused at 21° C. A combination of passive thermal shielding and active thermal control panels was used to control the over-all temperature.

Prevention of direct heating by the incident solar radiation was accomplished mainly by a mirror that encircled the slit plate. This mirror reflected the portion of the solar image not striking the slit plate back to the telescope mirror and out the front aperture. In addition, there was a heat rejection mirror surrounding the perimeter of the telescope mirror; this reflected out the front aperture any radiation that overfilled the mirror. These heat rejection mirrors kept differential heating of the instrument at a minimum, thus preventing significant smearing of the final image at the film plane during long exposures.

3.6 Film and Film Camera

Kodak Special Film types 104 and 101 were used. Both are VUV sensitive Schumann emulsions deposited on a thick gelatin pad carried on a 7-mil Estar base. The gelatin pad between the base and the emulsion contained a yellow antihalation dye to absorb scattered solar radiation longer than 2500 Å.

From 1000 A to 4000 A type 101 film is approximately two to five times faster than type 104. However, tests conducted prior to the Skylab mission revealed that type 101 film is disproportionately more susceptible than 104 to environmental effects. Therefore, the majority of the film strips used in the cameras were of type 104.

When received from Kodak, the film was in 100-ft rolls, 70 mm wide. Due to the great sensitivity to abrasion of these emulsions, each turn on the roll was separated from its neighbors by raised rails that consisted of a band of polystyrene beads secured to the gelatin and placed along each edge of the film. The strips of film for the spectrograph, measuring 35 mm x 250 mm, were cut from the center of the 70-mm wide rolls and mounted in flexible anodized aluminum holders. A chip of Kodak Plus-x panchromatic film was mounted at the end of each holder to record the diode matrix flasher exposure data. Two examples of the film strips and chips are shown in Fig. 10. Eight solar spectra and the diode array data exposures can be seen on each strip. The top strip is a flare spectrum in the short wavelength region (970-1970 A). The bottom is a limb scan exposure sequence containing both long and short wavelength spectra.

The camera carried 201 holders which were stacked in two columns of 100 each, one column above the other. As the camera was cycled, the perimeter of the strip to be exposed was pressed against a carrier which was shaped to the Rowland circle focal plane of the main grating and was registered to within 0.1 mm. The carrier was transported parallel to its long dimension in 3-mm steps, thus allowing eight exposures to be recorded on each strip. The camera was mounted to the instrument, as shown in Fig. 3.11, by a latch and guide rail system which provided easy installation and removal by the astronaut while maintaining accurate registration with the focal plane. Prior to being mounted in the instrument, the camera was stored in a sealed canister filled with nitrogen. After use on the instrument, the camera was returned to the canister and sealed while in the space vacuum.

3.7 Instrument Performance

The spectrograph operated well over the entire Skylab mission. There were no anomalies, except those connected with Schumann film, which are described elsewhere in this Guide (Sec. 4). One camera was exposed during SL-2, two during SL-3, and one on SL-4. A total of 6408 spectra was obtained.

In Fig. 3.12 there is reproduced a sample section of eight exposures made at the beginning of the first mission. This shows the 1170-1245 Å region, less than 10% of the entire coverage in the short wavelength position. These exposures were made in the automatic limb scan mode. Exposures of 160 sec were made between the white light limb and -12 sec of arc inside. The exposures made above the limb to +8 sec of arc were four times longer. This limb scan was carried out when an active region was on the limb.

The Lyman- α line of hydrogen, 1216 Å, is seen to reach greatest intensity in the chromosphere, 2 sec of arc above the limb. All images of it are greatly overexposed. The profile of the line is conspicuous; broad wings, the central maximum doubled by deep self-reversal caused mainly by the great optical density of the solar atmosphere at the center of the line and also by the telluric hydrogen absorption core. When observed close to the limb, the double peaks became so intense that their images were solarized. Between the solarized images one can see an extremely narrow non-solarized line; this is the telluric absorption core, whose width is 0.025 Å. The other chromospheric and low transition region lines, Si II, Si III, C III, N V, maximize at the same limb position, approximately, as does Ly- α .

The behavior of the coronal and high transition region lines is different. For example, Fe XII, 1242.0 Å, is extremely faint on the disk at -12 sec of arc. It is most intense above the limb and stays intense all the way to +8 sec of arc above the limb.

Shown on Figure 3.12 are several lines whose identifications are new*. Mg VII, 1189.8 Å, S X, 1196.2 Å and 1213.0 Å, S V, 1199.2 Å, and Fe XIII, 1216.4 Å. In older low dispersion spectra the intersystem line O V, 1218.4 Å was barely visible above the Lyman- α wing, much as is the case in Fig. 3.12 for Fe XIII, 1216.4 Å, which is three times closer to Ly- α than O V.

Within the 1000-Å short wavelength coverage of the spectrograph approximately 4000 lines can be resolved. Some 50% have been identified. In Fig. 3.12 there are present about 25 unidentified lines, most of them weak. An emission doublet of some interest can be seen at 1243.9 Å, 1240.4 Å, just to the right of the shorter component of N V in the exposure at +2 sec of arc. This is the transition Mg II $3s^2S_{1/2} - 4p^2P_{3/2, 1/2}$ the first members of the principal series of Mg II. In long exposures on the disk the two lines are present in absorption against the wing of Ly- α ; they are the Fraunhofer lines of shortest wavelength as yet obtained in the solar spectrum.

* G. D. Sandlin, G. E. Brueckner, and R. Tousey, Ap. J. 214, 898, 1977, Forbidden Lines of the Solar Corona and Transition Zone: 975-3000Å.

Figure Captions

- Fig. 3.1 The optical system of the XUV spectrograph in ATM.
- Fig. 3.2 The telescope and the pointing reference servo system that stabilized the sun's image on the slit; the long dimension of the slit lies in the plane of the figure.
- Fig. 3.3 Astigmatism of the Rowland mounting.
- Fig. 3.4 The pseudoastigmatism of the predisperser ruled with ten segments of different spacings.
- Fig. 3.5 Illumination of the main grating by the ten paneled predisperser for different wavelengths.
- Fig. 3.6 The decrease in length of the spectral lines achieved by use of the segmented predisperser.
- Fig. 3.7 The off-plane aberrations of the double-dispersion spectrograph and the effect of the segmented predisperser.
- Fig. 3.8 The spectral resolution of the ATM spectrograph, showing points plotted from measurements made prior to flight and curves calculated with a 3-D ray tracing computer program. The upper section is for the short wavelength range and the lower for the long.
- Fig. 3.9 The total reflectance of the instrument, including both main and predisperser gratings and the telescope mirror.
- Fig. 3.10 Photographs of two strips of film exposed by S082B.
- Fig. 3.11 The S082B spectrograph resting on a granite block and showing the thermal control panels. The camera is located at the front center of the photograph.
- Fig. 3.12 An example of spectra obtained during the limb scan mode. The wavelength range is 1170-1245 Å, about 1/10 of the entire coverage. Positive limb positions (in sec of arc) refer to positions above the limb.

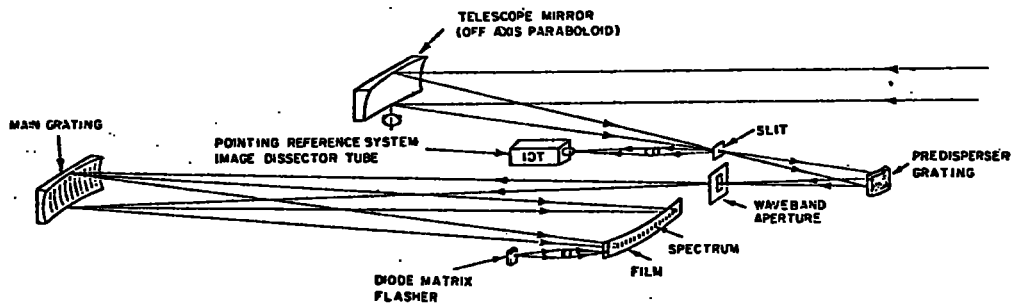


Fig. 1. The optical system of the XUV spectrograph in ATM.

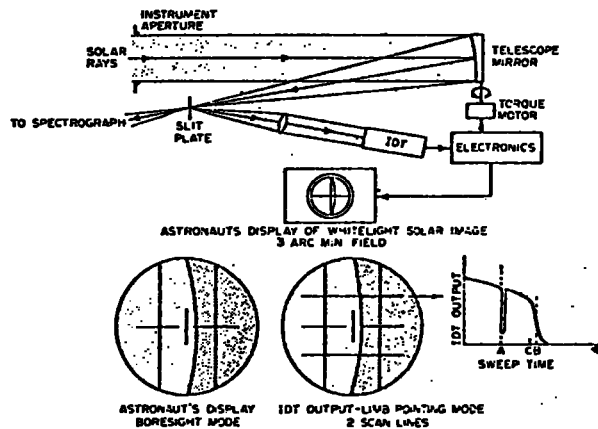


Fig. 2. The telescope and the pointing reference servo system that stabilized the sun's image on the slit; the long dimension of the slit lies in the plane of the figure.

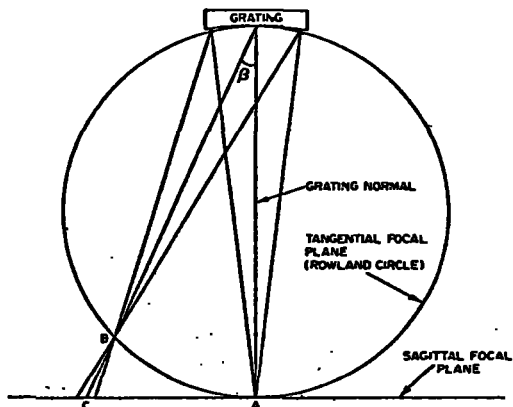


Fig. 3. Astigmatism of the Rowland mounting.

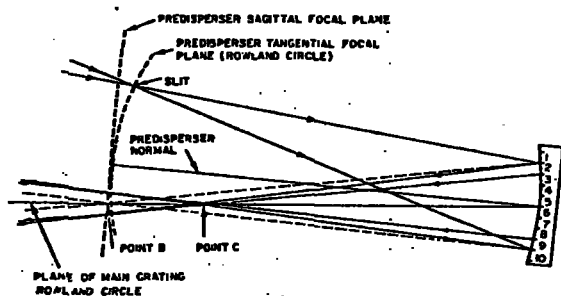


Fig. 4. The pseudoastigmatism of the predisperser ruled with ten segments of different spacings.

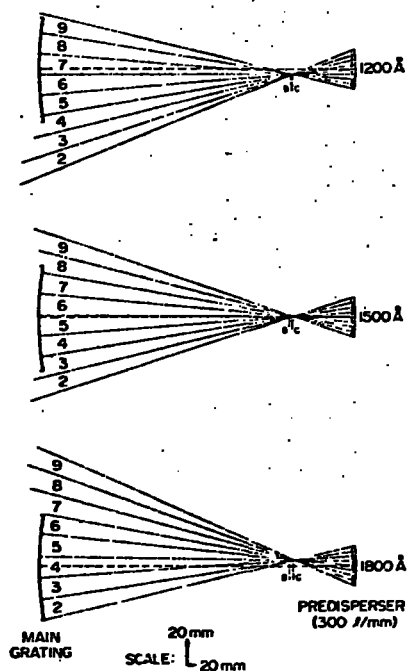


Fig. 5. Illumination of the main grating by the ten paneled predisperser for different wavelengths.

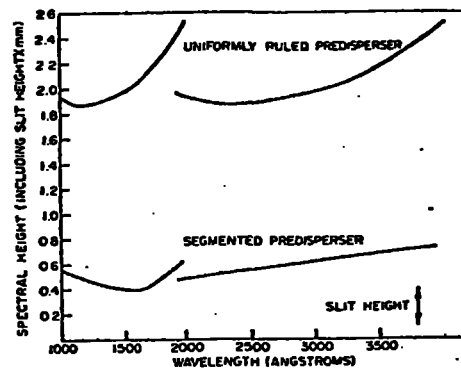


Fig. 6. The decrease in length of the spectral lines achieved by use of the segmented predisperser.

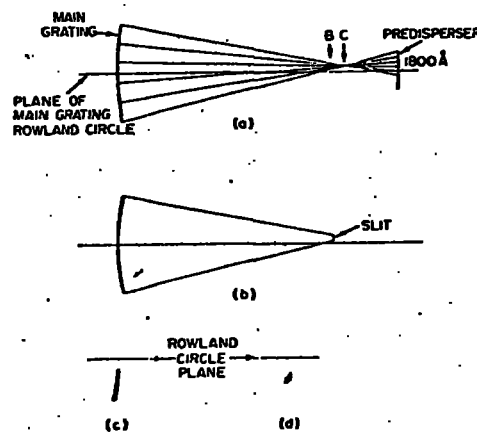


Fig. 7. The off-plane aberrations of the double-dispersion spectrograph and the effect of the segmented predisperser.

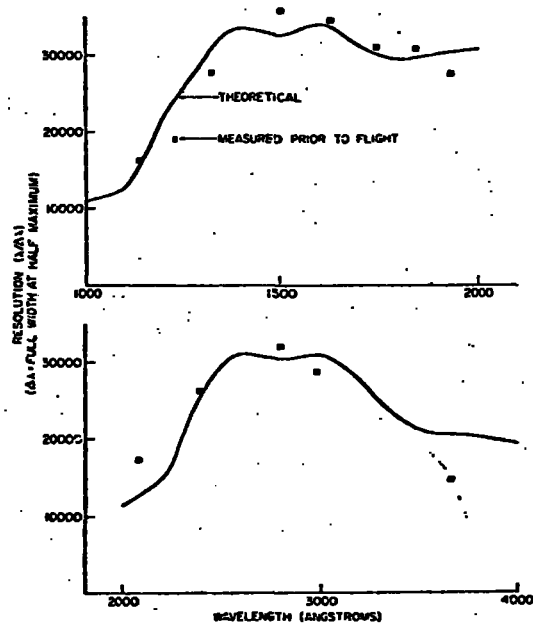


Fig. 8. The spectral resolution of the ATM spectrograph, showing points plotted from measurements made prior to flight and curves calculated with a 3-D ray tracing computer program. The upper section is for the short wavelength range and the lower for the long.

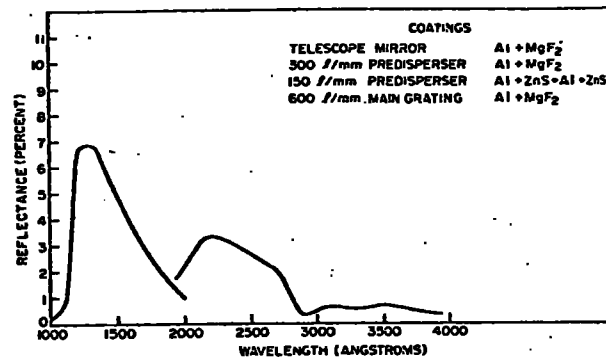


Fig. 9. The total reflectance of the instrument, including both main and predisperser gratings and the telescope mirror.

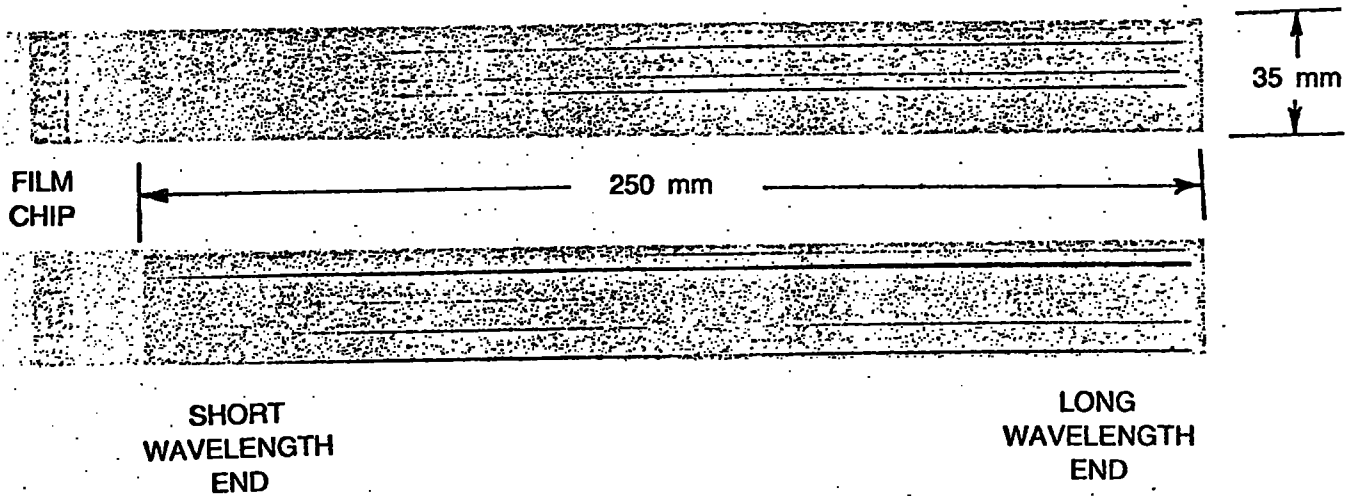


Fig. 10. Photographs of two strips of film exposed by S082B.

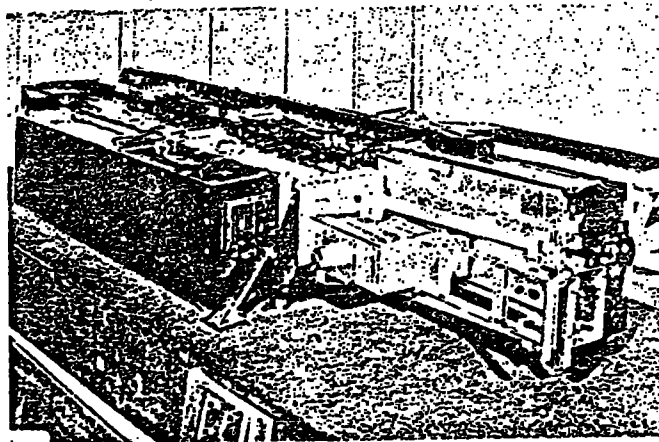


Fig. 11. The S082B spectrograph resting on a granite block and showing the thermal control panels. The camera is located at the front center of the photograph.

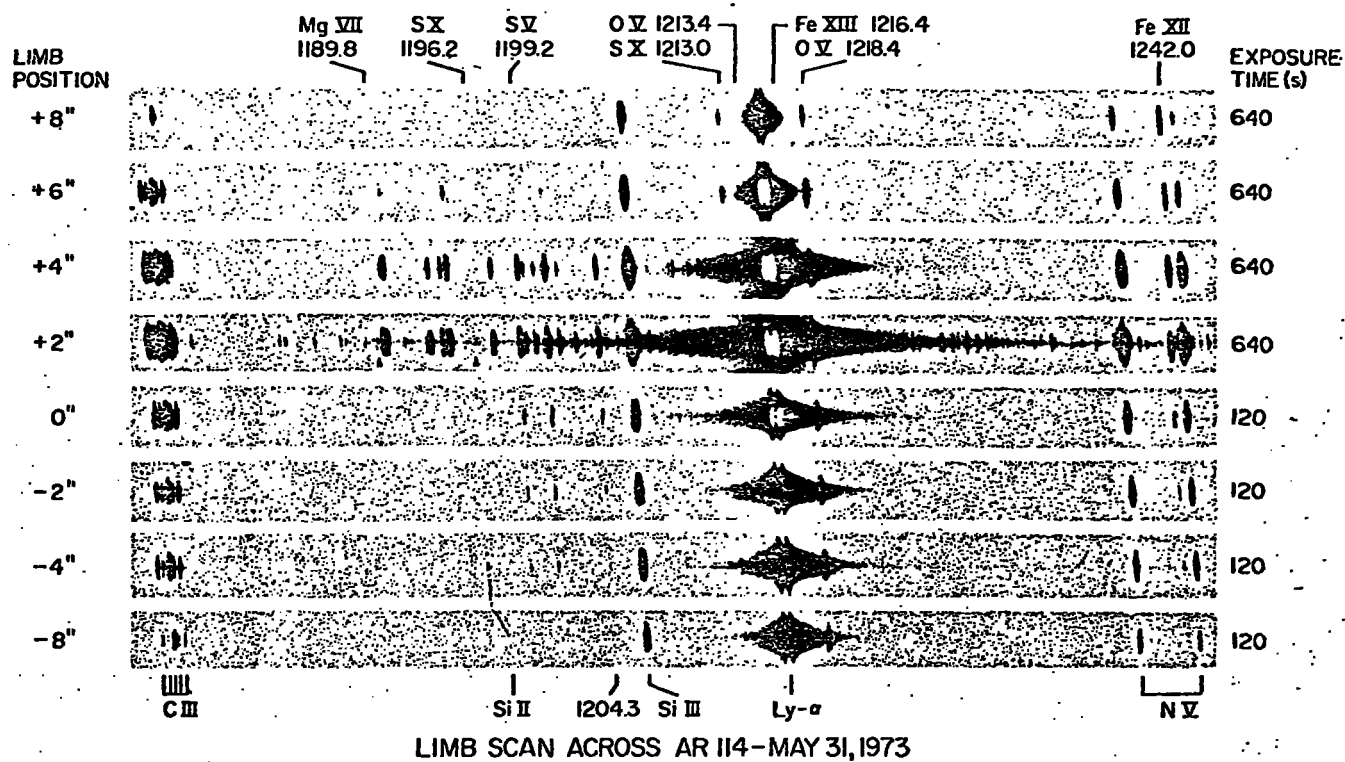


Fig. 2. An example of spectra obtained during the limb scan mode. The wavelength range is 1170–1245 Å, about $\frac{1}{10}$ of the entire coverage. Positive limb positions (in sec of arc) refer to positions above the limb.

4.0 FILM HISTORY*

Commencing in 1946, when V-2 rockets first made possible experimentation from above the earth's atmosphere, there has been an increasing need for photographic film with which to record the XUV spectrum of the sun. The emulsion type most sensitive to the XUV was invented by Schumann in 1892 and perfected by 1901. Schumann recognized the fact that gelatin is opaque to the XUV. As a result he developed an emulsion with just enough gelatin to hold the silverhalide crystal on the base material, but the layer of gelatin was so thin that it was effectively transparent to the XUV. These emulsions could not be touched without destroying them.

For 50 years Schumann plates were made by hand and in severely limited quantities. Eastman Kodak was first to produce a Schumann emulsion on a film base by machine coating. They also developed a method of preventing abrasion between turns of packaged rolls by coating each edge of the film with a spacer 0.2 mm thick, consisting of polystyrene beads held down with gelatin. They named the new, fast emulsion 101 and produced as 104 a slower, but finer-grained emulsion having the beaded spacers. All these emulsions were unprotected, hence extremely susceptible to abrasion. Although now nearly free from defects, fog problems and other effects have continued to arise; some are described in this Guide.

4.1 Batches

The film strips required by the XUV spectroheliograph (SO82A) and spectrograph (SO82B) were 250 mm long and 35 mm wide. To provide for this size, Eastman Kodak produced 104 and 101 films in special rolls, 70 mm in width, and 30 m (100 ft) in length. The required strips were cut from the center. Three rolls were sufficient to provide the 200 strips needed for each camera. Ten rolls were made from one batch of emulsion. Strict controls were required to produce the many batches of emulsion needed to manufacture film that was satisfactory for (ATM) experiments in the large quantity required. In the past it was not uncommon to find variations from batch to batch, and even within a single roll, on the order of a factor of 2 to 5. Eastman Kodak succeeded, however, in improving dramatically the over-all quality of both 104 and 101 films. Large quantities of these films were produced that were uniform to a degree never previously achieved; they were remarkably free from

*Material for this section has been extracted from a paper in Applied Optics, 16, 887, 1977, by M. E. VanHoosier, J.-D. F. Bartoe, G. E. Brueckner, N. P. Patterson, and R. Tousey. Experience with Schumann-type XUV Film on Skylab. More detailed information about the film may be found in in that source.

blemishes of all kinds. Generally, the sensitivity threshold did not change significantly with batch or from place to place over a roll. The maximum density D_{max} and the contrast varied between batches, but not greatly. Type 104 batches having D_{max} between 1.4 and 1.6 (as measured with a Grant microphotometer) were accepted for use in ATM.

4.2 Film Sequence Log

Each of 10 cameras exposed for experiments SO82A and SO82B during Skylab contained film strips cut from several different rolls, and each camera load of strips was developed in several different runs. A record was kept of the roll of film from which each film strip was cut, the emulsion batch in which that roll was manufactured, and the development run in which the film strip was developed. This record is known as the Film Sequence Log, and it is reproduced for SO82B in Appendix C. The emulsion batch appears as the second suffix in the film type number of each roll, i. e.

Film Type

104 - 06 - 05

(Type 104 emulsion)	(7 mil Estar base)	(batch 5)
------------------------	--------------------------	-----------

The full complement of film strips (approximately 201) was exposed in all SO82B cameras. Development run A was made as a test prior to the full tank runs.

4.3 Mounting

A major design problem in of both SO82 instruments was the camera. It was decided not to attempt to use Schumann film in roll form because of the many difficulties associated with abrasion, environment, static electrical effects, and precise registration of the film to the focal surface. Rather, each film strip was carried in its own metal holder, and approximately 200 strips were held in each camera.

The design of the metal holder involved the choice of a suitable metal and configuration so that, when bent into position, the film would lie precisely on the Rowland circle, within a tolerance of 0.2 mm. An equally important consideration was to choose a material for the holders that would not fog Schumann film.

Holders of two types were used for experiments S082A and S082B. The first choice was 0.25-mm stainless steel which was believed compatible with Schumann film. It was necessary, however, to increase its stiffness for the 2 m focal plane radius of the S082A instrument by stamping five depressed ribs lengthwise into each holder; otherwise the unsupported area would not conform properly to the Rowland circle. As discussed in articles about the S082A experiment, these grooves were found to be a source of fog.

The S082B focal plane radius was only 1 m, and the tolerance on conformity to the Rowland circle was very tight. For this instrument the holders were made of 0.8-mm thick aluminum sheet, which was sufficiently stiff and uniform so that ribs were not required. However, before forming the retaining lips, it was necessary to reduce by machining the thickness of the aluminum to be bent.

Use of aluminum for film holders had been avoided as long as possible, because of its long history of fogging Schumann film, from rocket experiments and experience in the laboratory. A test program was set up to investigate film fogging by metals. It was found that freshly machined aluminum did, indeed, fog types 104 and 101 films; but aluminum, if completely anodized, did not. Therefore, the aluminum holders were thoroughly anodized after machining and bending. These holders caused no fogging of flight film. Similar precautions were taken with all parts of the camera, even though they were not located close to the film. Black-anodized aluminum, made by dying black the anodized layer before it was dry, was found safe. Magnesium was not used because, when chemically blackened, it produced fog.

Figure 4.2 shows a partially disassembled view of a camera loaded with empty film holders. Each camera, of which 10 were flown on Skylab, was extremely complex. The quasi-carrousel design allowed the loaded film holders to be transferred sequentially and rapidly into and out of the focal position, from one stack of 100 to the other stack, while another transfer occurred at the back. When all the holders had made the circuit once, the camera was fully exposed. In flight, the only camera that malfunctioned was the one actually in place in the S082A instrument during the launch.

4.4 Processing the Film

Over the years of using Schumann type film, and after considerable additional experimentation, it was decided that D-19 mixed 1:1 with distilled water provides the greatest uniformity, freedom from chemical fog, and minimum Eberhardt, edge and adjacency effects. The following procedure was adopted to provide maximum control and uniform quality of the flight exposures.

One flight strip from each mission was selected and processed alone at the start, to ensure that each returned flight load had not received degradation which could be corrected by different processing. The remainder of the film was developed in batches of 40 flight strips and 10 laboratory - exposed control strips. The flight strips were left in their holders, together with the Plus-X data chip. All strips were attached to a rack in a vertical position. The solutions were held in large, stainless steel tanks. Each tank contained 40 liters of solution, a quantity considered sufficient to process the entire contents of one camera without depletion.

The rack of 50 film strips was first presoaked in a tank of distilled water for 4 minutes. This was an important step because it prevented infectious development by allowing the dried-out gelatin pad to swell. Otherwise, whiskers growing on exposed grains could touch adjacent unexposed grains, making them developable. Immersion in the water was done quickly, but smoothly; if strips are immersed unevenly, marks are produced by the stresses of nonuniform swelling. All solutions were maintained at 20° C. It was important to avoid elevated or changing temperatures, which would cause reticulation of the gelatin pad. Development was for 4 min., followed by 30 sec in acetic acid short-stop, 4 min. in Kodak acid fixer, a 20 min. wash in filtered tap water, removal to a class 10 K clean room, rinsing in distilled water, and hanging to dry.

An important part of the development process was the use of N₂ bubble agitation, introduced through an array of many small holes, roughly 3/4" apart, in a plenum at the bottom of the tank. A one second burst of N₂ was produced at 10 sec intervals. In addition, the entire film rack was moved laterally by hand, alternately parallel and perpendicular to the film, at a speed of about 1 cm per sec. This procedure had been found to produce uniform development.

The five development runs which were required for each camera could be completed in one day. The development process was controlled by including in each development the 10 control strips of film from the same batch on which

a standard series of exposures had been placed 48 hours earlier. These 2 cm by 10 cm strips were exposed to the continuum spectrum of a D2 lamp, dispersed by a McPherson normal-incidence monochromator/spectrograph. The exposure times were 1 and 10 sec. The intensity was reduced in steps of a factor of 2 by means of sectorized disks, covering the range of 1:100 in transmittance. The spectral range was 1650 to 2400 Å. Use of these control strips was mainly to serve as a check that the development was the same each time it was carried out. The H - D curves of control strips developed in various runs were found to agree to ± 0.02 in log E.

Finally, the dry film strips, while still in the clean room, were mounted between high quality glass plates of 1.25 mm thickness, which had been anti-reflection coated on the inside surfaces to minimize Newton's rings. The film strip was surrounded with a brass spacer, of thickness slightly greater than the film. This, together with the normal curl, prevented the emulsion from being touched by the glass. The sandwich was then sealed with plastic tape and stored in a vault.

4.5 Loss of D_{max} and Contrast

An unexpected film effect was a reduction in D_{max} and contrast on all of the flight film, apparently due to prolonged exposure to the hard vacuum in space. Figure 4.2 shows a comparison between the characteristic curves for Types 101 and 104 flight film and those for film samples from the same emulsion batch kept at 2° C in the laboratory. Especially conspicuous is the long, flat maximum on the flight film. This is followed by a sudden turn-down caused by solarization, for extremely high exposures (typical of solar flares). These curves show that there was no loss in threshold sensitivity. Film stored for an extended period under vacuum in the laboratory did not show this effect. That the loss was due to a cause other than degradation of the latent image was shown by sensitometric tests made post-flight on unexposed strips of flight film.

4.6 Fog

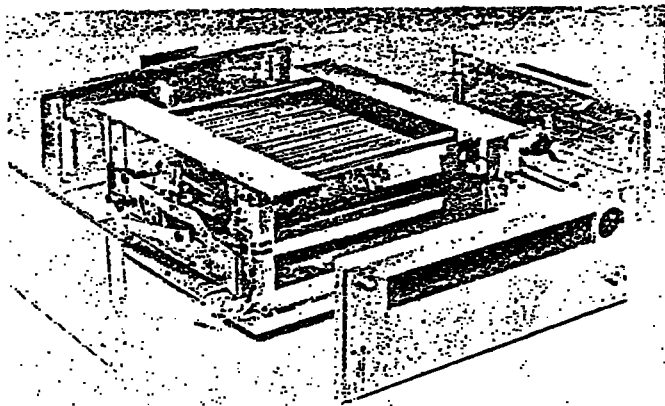
Fog levels expected from the proton flux did not materialize in flight. It had been realized that the fog prediction was not too certain, therefore a single strip of type 101 film was included as a test in most cameras on SL-2 and 3. The proton fog level for type 104 film was negligible and for type 101 only 0.02. The explanation appears to be that the proton flux from the South Atlantic anomaly was much less than was expected, and also that the shielding provided by the Skylab was more effective than calculated. Furthermore, high temperatures were never

experienced. No fogging of the film occurred due to ions, metallic surfaces, or contamination.

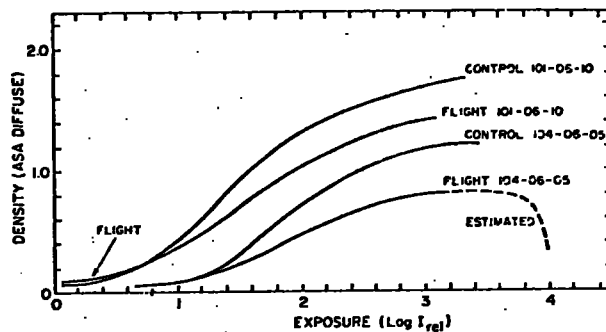
There was insufficient time to include any type 101 film in cameras resupplied in SL-3. However, some was included in the cameras for SL-4. The five times greater sensitivity made possible several investigations. It permitted recording coronal spectra to greater altitudes above limb than was possible with type 104. Through its use the profile of hydrogen Ly α as emitted from the extended hydrogen cloud surrounding the comet Kohoutek was photographed, and it extended to shorter wavelengths the spectral coverage of SO82B. This successful use of type 101 was, however, at the expense of added risk of fogging, reduced accuracy of calibration, and increased granularity.

Figure Captions

- Fig. 4.1 A photograph of a loaded and partially disassembled camera. Only the upper stack of 100 film holders can be seen. The closed shutter is seen in the plate at the right. All the actuator mechanisms were located at the sides.
- Fig. 4.2 Typical curves of density vs log exposure for Eastman Kodak types 101 and 104 film. One set applies to film that had been exposed to the space vacuum during Skylab, while the other is for control film kept at 2°C in the laboratory. The extension of the type 104 curve to large values of exposure shows the solarization response, as estimated.



4.1
Fig. 4.1 A photograph of a loaded and partially disassembled ~~SOSZA~~ camera. Only the upper stack of 100 film holders can be seen. The closed shutter is seen in the plate at the right. All the actuator mechanisms were located at the sides.



4.2
Fig. 4.2 Typical curves of density vs log exposure for Eastman Kodak types 101 and 104 film. One set applies to film that had been exposed to the space vacuum during Skylab, while the other is for control film kept at 2°C in the laboratory. The extension of the type 104 curve to large values of exposure shows the solarization response, as estimated.

5.0 CALIBRATION AND ABSOLUTE SPECTROPHOTOMETRY*

Handwritten:
Sec 5.3.2
new
2/14/78

Accuracy of calibration of instrumentation used in the extreme ultraviolet has always been a problem of great difficulty. Early in the ATM program it was proposed by HCO and by NRL that their instruments be calibrated by comparison with carefully standardized instrumentation flown in rockets. One calibration rocket (CALROC) flight per mission for each institution was considered to be the minimum required because the sensitivity of the ATM instruments was expected to change during the course of the nine months over which they would be used. The fundamental idea was to make simultaneous solar measurements using both rocket-borne and ATM instruments. Absolute intensities derived from the well-calibrated rocket instruments would then serve to calibrate the sun so that it could serve as a standard source with which to calibrate the ATM instruments.

The plan of NRL was to fly instruments almost exactly like those of ATM but reduced in size by a factor of two. The ATM spectrograph could operate in either of two wavelength ranges: 970-1940A, or 1940-3940A. In the latter, or "long wavelength" range, absolute intensities had already been well-determined by Tousey et al. (1) and by Broadfoot (2). Therefore the CALROC instrument could be simplified and improved over the ATM instrument by eliminating the long wavelength range and utilizing both the main and pre-disperser gratings in the first order. In this manner stray light which was present in the ATM instrument was eliminated from the CALROC instrument.

NRL, together with Ball Brothers Research Corporation (BBRC), Goddard Space Flight Center (GSFC), and the Ames Research Center, developed a command system by which the instrumentation section of the rocket, after separation from the booster, could be pointed at particular positions on the sun. This was done by a radio command link combined with a television system which displayed to the PI on the ground an H- α image of the sun reflected from the slit plate of the spectrograph. By command loop the PI could then orient the slit precisely during the flight to any desired solar feature.

The CALROC program required a great effort, but the results proved to be highly successful. In the remaining

* Material for this Section has been gathered from helpful discussions with Drs. K. R. Nicolas, O. Kjeldseth Moe, N. P. Patterson, J. W. Cook, G. A. Doschek, and U. Feldman. Portions of material have been extracted from References 3, 5, 6, 7, and 8, listed at the end of this Section.

paragraphs of this Section, methods of obtaining absolute solar intensities from the ATM data are discussed. First the CALROC instrument and the method used for its absolute calibration in the laboratory are described. Reduction of the CALROC solar exposures then gave absolute solar intensities, which were published in a spectral atlas for the range 1175 to 2100 Å (3). By comparison of identical spectral features measured by CALROC and ATM, a wavelength-dependent absolute sensitivity plot was produced for the ATM spectrograph during the second Skylab mission. A method which can be used to transfer this calibration to other film batches and other Skylab missions is then presented. Also included is a discussion of precautions to be observed in the photometry of the ATM film. Finally, the method and instrumental response curve needed to obtain absolute intensities from the long wavelength ATM data are provided.

5.1 CALROC Calibration

CALROC flights were made on June 13, 1973, Sept. 4, 1973 and Jan. 15, 1974. The calibration instrument, flown on a Black Brant VC rocket, was a 1/2 scale model of the ATM SO82B spectrograph and used a 1 m focal length off-axis parabolic mirror to focus a solar image onto the spectrograph slit. Behind the entrance slit was a double dispersion spectrograph. A predisperser grating, consisting of panels with slightly varying grating constant (average 200 lines mm^{-1}), formed a dispersed image of the slit on a slot which selected the wavelength band to be recorded and blocked all visible light from striking the main grating (2150 lines mm^{-1}), which was mounted in a Rowland configuration. Both gratings were used in the first order; this eliminated stray light which was present in the ATM instrument. (See Sec. 3.3). The film strips on the Rowland circle were 200 mm long and covered the spectrum from 1170 to 2100 Å with a dispersion of 4.7 Å mm and a spectral resolution of 0.07 Å, closely comparable to the ATM spectrograph (See Sec. 3).

An absolute calibration of the CALROC spectrograph was made in the laboratory utilizing a standard deuterium (D_2) lamp calibrated as a function of wavelength between 1650 Å and 2600 Å at the National Bureau of Standards (NBS) before and after the flights. For shorter wavelengths this source cannot be used as a standard because of the appearance of numerous D_2 molecular lines. Between 1250 Å and 1700 Å a relative spectral calibration was obtained after the flight using a high pressure argon arc as an intensity standard (Bridges and Ott, (4)). By matching this relative calibration from the argon arc to the deuterium lamp absolute calibration above 1700 Å, it was then possible to extend the absolute calibration of the rocket instrument to 1250 Å. A detailed description of the deuterium lamp calibration is given by Brueckner et al. (5), while Kjeldseth Moe et al. (3) have described the argon arc calibration.

Spectra of the deuterium lamp were exposed by the instrument before and after each flight to detect any change in instrument sensitivity. In addition, segments of the lamp spectrum were placed on each strip of the flight film prior to flight to minimize errors resulting from film inhomogeneities, development problems, and film environment during flight. These segments were exposed with the flight instrument, using a 1 m off-axis parabola as a collimator. Short of in-flight calibration, this method was as close as possible to an ideal calibration for irradiance measurements. The only optical element which had to be measured independently was the collimator mirror. Care was taken to assure that the illumination of all optical elements of the flight instrument was identical during the calibration and the solar exposures.

The film characteristic curves relating film density above fog level to relative exposure were constructed from a series of flight exposures in the manner described in Sec. 5.3.1. Fig. 5.1 gives an example of the CALROC characteristic curve.

Absolute solar intensities derived from the CALROC program for use in the ATM calibration have been published as "A Spectral Atlas of the Sun between 1175 and 2100 Å" (3), described in more detail in Sec. 8. The data have also been used in various other studies of the sun, which are listed in the Bibliography, Appendix D.

5.2 ATM Calibration

CALROC essentially calibrated the sun, making it a secondary standard source. As nearly as possible the CALROC instrument observed the same regions as the ATM, although at a time which was a few hours away from the ATM observations. The accuracy attained in pointing both instruments, together with the closeness in times of observation, made the calibration of the ATM intensities from CALROC both simple and accurate. Only a direct transfer of intensities from the CALROC spectra to the ATM spectra was involved, without the need to consider the possibility of changes in instrument or film sensitivity.

The instrument sensitivity curve derived from a comparison of ATM and CALROC exposures is presented in Fig. 5.2. (Kjeldseth Moe and Nicolas (6) and Nicolas (7)). The logarithm of exposure, E , ($=It$) is plotted vs. wavelength. Absolute units on the ordinate scale are given in terms of the intensity, I , of the source in $\text{ergs cm}^{-2} \text{s}^{-1} \text{sr}^{-1} \text{Å}^{-1}$ required to produce an exposure of density 0.30 in 1 sec. Above 1500 Å the curve was derived from measurements of the continuum and also of emission lines from neutral and singly ionized atoms.

Below 1500 Å, only lines from neutral and singly ionized species were used (7).

In addition, the calibration curve has been modified to incorporate more accurate data obtained from a reflight of the CALROC instrument on Oct. 22, 1976. At that time, the argon arc had become available as a calibration source, and measurements of the arc intensity were made close to the date of flight, both before and after launch.

For photometry on the linear part of the film characteristic curve, as described in Sec. 5.3.1, the estimated accuracy of intensity measurements derived from the data of Fig. 5.2 is 50% rms. The uncertainties in the film characteristic curve, in the original deuterium lamp calibration, in the relative calibration with the argon arc, and in the transfer of the rocket calibration to the ATM instrument all contribute to the total error.

An independent calibration of the short wavelength ATM data has been published by Doschek, Feldman, VanHoosier, and Bartoe (8). They compared arbitrary continuum intensities obtained from the Skylab spectra with the absolute intensities at sun center in the quiet sun continuum published by Samain et al. (9). From the comparison they derived conversion factors to place their line intensities on an absolute scale. Their intensities thus converted to absolute values agree well with the spectral intensities derived from Fig. 5.2 between 1400Å and 1700Å. Above 1700Å the values agree to within a factor of 2, with Doschek et al. high by a factor of about 1.8 at 1900Å.

Below 1400Å, where the ATM continuum became too weak to measure, Doschek et al. made use of the reflectivity curve for the S082B instrument (10) for their determination of conversion factors. Absolute values for their intensities in this spectral range lie below the CALROC calibration by at most a factor of 2.

5.3 Photometry of S082B Spectra

All intensity measurements of the S082B data of NRL have been derived from specular density measurements of the film made with a Grant microdensitometer, operated under control of a PDP-8 minicomputer. Various members of the staff have developed individual methods and computer programs for reducing the data. Investigators analysing the spectra may wish to make collaborative arrangements to utilize this expertise.

5.3.1 Characteristic Curves

The film characteristic curves must be constructed from the flight exposures. The method consists of comparing film densities above fog level at exactly the same wavelengths on exposures taken with different exposure times but at the same pointing. Spectral features are selected to cover a wide range of intensities. Thus many sets of film densities vs. exposure are obtained. The curve of density vs. log exposure ($\log E$) is synthesized by sliding the many sets of points independently along the $\log E$ axis until a best fit to an average curve is obtained. The method assumes that a possible reciprocity failure is small and can be disregarded. The assumption is valid in general for exposure times within a factor of 10 of one another. Exposures farther apart must be investigated on an individual basis. The curve should be normalized to a standard position of $\log E = 0.00$ at $D = 0.30$ for a 1 sec exposure in order to make direct use of the absolute calibration data of Fig. 5.2, as described in Sec. 5.3.2 below.

Figure 5.3 shows two representative H&D curves developed in the above manner for the wavelength regions shorter and longer than 1400 Å. It was found from examination of small wavelength intervals throughout the spectral range that for these particular exposures, from one film batch and development run, there was a continuous transition in the slope of the quasilinear part of the characteristic curve with increasing wavelength. Other film batch and development runs have not always shown this.

In deriving the ATM characteristic curves, attention must be paid to the film batch number and development run. For this purpose the "Film Sequence Log" given in Appendix C lists each film strip or "plate," and the batch number of the film roll from which the strip was cut. Also included is the development run in which the film was developed. The characteristic curves may vary with each of these parameters. (See Sec. 4 for a discussion of the ATM film). For one batch and development run it is often possible to cover the range 1175-1960 Å with two curves, for wavelengths above and below 1400 Å, respectively. The shape of these characteristic curves is similar for a number of batch number and development runs, but can differ and should be examined. There is no "standard" characteristic curve.

Scatter of the data points about the final curves obtained using the above method varies considerably, depending to some extent on the spectral width of the band from which the points are selected. There is usually increased scatter at film densities below about 0.05 above fog level, the toe region of the curve, and also in the shoulder of the curve. Photometry in these ranges should be avoided, if at all possible.

5.3.2 Conversion to Absolute Intensity

The absolute intensity, I_{Abs} , for any exposure E , ($=It$), at any wavelength, λ , is found from the relationship

$$\log I_{\text{Abs}} (\lambda) = \log E_{\text{Abs}} (\lambda) - \log t + \Delta \log E_{\text{rel}}. \quad (5.1)$$

$\log E_{\text{Abs}}$ values are read from Fig. 5.2. Several of the values which make a convenient table for computer use have also been listed in Table 5.1. $\Delta \log E_{\text{rel}}$ is the log exposure correction required to take into account the actual measured density of the particular feature. It is read directly from the H-D curve which is normalized for $\log E = 0.0$ at $D = 0.3$. Exposure time is t .

To illustrate the method, Table 5.3 lists values for the long wavelength relative characteristic curve of Fig. 5.3. A film density of 0.4 at 1500 Å on an exposure of 10 sec would give an absolute intensity whose log is 4.891-1.000+0.238. The absolute intensity is then 1.35×10^4 ergs $\text{cm}^{-2} \text{ s}^{-1} \text{ sr}^{-1} \text{ Å}^{-1}$.

5.4 Slew Calibrations and Variations in the ATM Sensitivity Curve

Special calibration exposures under conditions as nearly identical as possible were programed during the Skylab missions to aid in evaluating the several instrumental parameters which were susceptible to variation with time. These include the absolute sensitivity of the film and the reflectivities of the optical surfaces. The exposures were programed every several days and were made with the ATM spectrograph pointed to a quiet region 300" inside the solar limb ($\mu = 0.73$). The instrument was slewed back and forth in a direction perpendicular to the slit length to average out fluctuations along the slit and thereby covered a quiet solar area of one square arc min. on a regular basis. Throughout the mission other exposures useful as checks on the absolute calibration were made at quiet region pointings 12" and 25" inside the limb, where instrumental stray light was low.

A listing of the slew exposures is given in Table 5.2, which is organized by film groups. Plates from a common film batch, roll, and development are listed together opposite columns containing the identification numbers of those parameters. Serial numbers of the plates containing slew exposures and the day of year date of the exposures are given opposite the group of plates within which they are found. A more detailed listing, which includes exposure frame and exposure time, is available among the Skylab documents at NRL.

C. Y. Yang, N. P. Patterson, and O. Kjeldseth Moe have made a thorough study of the slew exposures on 104 film (11). They found that the most consistent information was obtained from densitometer scans of continuum areas between 1914 and 1956A, which were almost completely free of scattered light. Scans of emission lines were difficult to evaluate because of variations in the amount of network cells or boundary areas included in the slewed region. Other difficulties encountered with the slew exposures involved the manual control of the exposures, with errors up to $\pm 1/4$ sec. at the beginning and end of an exposure. A "worst case" error was observed for 2 exposures taken on the same day by the same astronaut, differing in relative exposure by 44%. Three days later the same conditions registered a relative exposure difference of only 20%. A plot including the slew measurements from all missions shows that variations in exposure were within $\pm 25\%$, and that no significant degradation of the instrument or optics could be detected.

From Table 5.2 it may be noted that each of the cameras used with the S082B instrument contained film from only one batch, and that each camera contained a different batch. Although no differences in the slew calibrations were noted which might correlate to batch, roll, or development run, several investigators have noticed variations in D_{\max} and contrast when H-D curves have been plotted. It is therefore recommended that the absolute value of the sensitivity curve of Fig. 5.2 be checked at one or more wavelengths.

The absolute sensitivity curve can be checked by comparing absolute intensities derived from selected regions of slewed spectra closest to the spectra being interpreted with values contained in the CALROC spectral atlas published by Kjeldseth Moe et al. (3). From the comparison, a correction factor for Fig. 5.2 at one or more wavelengths can be obtained. Assuming that film sensitivity remains uniform with wavelength throughout the Skylab missions, the entire curve for Fig. 5.2 can then be shifted to match the corrected points. The best spectral regions to use for the comparison measurements lie above 1850A or below 1500A, where the first order stray light is minimum. (See Sec. 3.3 for a discussion of the stray light.) Above 1950A there is a mixture of continuum, absorption and emission features, while below 1500A, only emission lines are available. Although in principle only one region needs to be checked, it is useful to compare several in order to obtain an estimate of the error in calibration.

5.5 Curvature of Spectra

Both the ATM and the CALROC spectra are bowed along the dispersion, the ends of each spectrum line deviating several hundred micrometers from a tangent to the middle position. To ensure that the photometer slit always stays in the region of uniform exposure, densitometry of the spectra must be

performed in segments, or a computer program may be devised to control the scan automatically, the exact procedure depending upon the user's project.

5.6 Long Wavelength Calibration

No direct intensity calibration of the long wavelength range of the spectrograph was made. It was considered unnecessary, because the intensity distribution in the solar spectrum from 2000 to 3000A, approximately, is well known and is believed not to vary significantly with changing solar conditions.

The steps required to convert film density measured from a long wavelength spectrum to absolute units have been described by Doschek, Feldman, and Cohen (12). The conversion begins with the establishment of a characteristic curve for the film batch of interest, as described in Sec. 5.3.1 above. Relative intensities derived from the characteristic curve are then converted to absolute intensities by reference to one of several published solar atlases covering the spectral region, such as Tousey, et al. (1) 1974, or Broadfoot (2) 1972.

The major difficulty encountered in obtaining absolute values for the ATM data involves selecting the proper correction for limb darkening in order to relate to the values tabulated in the atlases, which apply to the radiation from the total sun. Doschek et al. made use of the value from Allen (13) for 2800A based on work by Bonnet (14). Depending upon the individual research problem, each investigator will undoubtedly select his own approach to this correction. The limb darkening function is by no means independent of wavelength in the UV. A forthcoming publication by Kjeldseth Moe and Milone (15) lists coefficients for limb darkening equations, derived as functions of from the ATM data.

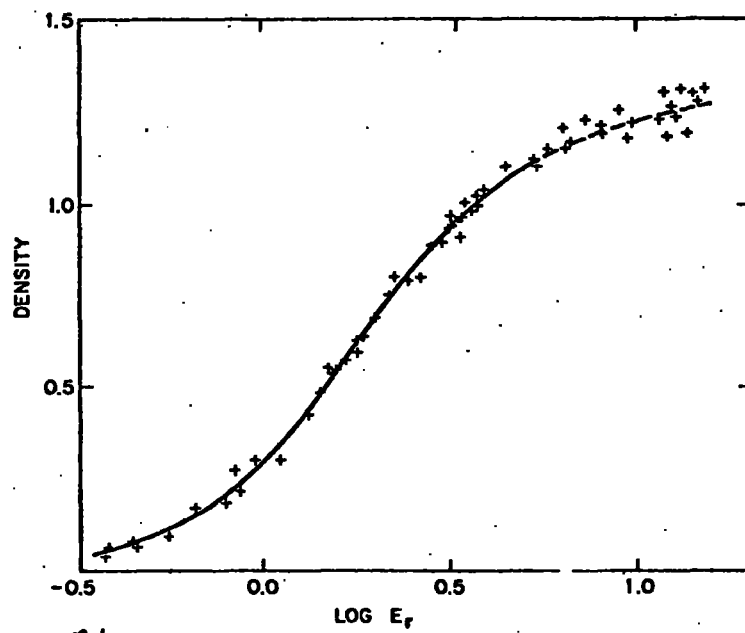
5.3 References

1. Tousey, R., E. F. Milone, J. D. Purcell, W. Palm Schneider, and S. G. Tilford, NRL Rept. 7788, 1974 "An Atlas of the Solar Ultraviolet Spectrum Between 2226 and 2992 Angstroms."
2. Broadfoot, A. Lyle, Ap. J. 173, 681-689, 1972, "The Solar Spectrum 2100-3200 A".
3. Kjeldseth Moe, O., M. E. VanHoosier, J.-D.F. Bartoe, and G. E. Brueckner, NRL Report 8056, 1976 "A Spectral Atlas of the Sun Between 1175 and 2100 Angstroms."
4. Bridges, J. M., and W. R. Ott, App. Optics, 16, 367-376, 1977. "Vacuum Ultraviolet Radiometry. 3: The Argon Mini-arc as a New Secondary Standard of Spectral Radiance".
5. Brueckner, G. E., J.-D. F. Bartoe, O. Kjeldseth Moe and M. E. VanHoosier, Ap. J. 209, 935-944, 1976, "Absolute Solar Ultraviolet Intensities and Their Variations with Solar Activity. I. The Wavelength Region 1750-2100 A."
6. Kjeldseth Moe, O. and K. R. Nicolas, Ap. J. 211, 579-586, 1977, "Emission Measures, Electron Densities and Non-thermal Velocities from Optically Thin UV Lines Near a Quiet Solar Limb."
7. Nicolas, K. R., Ph. D. Thesis, University of Maryland. 1977, "The Application of Si III Line Intensity Ratios to Determine the Solar Transition Zone Density and Pressure."
8. Doschek, G. A., U. Feldman, M. E. VanHoosier, and J.-D. F. Bartoe, Ap. J. Suppl. 31, 417-443, 1976, "The Emission-line Spectrum Above the Limb of the Quiet Sun: 1175-1940A."
9. Samain, D., R. M. Bonnet, R. Gayet, and C. Ligambert, Astr. and Ap. 39, 71-81, 1975, "Stigmatic Spectra of the Sun Between 1200A and 2100A."
10. Bartoe, J.-D. F., G. E. Brueckner, J. D. Purcell, and R. Tousey, Appl. Opt. 16, 879-886, 1977, "Extreme Ultraviolet Spectrograph ATM Experiment S082B."
11. Yang, C. Y., N. P. Patterson, and O. Kjeldseth Moe, private communication.
12. Doschek, G. A., U. Feldman, and Leonard Cohen, Ap. J. Suppl. 33, 101-111, 1977, "Chromospheric Limb Spectra from Skylab: 2000 to 3200A."

13. Allen, C. W., "Astrophysical Quantities" (London: Athlone) p. 172, 1973.
14. Bonnet, R., Ann. d'Ap. 31, 597, 1968.
15. Kjeldseth Moe, O. and E. F. Milone, submitted to Ap. J. Suppl., "Limb Darkening 1945A to 3245A for the Quiet Sun from Skylab Data."

Figure Captions

- Fig. 5.1 Example of film characteristic curve determined from the CALROC exposures. Crosses mark the observed points shifted along the exposure axis to form the best possible average curve, Kjeldseth Moe et al. (3).
- Fig. 5.2 Absolute calibration curve for ATM 104-type film. Prepared by Kjeldseth Moe and Nicolas (6) and (7).
- Fig. 5.3 Example of relative characteristic curves for one film batch and development run on ATM 104-type film.
- Fig. 5.3 (a) Wavelengths shorter than 1400 Å.
- Fig. 5.3 (b) Wavelengths longer than 1400 Å.



5.1
Fig. 3 — Example of film characteristic curve determined from the flight exposures. Crosses mark the observed points shifted along the exposure axis to form the best possible average curve.

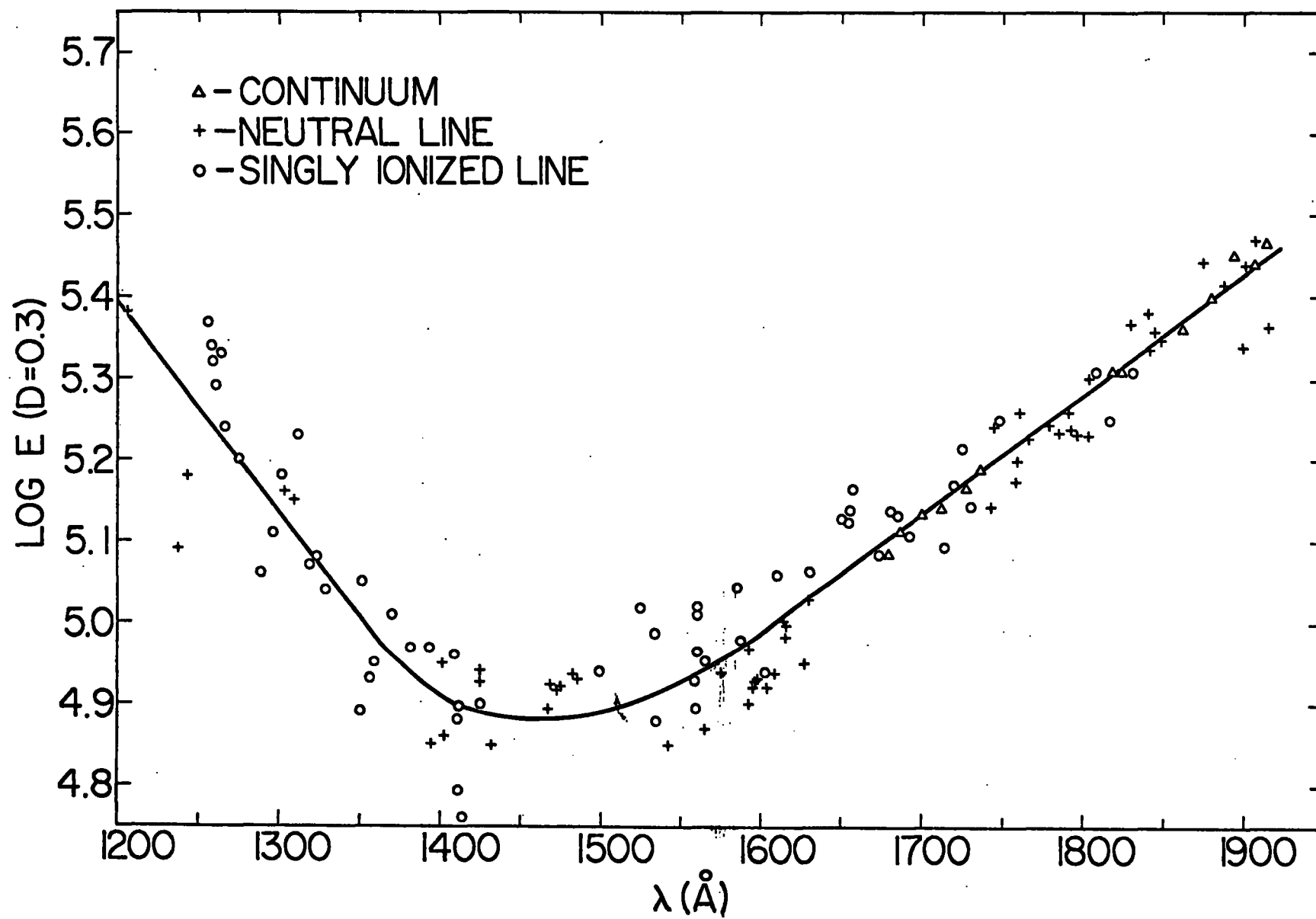


Fig. 5.2

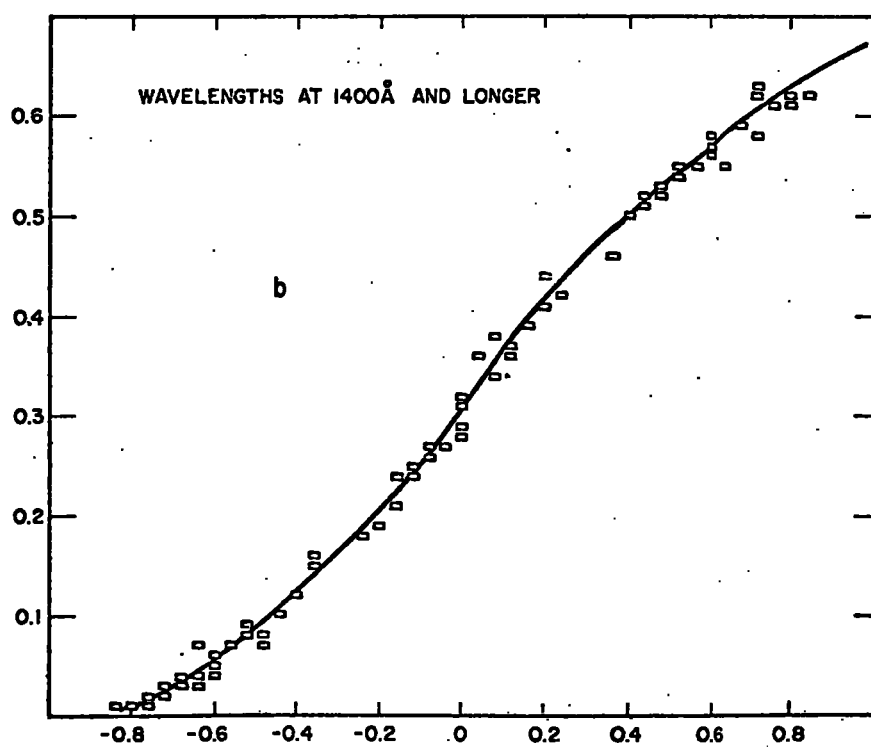
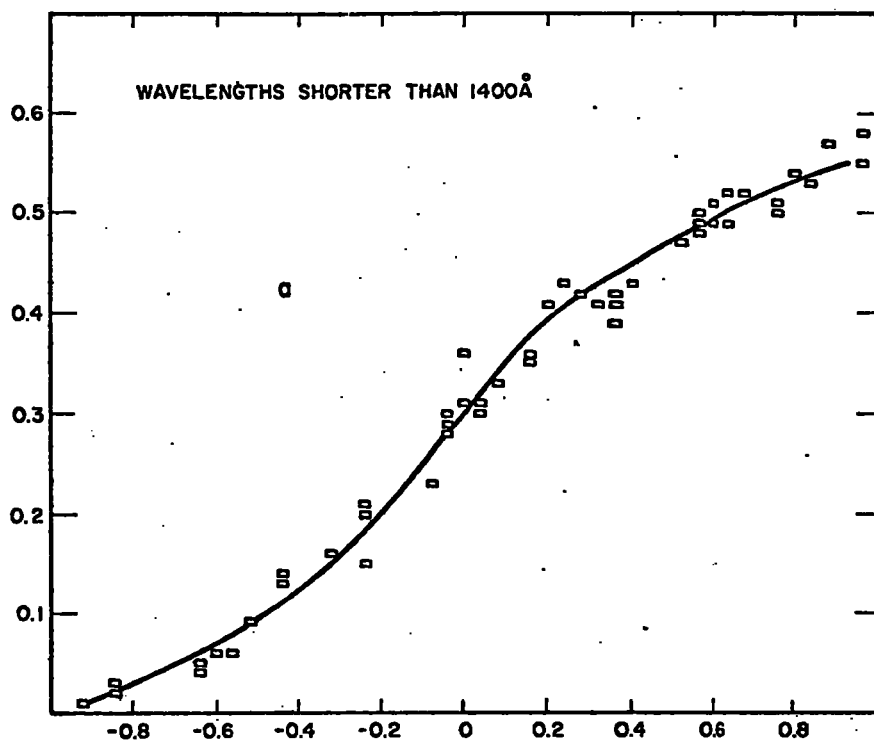


Fig 5.3

Table 5.1 Absolute Calibration of S082B Instrument (104 film)

Wavelength	Log E _{Abs} (D=0.3)
1160.0	5.497
1200.0	5.394
1206.0	5.379
1400.0	4.883
1450.0	4.884
1500.0	4.891
1514.0	4.900
1535.0	4.915
1557.5	4.935
1577.0	4.958
1600.0	4.989
1900.0	5.425
1960.0	5.512

Table 5.2 Data from Fig. 5.3 Characteristic Curve

Density	$\Delta \text{Log } E_{\text{rel}} (\lambda)$
0.000	0.954
0.020	0.835
0.040	0.729
0.060	0.633
0.080	0.548
0.100	0.472
0.150	0.316
0.200	0.196
0.250	0.095
0.300	0.000
0.350	0.106
0.400	0.238
0.450	0.412
0.500	0.643
0.520	0.755
0.540	0.879
0.560	1.017
0.580	1.170
0.600	1.338

Table 5.2 S082B Slew Exposures and Film History

<u>Mission</u>	<u>Plate No.</u>	<u>DOY</u>	<u>Slew</u> <u>Plate No.</u>	<u>Batch</u>	<u>Roll</u>	<u>DevRun</u>
SL-2 Camera B1	1B001			04	6A	3
	1B002			04	3	1
	1B003-1B018	150	1B011	04	7B	1
	1B019-1B041	153	1B035	04	8A	1
	1B042-1B078	153	1B061/2	04	8A	2
		157/158	1B075			
	1B079-1B081			04	7B	2
	1B082-1B103	161	1B083	04	7B	3
	1B104-1B107	162	1B106	04	7B	5
	1B108-1B142			04	7A	5
	1B143-1B177	164	1B145/6	04	7A	4
	1B178-1B182			04	7B	4
	1B183-1B201	167	1B192	04	7B	3
		168	1B194			
SL-3 Camera B2	2B001			06	3	1
	2B002			06	2	A
	2B003-2B021	220	2B014	06	2	1
	2B022-2B040			06	1	1
	2B041-2B080	225	2B057/8	06		
		225	2B064/5		1	2
	2B081-2B091			06	1	3
	2B092-2B103			06	2	3
	2B104-2B144	229	2B140	06	2	5
	2B145-2B150			06	2	4
	2B151			05(101)	3(101)	4
	2B152-2B184	231	2B171	06	3	4
		231	2B175			
	2B185-2B192			06	3	3
	2B193-2B201	233	2B194	06	2	3
		234	2B198/9			
		235	2B200			

Table 5.2 (Cont.) S082B Slew Exposures and Film History

<u>Mission</u>	<u>Plate No.</u>	<u>DOY</u>	<u>Slew</u> <u>Plate No.</u>	<u>Batch</u>	<u>Roll</u>	<u>DevRun</u>
SL-3 Camera B3	2B301-2B303	237	2B303	06	3	1
	2B304	237	2B304	05(101)	3(101)	1
	2B305-2B339	238	2B332/3	05	17	1
	2B340-2B341			05	17	2
	2B342-2B376	241	2B355/6/7	05	18	2
	2B377-2B380			05	17	2
	2B381-2B401	244	2B387	05	17	3
		244	2B391/2			
	2B402			05	17	5
	2B403-2B439	247	2B418/19	CALROC II	16	05
		247	2B426/7			
	2B440-2B479	249	2B446	05	16	4
		251	2B465			
		254	2B477			
	2B480-2B499	255	2B480/1	05	17	3
		257	2B483			
		258	2B488			
		260	2B492			
		262	2B498			
	2B500			05	17	A
	2B501			05	17	1
SL-4 Camera B4	3B001-3B017	333	3B004	08	8	4
	3B018-3B036	340	3B026/7	08	8	3
	3B037-3B047			08	8	1
	3B048-3B077			08	9	1
	3B078-3B100			08	9	2
	3B101-3B108			08	9	4
	3B109-3B123			10(101)	4	
	3B124-3B158	007	3B156/7	10(101)	4	5
	3B159-3B164	011	3B159/60	08	8	5
	3B165			08	8	1
	3B166-3B184	016	3B175	CALROC III	8	3
	3B185-3B201	030	3B200/01		8	2

The S082B flight film is kept in a secure area at the Naval Research Laboratory, Washington, D. C. Anyone who needs to perform an analysis from the original film should contact Dr. Richard Tousey, Code 7140, Principal Investigator, or Mr. Richard Schumacher, Code 7149, Program Manager.

Individual flight film strips are 35 x 250 mm in size and have been mounted for protection between 2 x 12 inch glass plates separated by thin brass spacers. Now referred to as "plates", all original material, consisting of 6408 spectra, has been copied at 1.8-times magnification onto 70-mm Kodak 2421 Aerial Duplicating roll film (Estar Base) and archived at the National Space Science Data Center (NSSDC). A 21-step wedge was also enlarged and photographed with the plates to enable the generation of transfer curves from flight film to users' copies. Members of the scientific community may obtain high quality fourth-generation positives and fifth-generation negatives from NSSDC (the flight film is considered first generation). Also available with these data are film catalogs on magnetic tape or microfiche and the "NRL/ATM User's Guide to Experiment S082B."

Figure 6.1 illustrates the photographic history of copies available for distribution to interested users. The master positive copy, produced at NRL, was used to make a contact working negative at NSSDC, and a working positive was then printed from the first working negative. Users' copies, as indicated, are then produced from the working copies. During the entire photographic procedure, care was taken to produce a high quality uniform product, and good quality control is exercised at NSSDC in the film processing. With multiple generation copies, however, there is some loss of fine detail in the fainter spectral exposures. It is expected that the copies will be useful primarily as intermediate negatives or positives from which prints can be made, or they can be used in various qualitative or survey-type investigations.

6.1 Photographic Procedures

In the duplication of the flight exposures it was found necessary to develop photographic equipment for the purpose. This equipment, the duplicating film, and the processing were selected to obtain optimum resolution, moderate grain compression on the copy film, and to retain the full density range of the data. In the enlarger, a 600W quartz lamp was used to obtain maximum resolution, acutance, and image contrast. This point light source was adjusted in position to minimize color fringing and parallax and to achieve best uniformity of illumination. The uniformity attained was found to be within +6% over the entire film plane. The lens was selected to minimize distortions and curvature of field.

Alignment of the system was achieved with a helium-neon autocollimating laser, using three-point control at the lens board and at the carrier for the film magazine. A vacuum back was used to hold the film flat at the enlarging surface.

The film was stored at 55° F until 24 hours prior to use and was refrigerated after exposure until time to be processed. These precautions were taken to minimize latent image loss and fogging of the film.

The plates were copied in small groups. At the beginning and end of each photographic session, the film was given a sensitometric exposure using a Kodak Process Control Sensitometer, Model 101. These frames reside on the film at NSSDC, and were used primarily to check the uniformity of film development from beginning to end of a particular group. A great amount of credit is due NSSDC in maintaining its processor control to such a degree that no significant differences could be measured from end to end in the various development runs.

The processor was a Kodak Model 11 Versamat with one rack, employing Hunt E. R. Aeroflo (Regular) developer at 85° F. The film was of one batch number and was processed to a gamma of 1.0. Sensitometric strips at NSSDC developed at intervals during the runs verified the gamma to a tolerance of about 0.02 as derived from measurements with a Macbeth Model TR524 densitometer (diffuse density).

6.2 Transfer Curves

Of more importance to a user who would attempt rough photometric use of the film is the 21 step Kodak calibrated wedge which was photographed with the copy camera at least once during each copy session at NRL. The film in the wedge conforms closely to the dimensions and granularity of the flight film and was mounted identically between glass plates of the same size and thickness as the S082B mounting plates. Table 6.1 is a listing of the various exposures, giving the location of a particular wedge whose exposure and general history matches a group of flight frames. The symbols in front of the plate numbers indicate a wedge image just prior to or just after that plate. For example, a wedge exposed and processed with plate number 2B148 will be found just before plate 2B146 and another just before plate 2B151 on the roll film. Although the wedge in front of 2B161 was processed at the same time, it was exposed nearer in time to plates 2B161 through 2B201, indicated by a semicolon dividing the groups in the table. Frequent use was made of the step wedge to insure evaluation of possible latent image loss or changes caused by differences in the development process which might occur from one group of exposures to another. In either case a transfer curve can be plotted

for any particular group of exposures by plotting step densities of the wedge listed in Table 6.2 against wedge densities measured from the users' copy.

Typical transfer curves derived from the wedge images are shown in Figs. 6.2 and 6.3. Figure 6.2 characterizes the master positive film archived at NSSDC. Diffuse densities of the copy were measured on a Macbeth Model TD 100A densitometer and are plotted against the Table 6.2 specular densities of the wedge itself, obtained with the the NRL precision Grant microdensitometer. Both specular and diffuse step densities of the wedge are given in Table 6.2. Specular density was used in this case in order to relate to the various phenomena measured on the flight film by members of the NRL data analysis team. Since most data of value fall between about 0.10 and 1.00 specular density units on the flight film, the copy data were deemed useful when the transfer curve was straight in that density range. As shown in Fig. 6.3, a good curve was also maintained for the user's generations of film, with D_{max} (diffuse) of about 1.8 for the Users' Positive and about 2.0 for the User's Negative. D_{min} values for the Positives and Negatives are 0.22 and 0.35 respectively.

6.3 Image Degradation

Mounted between glass plates holding the Kodak calibrated step wedge discussed in Section 6.2 were two precision resolution film targets of the standard Air Force 1951 type. One, a medium contrast target, had a contrast ratio of 6.3:1 for a density difference (ΔD) of 0.8 between the lines and the background. This condition is close to that of the S082B spectra, where D_{max} (specular), is about 1.0 and D_{min} about 0.1. An opaque line target on a clear background was selected to correspond with the negative spectral lines on the flight film. Resolution range of the target was one to 228 line pairs per mm.

The second target was high contrast, with a contrast ratio of 100:1 and $\Delta D = 2.0$ or higher. An exposure of both targets was obtained each time the wedge was photographed (Table 6.1). Plate 1B168 was also photographed at the beginning of each copy session to provide a standard by which to judge loss of spectral detail from generation to generation as subsequent contact prints were made.

Enlarged prints on Kodak polycontrast RC paper were made from each copy generation and the flight film, from in selected wavelength regions. Exposures were adjusted slightly to achieve approximately equal densities from each copy.

As could be seen from the enlarged paper prints, resolution was lost between the original film and the first copy. Compared with about 83 line pairs/mm resolution of the flight film, about 53 line pairs/mm could be resolved on the medium contrast targets of the copies. No significant differences among the copies up to 5th generation could be measured, except that slightly better resolution could be observed from the negative copy targets than with the positive copy targets. Slightly more resolution was lost in the high contrast targets, which averaged about 46 line pairs/mm.

6.4 Film Catalog

A complete listing of the S082B exposures, Appendix B, is contained in a microfiche catalog of 5 parts located in pockets attached to this Guide. Table 6.3 is a sample sheet showing the film or plate number (each plate contains 8 exposures), day of year date of exposure, time of shutter opening, exposure duration, and pointing information in yaw, pitch, and roll. The data were derived from binary coded decimal information projected onto a film chip attached to each S082B film strip. The time-of-day recorded by the diode array was mission elapsed time (MET) furnished by an ATM on-board computer. This computer time varied from Greenwich Mean Time (GMT) by as much as a few seconds and required periodic updates by ground command. The times listed in Appendix B have been corrected by the appropriate update information.

Pitch and yaw are given in arc sec, while roll is an arc min. For correct roll information, one must use the "Reconstructed Roll" referred to in several documents listed in Appendix A.

The column headed "off" gives the Pointing Reference System (PRS) limb offset in arc sec. A minus sign indicates a position on the solar disc. Fifty (50) indicates the PRS is off on in white light display state.

A zero (0) or one (1) in any one of the places in the "mode" 4 bit column had the following meanings:

Auto Step	X	X	X	X	0 = NRL bias not in
Auto			Flare		1 = NRL bias in

Errors that have been found to be diode array errors have been marked with a \$ symbol. An exception to this symbol is that minus (-) offset errors are corrected with a plus (+) and are the only plus marks found in the log.

It will be noted that 4 cameras were used to supply the film for the 3 manned missions. The cameras and film traceability information, including development runs, are listed in Appendix C, Film Sequence Log, described in Section 4.2 of this Guide. The cameras carried film strips of the following numbers:

<u>Camera</u>	<u>Film Strip or Plate No.</u>	<u>Mission</u>
1.	1B001 - 1B201	SL-1/2
2.	2B001 - 2B201	SL-3
3.	2B301 - 1B501	SL-3
4.	3B001 - 3B201	SL-4

Other listings of the data are contained in documents described in Appendix A, Skylab Documentation.

Exposure times available for the automatic and flare mode operation of SO82B are given in Tables 6.4 and 6.5, respectively. Normal exposures on the solar disc were those listed under the "Zone 1" column. Times shown should be accurate to within a millisecond.

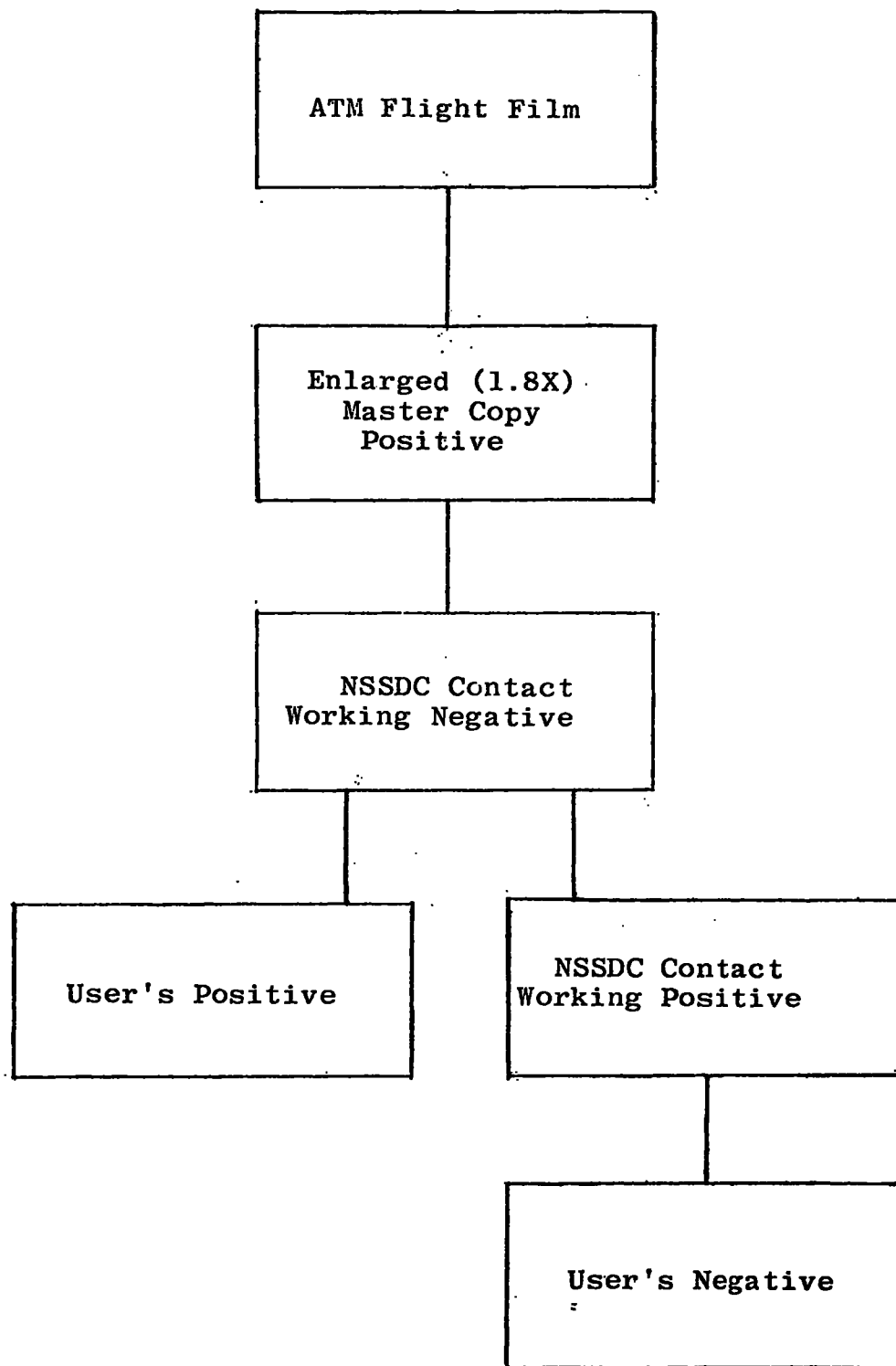


Fig. 6.1 — Duplication process for NRL/ATM photographic data

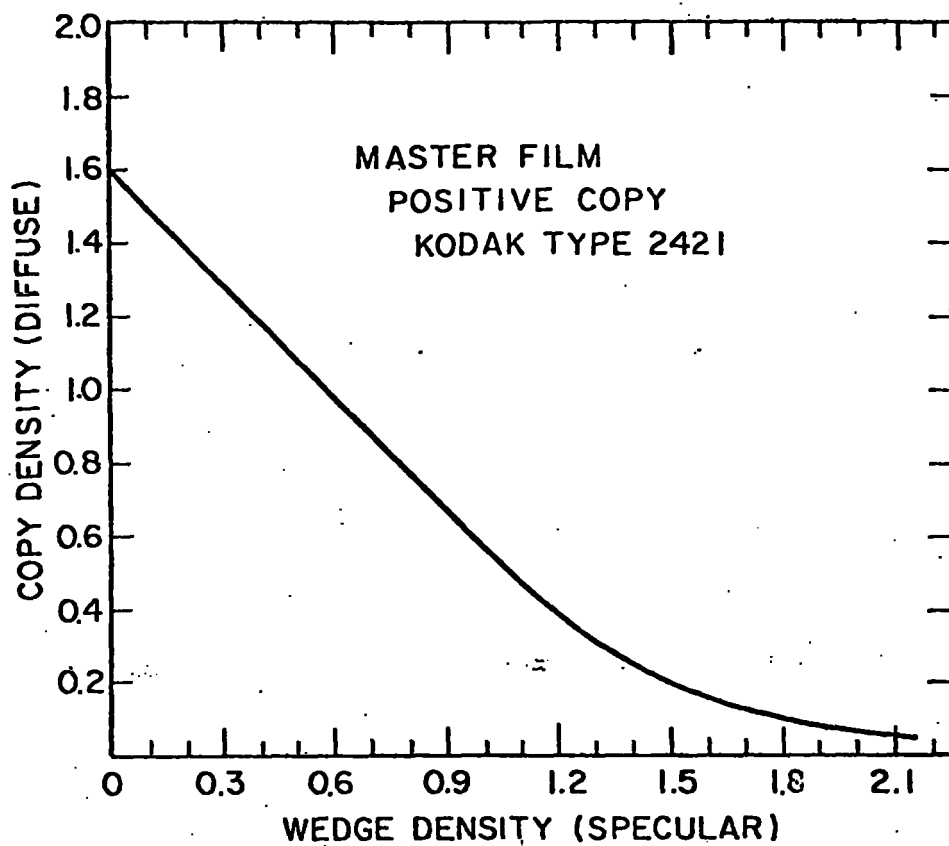


Fig. 6.2 — NSSDC archived master

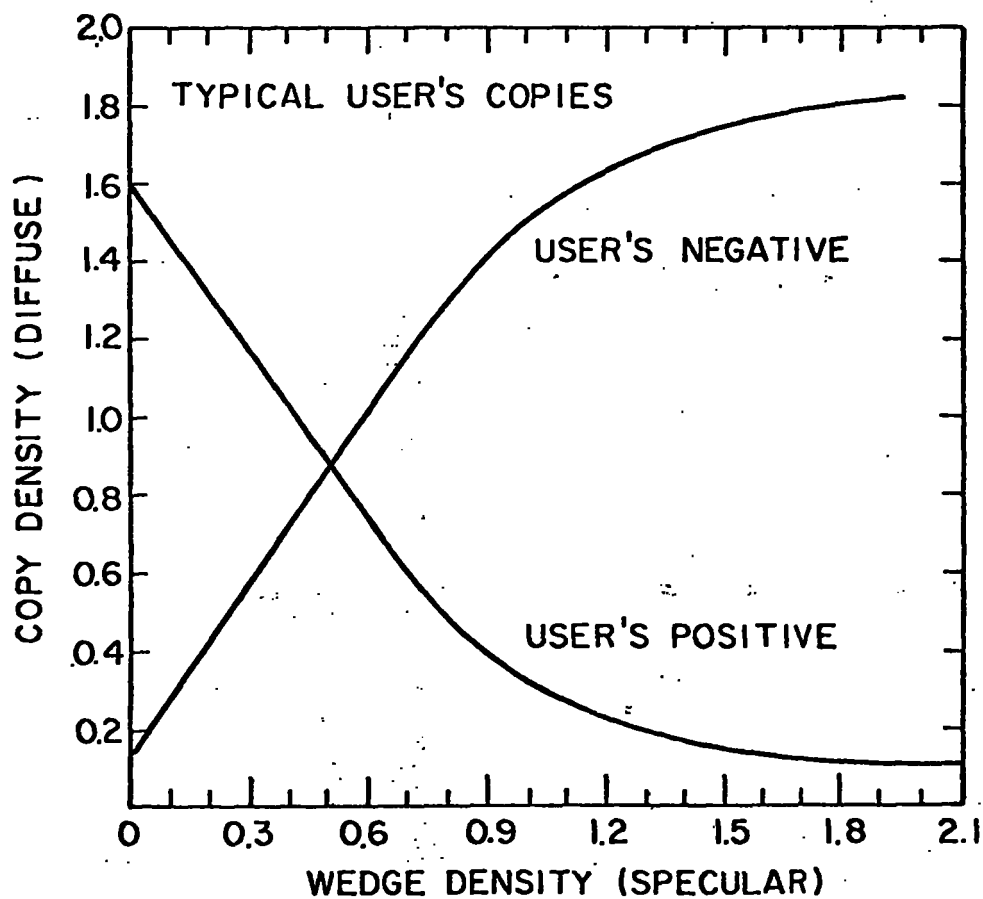


Fig. 6.3 — Transfer curves

Table 6.1 Location of Step Wedges Filmed with Groups of S082B Plates

Film Groups	Copy Roll*	Wedge Locations
1B001-1B015	2	<1B001, >1B015
1B016-1B030	2	<1B012, >1B030
1B031-1B080	3	<1B031, >1B080
1B081-1B140	3	<1B081
1B141-1B200	3	<1B141, >1B150, >1B165; <1B166, >1B200
1B201, 2B001-2B050	3	<1B201, >2B025, >2B050
2B051-2B100	3	<2B051; <2B076, >2B100
2B101-2B145	3	<2B101; <2B126
2B146-2B201	4	<2B146, <2B151; <2B161
2B301-2B350	4	<2B301, >2B350
2B351-2B400	4	<2B351, >2B400
2B401-2B444	4	<2B401, >2B440
2B445-2B501	4	<2B445, >2B501
3B001-3B095	4	<3B001, >3B025, >3B050; <3B051, >3B075
3B096-3B100	5	<3B096
3B101-3B125	5	<3B101, >3B125
3B126-3B201	5	<3B126; <3B151; <3B176; <3B201

* Copy film was Eastman Kodak type 2421, in 4 different rolls, all of same batch numbers.

< Exposure just prior to XBXXX plate

> Exposure just after XBXXX plate.

; Pause in exposure of plates just prior to next wedge listed.

Time lapse of 1 hour to overnight may exist between wedges.

STRIP NR	DOY	HR/MN/SEC	EXPTIME	YAW	PITCH	ROLL	OFF	MODE
2B121-1	228	18/38/14.75	0.25	-966.	-7.	10210.	50.	0101
2B121-2	228	18/38/17.00	10.00	-966.	-7.	10210.	50.	0101
2B121-3	228	18/38/28.75	1.25	-966.	-7.	10210.	50.	0101
2B121-4	228	18/38/32.00	40.00	-966.	-7.	10210.	50.	0101
2B121-5	228	18/39/13.75	5.00	-966.	-7.	10210.	50.	0101
2B121-6	228	18/39/20.75	160.00	-966.	-7.	10210.	50.	0101
2B121-7	228	18/42/ 2.50	20.00	-966.	-7.	10207.	50.	0101
2B121-8	228	18/50/18.25	359.50	-984.	0.	10143.	50.	0001
2B122-1	228	19/59/26.75	958.75	-969.	2.	10287.	25.	0001
2B122-2	228	20/17/48.00	602.25	-969.	22.	9497.	25.	0001
2B122-3	228	21/11/49.25	2.50	-944.	-31.	-7793.	-13.	1001
2B122-4	228	21/11/53.50	0.25	-944.	-31.	-7793.	-12.	1001
2B122-5	228	21/11/55.75	10.00	-944.	-31.	-7793.	-12.	1001
2B122-6	228	21/12/ 7.75	1.25	-944.	-31.	-7793.	-12.	1001
2B122-7	228	21/12/10.75	40.00	-944.	-31.	-7793.	-11.	1001
2B122-8	228	21/12/52.50	5.00	-944.	-31.	-7793.	-12.	1001
2B123-1	228	21/13/ 1.25	159.75	-944.	-31.	-7793.	-12.	1001
2B123-2	228	21/15/43.00	19.75	-944.	-31.	-7793.	-12.	1001
2B123-3	228	21/16/ 4.75	2.50	-944.	-31.	-7793.	-3.	1001
2B123-4	228	21/16/ 9.00	0.50	-944.	-31.	-7793.	-4.	1001
2B123-5	228	21/16/11.25	10.00	-944.	-31.	-7793.	-4.	1001
2B123-6	228	21/16/23.00	1.25	-944.	-31.	-7793.	-4.	1001
2B123-7	228	21/16/26.00	40.00	-944.	-31.	-7793.	-4.	1001
2B123-8	228	21/17/ 8.00	4.00	-944.	-31.	-7793.	-4.	1001
2B124-1	228	21/17/16.50	160.00	-944.	-31.	-7793.	-4.	1001
2B124-2	228	21/19/58.25	20.00	-944.	-31.	-7793.	-4.	1001
2B124-3	228	21/20/20.00	2.50	-944.	-31.	-7793.	-2.	1001
2B124-4	228	21/20/24.50	0.00\$	-944.	-31.	-7793.	-2.	1001
2B124-5	228	21/20/26.75	10.00	-944.	-31.	-7793.	-1.	1001
2B124-6	228	21/20/38.50	1.25	-944.	-31.	-7793.	-2.	1001
2B124-7	228	21/20/41.50	40.00	-944.	-31.	-7793.	-2.	1001
2B124-8	228	21/21/23.50	4.50	-944.	-31.	-7792.	-2.	1001
2B125-1	228	21/21/32.00	160.00	-944.	-31.	-7793.	-2.	1001
2B125-2	228	21/24/13.75	20.00	-944.	-31.	-7793.	-2.	1001
2B125-3	228	21/24/35.50	2.50	-944.	-31.	-7793.	0.	1001
2B125-4	228	21/24/39.75	0.50	-944.	-31.	-7793.	-1.	1001
2B125-5	228	21/24/42.00	10.00	-944.	-31.	-7793.	0.	1001
2B125-6	228	21/24/53.75	1.25	-944.	-31.	-7793.	-1.	1001
2B125-7	228	21/24/56.75	39.25	-944.	-31.	-7793.	0.	1001
2B125-8	228	21/25/38.75	5.00	-944.	-31.	-7793.	0.	1001

Table 6.3

STEP DENSITIES OF KODAK CALIBRATED WEDGE

Step	Density	
	Specular*	Diffuse+
1	.135	.12
2	.275	.22
3	.400	.32
4	.535	.42
5	.660	.51
6	.795	.61
7	.935	.71
8	1.06	.81
9	1.19	.91
10	1.32	1.00
11	1.44	1.10
12	1.58	1.20
13	1.72	1.30
14	1.84	1.39
15	1.99	1.50
16	2.09	1.58
17	2.21	1.68
18	2.35	1.78

* Measured with Grant Microdensitometer
 (above clear film step)

+ Kodak Calibration

Table 6.4 AUTO MODE EIGHT EXPOSURE SEQUENCE

Exposure Number	ZONE 1 Duration (Sec)		ZONE 2 Duration (Sec)		ZONE 3 Duration (Sec)	
	LW	SW	LW	SW	LW	SW
1	.312		2.5		4.0	
2		2.5		10.0		16.0
3	1.25		10.0		16.0	
4		10.0		40.0		64.0
5	5.0		40.0		64.0	
6		40.0		160.0		256.0
7	20.0		160.0		256.0	
8		160.0			640.0	1024.0
	253 Sec	4.2 Min	1076 Sec	17.9 Min	1714 Sec	28.6 Min

LW: Long Wavelength Range
SW: Short Wavelength Range

Zone 1: Sun Center to +1 arc sec or with PRS Off or in WL Display
Zone 2: +2 to +9 arc sec off limb and in Limb Scan or Limb PTG
Zone 3: +10 arc sec or greater off limb and in Limb Scan or Limb PTG
Moving from Zone 1 to Zone 2 increases exposure by factor of 4
Moving from Zone 2 to Zone 3 increases exposure by factor of 1.6

Table 6.5 SO82B FLARE MODE, 48 Exposure Sequence

(12.8 min)

<u>Exp No.</u>	<u>WL</u>	<u>Duration (Sec)</u>	<u>Exp No.</u>	<u>WL</u>	<u>Duration (Sec)</u>	<u>Exp No.</u>	<u>WL</u>	<u>Duration (Sec)</u>
1	S	0.312	17	S	0.321	33	S	1.250
2	S	1.250	18	S	1.250	34	S	5.000
3	S	5.000	19	S	5.000	35	S	20.000
4	S	20.000	20	S	20.000	36	S	80.000
5	S	0.312	21	L	0.156	37	L	0.156
6	S	1.250	22	L	0.625	38	L	0.625
7	S	5.000	23	L	2.500	39	L	2.500
8	S	20.000	24	L	10.000	40	L	10.000
9	S	0.156	25	S	1.25	2 min wait		
10	S	0.625	26	S	5.000	41	S	1.250
11	S	2.500	27	S	20.000	42	S	5.000
12	S	10.000	28	S	80.000	43	S	20.000
13	S	0.312	29	L	0.156	44	S	80.000
14	S	1.250	30	L	0.625	45	L	0.256
15	S	5.000	31	L	2.500	46	L	0.625
16	S	20.000	32	L	10.000	47	L	2.500
			2 min wait			48	L	10.000

7.0 OBSERVING PROGRAMS*

In support of the ATM experiments carried out from Skylab, a number of large and important programs of solar research were carried out from the ground, both by solar observations all over the world, and by experiments flown in rockets. In addition, a complex plan was developed for coordinating the individual Skylab observations, to optimize the return from each instrument and to produce the most valuable observations for solar physics. As a result, a large number of instruments covering the spectrum from the visible to x-rays were brought to focus on given solar targets, such as flares, and many times more data were acquired than could otherwise have been gathered. Thus, a massive attack was made on problems of solar physics during Skylab's nine months, which might well be called "the year of the sun".

7.1 The Joint Observing Program

The Joint Observing Program (JOP) was devised to make it feasible to use simultaneously the maximum number of instruments to produce the most valuable solar results. The key to accomplishing this was to plan the observations in a way that offered the best chance of contributing to the solution of the most important problems in solar physics. A list was drawn up that covered the problems which the ATM instruments were expected to be most likely to explain, such as the mechanism for transfer of energy through the solar atmosphere, or the trigger mechanism of solar flares and what goes on during flares. Observations relevant to each of these problems were listed, instrument by instrument. From this analysis, a set of JOP's was developed that came close to making use of every experiment during all the time allotted to ATM. There were many constraints because the observations desired for one instrument were often not compatible with those for another. The complex set of JOP's took the form of an illustrated manual containing detailed instructions for the operation of each JOP, of which there were 13 in SL-2. To implement the JOP's, a further subdivision into "building blocks" (BB), or elemental operational sequences, was required. There were 23 building blocks, which could be combined so as to carry out any of the JOP's. A small portion of this manual, actually about one percent, is reproduced in Figure 7.1.

*Material for this section has been extracted from a paper by R. Tousey, Applied Optics 16, 825, 1977, Apollo Telescope Mount of Skylab: an Overview".

In planning the JOPs during the mission, the prevailing solar conditions were first considered. Once decided between, for example, active regions, JOP-2, or limb scans, JOP-5, the building blocks were chosen to accomplish the particular JOP in the best way. Time blocks were controlled to one minute units, and since the time available per orbit was a maximum of 55 minutes, and often much less, the perfect fit was rare.

The JOP system worked so well in SL-2 that the number of JOP's was increased in the following missions, reaching 27 for SL-4. In addition, so much confidence in the crew was developed that by late SL-4 free time was given to them in substantial amounts for observing events of opportunity which appeared to be of interest - the so-called "shopping list". Appendix A of this Guide contains a description of the JOP Summary Sheets available at NRL as a reference document and an abbreviated listing of the JOPS for SL-3.

7.2 The Calibration Rocket Program - CALROC

Accuracy of calibration of instrumentation used in the extreme ultraviolet has always been a problem of extreme difficulty, yet its importance for solar research cannot be underestimated. Early in the ATM program it was proposed by HCO and by NRL that their instruments be calibrated by reference to carefully standardized instrumentation flown in rockets. One rocket flight per mission for each institution was the minimum acceptable because the sensitivity of the ATM instruments was expected to change during the course of the nine months over which they would be used. The fundamental idea was to make at the same time the same measurements of solar radiation using both the rocket-borne and the ATM instruments. The rocket instruments had been carefully and recently calibrated before flight. Therefore they could be used to "standardize" the sun so that it could serve as a standard source with which to calibrate the ATM instruments.

The plan of NRL was to fly instruments almost exactly like those of ATM but reduced in size by a factor of two. The Harvard CALROC instrument was designed in a similar fashion. NRL, together with BBRC and the Ames Research Center, developed a command system by which the instrumentation section, after separation from the booster, could be pointed at particular places on the sun. This was done by a radio command link, combined with a television system that permitted the PI on the ground to watch a display showing in real time the sun's image in H- α on the slit plate of the rocket instrument and the precise location of the slit on the sun.

The CALROC program required a great effort but the results proved to be highly successful. In addition to being essential for ATM, the project served also to provide for the scientific community in general vehicles of much greater sophistication for use in ongoing solar research than were available prior to Skylab.

Section 5 of this Guide deals with the calibration results from the program.

7.3 Solar Forecast Services

It was extremely important not only for planning purposes but also for making changes in near real time in the observing program being conducted by the ATM crewman to have up-to-the-minute information on solar activity. Although the crewman himself could observe changes in solar activity in real time, it was hardly possible for the crew to maintain the continuous monitoring of the sun necessary to detect all events because time was required for other activities and for sleeping. Monitoring on a 24 hour basis was done through the network of ground-based solar observatories maintained by the National Oceanic and Atmospheric Administration (NOAA) with support from the Air Weather Service and with information sent to them by other observatories all over the world.

NOAA solar forecasters were stationed in the ATM control center around the clock. They made an invaluable contribution by providing timely and complete knowledge of solar conditions to the ATM team who produced the detailed planning of the observing program, and also to the ATM science Czar in the ATM mission control center.

Complete information on the sun was made a matter of record by NOAA. All this material was distributed to each ATM PI after the completion of the mission for use in the interpretation of the data gathered by his solar instruments in ATM. Appendix A lists this data available among the reference material at NRL.

7.4 Skylab Associated Solar Programs

Many associated solar programs were carried on for the most part by ground-based observatories and to a lesser extent by space experimentation. The Coordinated Observing Program (COP) spearheaded by HCO, made continuously available by radio broadcast the observations actually being carried out by ATM together with those planned for the following day. This information was received by as many as 250 different groups located all over the world. Separate from this was the Skylab

ground-based astronomy program through which some eight or ten major observatories were funded to make specialized observations of a character closely related to the objectives of the ATM experiments. In addition, there was the ATM guest investigator program. This took the form of proposals from a large number of solar physicists and astronomers to provide post-mission relevant observational material or specialized interpretative skills in exchange for data gathered by ATM. In effect the guest investigator program was simply a large collection of agreements between collaborating scientists and PI's to share data. These various collaborative programs have proved to be most rewarding.

As a new experiment in collaboration, NASA, through the NSF and NCAR, has provided support for a series of Skylab Workshops which commenced in October 1975. These Workshops were organized by the High Altitude Observatory. The first was devoted to the study of coronal holes and the second dealt with the problem of explaining the flare mechanism.

Figure Captions

Fig. 7.1 A sample section from the volume that contained detailed instructions to the crew concerning the operation of the ATM instruments. The top section is the first step in JOP 2B, at the right are listed setup times (SU), operation times, and total elapsed times, in this case 44 min. The Building Blocks (BB) are shown in the lower left, and operation A-E are defined in the five columns. The sample H- α image shows suggested slit positions for S082B with the S055 square slit located at its center.

JOP 2B - ACTIVE REGIONS: Long Term Evolution - Disc (R<.9R₀)

Step	BB	Target	$\Delta T/\Sigma \Delta T$
(1)	4A	<ul style="list-style-type: none"> Roll 82A XUV dispersion clear of active region. Point 55 OFFSET so that 55 MAR covers most of active region. Record pointing coordinates RL+/- _____ U+/D- _____ L-/R+ _____. 	SU: 4 7/10
	B	<ul style="list-style-type: none"> Point Hα1 at a Hα bright point. Roll slit for uniform emission. Maximize DET 1 or 3. 	SU: 3 6/20
	C	<ul style="list-style-type: none"> Repeat B at a second Hα1 bright point. 	SU: 3 6/29
	D	<ul style="list-style-type: none"> Point Hα1 at a relatively dark Hα area. Roll 82B slit for uniform emission. 	SU: 2 5/36
	E	<ul style="list-style-type: none"> Pointing and roll same as 4A. Repoint 82B slit for uniform emission. 	SU: 2 6/44

BB4: SPATIAL AND SPECTRAL RESOLUTION.- BRIGHT FEATURES

TIME (Min)	31	26	21	16	11	6	1
BB SUBPART	A 55 OFFSET PTC	B H α 1 PTC	C H α 1 PTC	D H α 1 PTC	E 55 OFFSET PTC		
H α 1	2 FR/MIN						
X-RAY TELE 56	PATROL H	ACT 1 EXP H	ACT 1 EXP L				PATROL
XUV SPECT 82A	AUTO 1 WY EXP						
XUV SLIT 82B		AUTO	AUTO	AUTO	AUTO		
WLC 52							
SCAN SPECT 55A	HAR Det 1 Grt	GAS Det 1 Grt	GAS Det 1 Grt	GAS Det 1 Grt	HAR Det A11 Grt		
X-RAY SPECT 54	H 2 0 5 256	H 5 0 5 256	H 6 0 5 256	H 1 3 0 5 256	H 1 3 0 5 256		
TIME (Min)	0	5	10	15	20	25	30

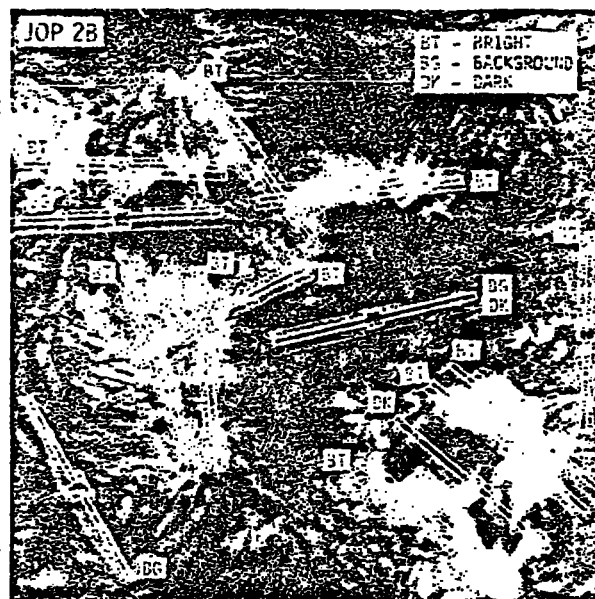


Fig. 2 A sample section from the volume that contained detailed instructions to the crew concerning the operation of the ATM instruments. The top section is the first step in JOP 2B, at the right are listed setup times (SU), operation times, and total elapsed times, in this case 44 min. The Building Blocks (BB) are shown in the lower left, and operations A-E are defined in the five columns. The sample H- α image shows suggested slit positions for S082B with the S055 square slit located at its center.

8.0 SPECTRAL ATLAS*

Atlases of the solar ultraviolet radiation have been presented for the wavelength region 2226 - 2992 Å by Tousey et al. (1) and for the region 2988 - 3629 Å by Brueckner (2). However, correspondingly complete information on line profiles and continua with good spectral resolution and reliable calibration of absolute intensity have not been published for wavelengths below 2226 Å. Data from the CALROC program, which had good absolute intensity calibration, have been used to compile "A Spectral Atlas of the Sun between 1175 and 2100 Å". This Atlas is available in three forms: an 8x10 inch document, NRL Report 8056; a 12x21 inch hardbound volume, NRL Report 8057; and magnetic computer tapes, World Data Center - A for Rockets and Satellites identification number RS-12A.

The atlas presents the absolute intensity of two quiet regions, one located 300" inside the solar limb ($\cos \theta = 0.73$) and representative of the spectrum of most of the disk. The other quiet region is located 50" inside the limb ($\cos \theta = 0.32$) and is more representative of a limb spectrum. In addition, the spectrum of active region McMath 508 is presented for wavelengths longer than 1680 Å. The logarithm of the specific intensity in $\text{erg cm}^{-2} \text{s}^{-1} \text{sr}^{-1} \text{Å}^{-1}$ is plotted vs wavelength in Angstroms. The spectra of the quiet regions and the active region are plotted above each other on the same page. This facilitates comparison of details in the three types of spectra. The wavelength axis is marked in .1Å intervals and logarithmic intensity levels are labeled in .10 intervals.

For wavelengths below 1400 Å only isolated emission lines are displayed. The continuum between lines is too weak to be recorded even with the longest exposure times (see Table 8.1). For wavelengths below 1200 Å only the emission lines at the limb position (50") are shown; the corresponding spectral features on the disk (300") fall below the detection limit. The active region spectrum is shown only at wavelengths above 1680 Å because exposure conditions during flight did not permit reliable calibration for shorter wavelengths.

Information on the exposures used to prepare the Atlas is given in Table 8.1. For the exposures at 50" inside the limb and in the active region, the full spatial resolution of the instrument (2" by 60") was used. During the

*Material for this section has been obtained from NRL Report 8056, (1976) "A Spectral Atlas of the Sun Between 1175 and 2100 Angstroms", by O. Kjeldseth Moe, M. E. VanHoosier, J.-D. F. Bartoe, and G. E. Brueckner

exposures at 300" inside the limb the slit was moved back and forth perpendicular to its length, covering an area of about 60" by 60" on the solar disk. This was done to average the inhomogeneous solar emission associated with the chromospheric network.

The quiet solar regions were selected carefully to avoid any solar activity, coronal holes, or filament channels. In the case of the active region 90% of the slit was covered by the plage. Figure 8.1 is a detailed drawing of the location of the spectrograph slit inside the plage.

Intensity calibrations for the Atlas were made as described in Section 5 of this Guide. The scans presented in the atlas were smoothed by removing high-frequency noise in the film emulsion and photometry using a Fourier filtering technique described by Nicolas et al. (3) A low-frequency component caused by grain clumps in the emulsion of size 10 μ m could not be removed by filtering without degrading the effective instrumental width. These grain clumps may distort slightly the intensities and profiles. Broadening caused by the instrument profile has not been removed from the atlas spectra, because the shape of the instrument profile is not known in enough detail. Furthermore, the low-frequency noise component still present in the data may cause strong distortions if deconvolution is attempted. One may estimate the line widths from

$$\Delta \lambda_T \approx (\Delta \lambda_o^2 - \Delta \lambda^2)^{\frac{1}{2}}$$

? where $\Delta \lambda_o$ is the observed line width, $\Delta \lambda$ the instrumental width, and $\Delta \lambda_T$ the true width of the line profile.
 ? Theoretical calculations using a ray-tracing method gave a constant instrumental width of 0.055 Å for all wavelengths between 1200 and 2100 Å. This should be regarded as a lower limit since the effect of the film emulsion has not been taken into account. From the width of the narrowest emission lines in the spectrum, it seems more likely that the effective instrumental width is 0.07 Å.

The Ly α line presented a special problem. On the 1974 CALROC flight this line became seriously overexposed in the line core, even for the shortest exposure times at the 50" and 300" pointings. The central region (1 Å wide) of the line was therefore omitted from the atlas. Fig. 8.2 is a sample page from the Atlas. The high resolution spectra presented have been compared with results obtained by others in order to evaluate the reliability of the absolute intensities. In so doing, care was taken to deresolve the CALROC spectra to fit the lower resolution of the other investigators. The agreement is illustrated in Fig. 8.3, showing the mean intensity of the sun averaged

over 10 Å intervals as given by various observers. For this figure the Atlas intensities at 300" inside the limb were converted to solar mean intensities using the center-to-limb variations given by Samain et al. (4). All the intensities agree within the Atlas error limit of + 25%. A separate publication is being prepared listing the intensities averaged over wavelength intervals ranging from 0.1 to 10.0 Å bandwidths.

8.1 References

1. R. Tousey, E. F. Milone, J. D. Purcell, W. Palm Schneider, and S. G. Tilford, "An Atlas of the Solar Ultraviolet Spectrum Between 2226 and 2992 Angstroms," NRL Report 7788, 1974.
2. G. Brueckner, Photometric Atlas of the Near Ultraviolet Solar Spectrum 2988 A-3629 A, Vandenhoeck and Ruprecht, Gottingen, 1960.
3. K. R. Nicolas, G. E. Brueckner, R. Tousey, D. A. Tripp, O. E. White, and R. G. Athay, submitted to Solar Physics (1977). *published(?) 1974*
4. D. Samain, R. M. Bonnet, R. Gayet, and C. Lizambert, Astron. Astrophys. 39, 71 (1975).
5. D. Samain and P. C. Simon, to be published in Solar Physics, (1977).
6. G. J. Rottman, Trans. Amer. Geophys. Union 56, 1157 (1974).
7. L. Heroux and R. A. Swirbalus, J. Geophys. Res. 81, 436 (1976).

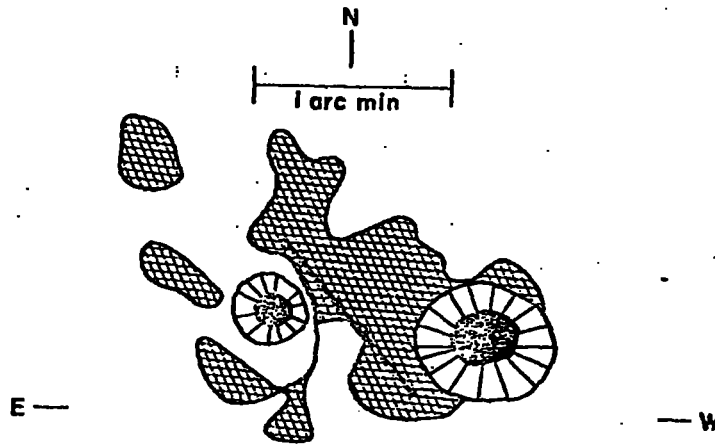
Figure Captions

Fig. 8.1 Position of the spectrograph slit inside active region McMath 508 on September 4, 1973.

Fig. 8.2 Sample Atlas Page

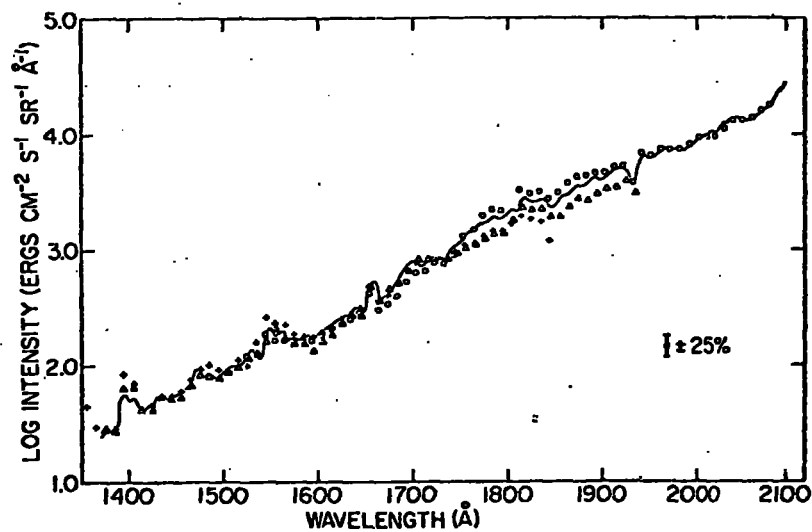
Fig. 8.3 Comparison of solar mean intensities averaged over 10 Å intervals. The full line represent the NRL CALROC data used in the atlas. Open circles are the observations of Samain and Simon (5) crosses the observations of Rottman (6), and triangles the observations of Heroux and Swirbalus (7).

~~Fig. 8.4 Sample page from Atlas.~~



8.1
Fig. 3 — Position of the spectrograph slit inside active region
McMath 508 on September 4, 1973.

Fig 8.3. Sample Atlas page



8.3
Fig. 3 — Comparison of solar mean intensities averaged over 10 Å intervals. The full line represent the NRL CALROC data used in the atlas. Open circles are the observations of Samain and Simon [10], crosses the observations of Rottman [6], and triangles the observations of Heroux and Swirbalus [7].

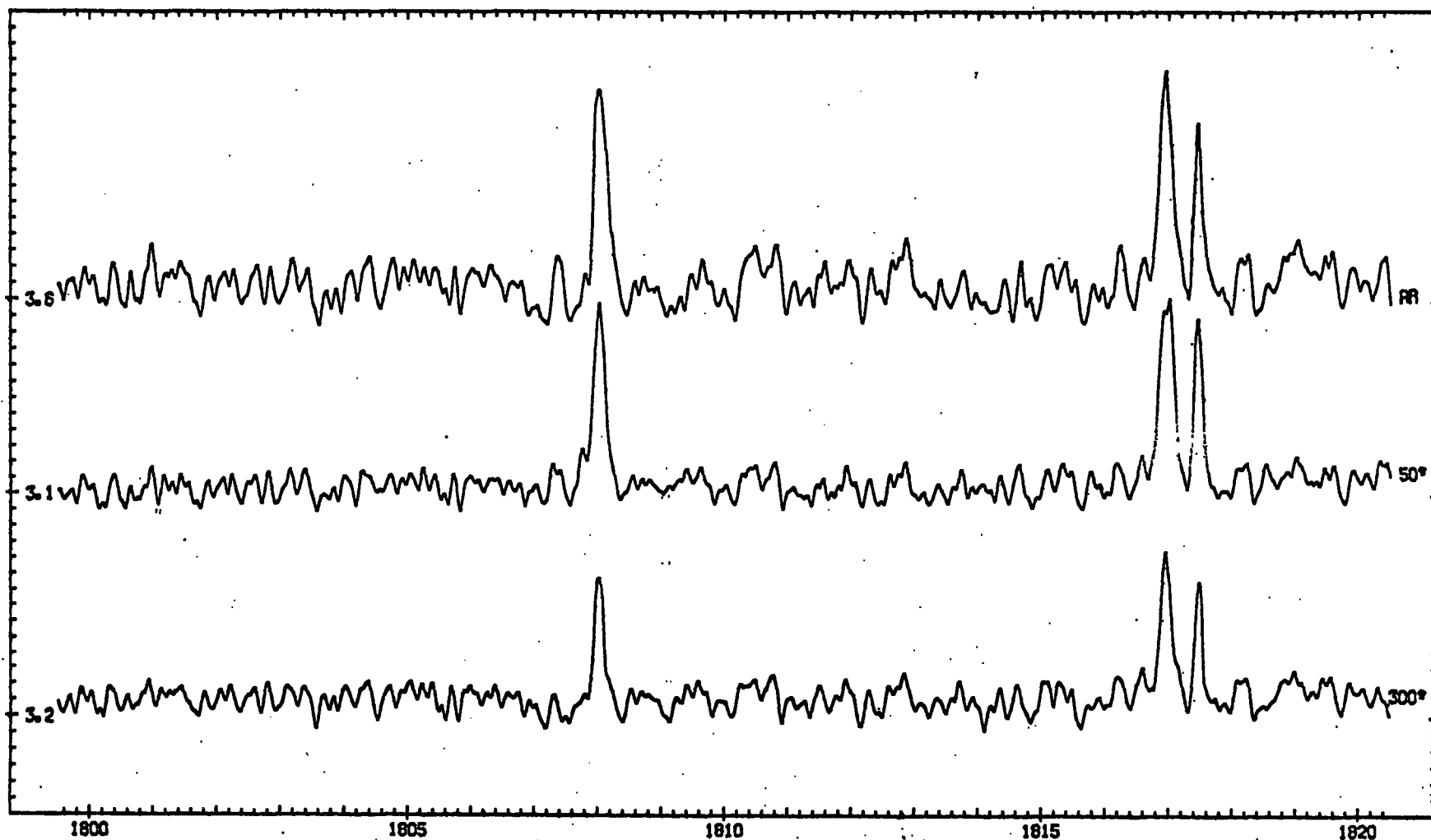


Fig 8.2 Sample page from atlas. (To be selected - probably not this one).

8.1
Table 3 — Data for Exposures Used to Make the Atlas

Date	Target	Exposure Time (s)	Altitude at Start of Exposure (km)
Sept. 4, 1973	Active Region	5.45	120.4
	McMath 508	1.07	111.3
Jan. 15, 1974	300" ± 30"	55.45	174.0
		1.95	218.7
		9.45	220.1
		31.45	224.8
		39.45	234.2
	50"	3.45	230.6
		9.45	227.4
		111.45	225.9

APPENDIX A. Skylab Documentation*

(1) NRL/ATM Exposure Catalog

Vol. I (Rev A) Time Listing
Vol. II (Rev A) Joint Observing Program Listing
Vol. III (Rev A) Target Listing

These three volumes list the time, JOP, step and building block, the target, exposure time and wavelength band of each S082A (and S082B) exposure. They also include notes identifying special events, sequences and pointings.

(2) NRL/ATM Mission Engineering Data Book (Rev A)

This catalog (one volume for each of the four S082B cameras) lists: the opening and closing time of the camera shutter for each exposure and the corresponding exact exposure time, wavelength band, and instrument operating mode; other instruments operating at the time, and their modes; and a verification of correct temperatures throughout the S082B instrument during the exposure.

For each exposure, the values are also given for the reconstructed ("correct") ATM roll position, ROLL or Γ_{RR} , the maximum excursion of any disturbance in the ATM pointing position during the exposure, the S082B BIAS, the beta angle of the Skylab orbit, the altitude of the Skylab and its line of sight to the sun, and the orbit number.

This catalog also includes traceability charts for each film strip, the temperature and radiation histories of each camera, and transmission curves and pinhole maps for each aluminum filter.

(3) ATM Mission Operation Log (Vols. 1-5, and magnetic tape)

This catalog, prepared for S055, lists the time, pointing, operating modes and other information, for all observations by every ATM instrument (S052, S054, S055, S056, S082A, S082B and H α 1).

It should be noted that the ATM roll position values throughout this catalog are not the reconstructed ("correct") values.

(4) User's Guide for Reconstructed Roll Reference (Γ_{RR})

* This Appendix was prepared by N. Paul Patterson, Ball Brothers Research Corporation.

- (5) Reconstructed Roll Reference Data (6 vols.)
- (6) Roll Reference Determination Summary Report
- (7) Skylab Apollo Telescope Mount Pointing Reference Handbook

The first three of these documents provide information from which a user can determine the correct value of the ATM roll position ($\Gamma_{RR} = \text{GAMMARR} = \text{EXP ROLL} = \text{ROLL}$), and ascertain its uncertainty ($\sim +40$ arc-min). The roll value corresponds to the angle, in arc-min, between solar north and the UP pointing axis of the ATM (parallel to the axis of the S082B slit, and at right angles to the S055 raster lines). The error and uncertainty of the telemetered values developed as a result of the failure of the star-tracker roll reference during the mission.

The pointing bias required to coalign the center of the S082B slit with the ATM fine sun-sensor, and its variation over the mission is discussed in the fourth document.

- (8) ATM JOP Summary Sheets (with Shopping Lists), SL 1/2, SL-3, SL-4.

This set of documents consists of copies of plastic sheets used by the astronaut operating the ATM control panel. These sheets, with guidelines for their use in each of the JOPs, provided explicit, self-contained, step-by-step instructions for pointing and operating the ATM experiments in unison. Photographic examples of solar features, and abbreviated descriptions of desired pointings are shown together with various combinations ("Building Blocks") of simultaneously operated instrument modes. Each sheet summarized all the information needed by Skylab crews and solar scientists to coordinate observations with the daily scientific objectives. A schedule was telemetered every morning to the crews, which gave suggestions for observations and operating modes, and guidelines for responding to flares and other interesting events.

The sheets evolved through an iterative process, during many months of practice on the ATM simulator, and much discussion in meetings between scientists representing the ATM experimenter groups. The sheets changed from one manned phase to the next. New JOPs were added, a few were dropped, and the operating strategies were made more efficient and flexible. JOP and step numberings are therefore not always the same from one mission to another. A simplified listing of Joint Observing Programs for SL-3 follows:

JOP 1	Chromospheric Network	JOP 10	Lunar Libration Clouds
JOP 2	Active Regions	JOP 11	Chromospheric Oscillations and Heating
JOP 3	Flares	JOP 12	Calibrations
JOP 4	Prominences	JOP 13	Night Sky Objects
JOP 5	Constant Latitude Studies	JOP 14	Eclipse (deleted for SL-3)
JOP 6	Synoptic Observations	JOP 15	Coronal Holes
JOP 7	Atmospheric Extinction		
JOP 8	Coronal Transients	JOP 16	Disk Transients
JOP 9	Solar Wind	JOP 17	Bright Points

Because of the formality of the NASA mission protocol which regulated the implementation of the JOP programs, a sheet of informal "Shopping List" items was included on each of the last two manned phases. These provided the astronaut with a list of pet projects for each of the experimenter groups, that he could conduct at his discretion when time was available.

(9) ATM Experiments Reference Book (SL 1/2, SL-3, SL-4)

This document is a copy of a book used as a training text and carried on board Skylab for crew reference during each manned phase. It provides a detailed discussion of the background, rationale and scientific objectives of each of the JOPs. Specific terms are defined, and photographs are given of features as they would appear in H and XUV emissions. Graphs and tables of filter transmissions, detector positions of XUV lines, and other information useful to the ATM operator are included. In addition, technical data is included on each of the ATM instruments and monitors, as well as teleprinter abbreviations, and ATM scheduling conventions.

(10) NOAA/Skylab Solar Data Books

Several dozen loose-leaf volumes containing copies of the solar photographs and data provided ATM experimenters by NOAA during the Skylab mission.

(11) Skylab ATM H-Alpha Atlas, and Atlas Guide (49 vols.)

Copies of photographs taken by the H α telescope on ATM (H α 1). A print is included with a scale of 2 arc-min per inch, for the beginning and end of each orbit, for each significant ATM pointing change, and, when no pointing change occurred, at 15 minute intervals, for the entire Skylab mission.

(12) NRL Science Console Execution Log Books

Roughly two dozen loose-leaf volumes containing information pertinent to the operation of NRL's two instruments on the ATM, logged in real-time by NRL representatives who manned consoles in the mission control center round-the-clock. These logs contain summary charts of the orbits in which the ATM was operated, and the as-flown schedule of ATM operations relative to orbital sunrise and sunset. Of particular value to users of S082B data, are notes of crew-reported solar events, operating errors, and special observations with the S082B instrument.

(13) Skylab Astronaut-Ground Voice Transcripts

This is a complete set of all voice communication between the Skylab astronauts and the ground, of both live conversations and comments taped on an onboard recorder and dumped. In addition, a set of transcripts is available edited for ATM-related communications.

(14) Skylab Operational Handbook, (Vol. I and II)

Detailed diagrams of ATM instruments, as well as the ATM, and the checklists of their operating procedures.

Appendix C*

Camera No B1 SL 1/2
Sequence Log

ATM No	Film Roll	Strip Cut	Dev Run	ATM No	Film Roll	Strip Cut	Dev Run	ATM No	Film Roll	Strip Cut	Dev Run	ATM No	Film Roll	Strip Cut	Dev Run
1B001	6A-3		3	1B051	8A-40			1B101	7B-11			1B151	7A-33		
1B002	3		1	1B052	8A-41			1B102	7B-10			1B152	7A-32		
1B003	7B-62			1B053	8A-42			1B103	7B-09			1B153	7A-31		
1B004	7B-63			1B054	8A-43			1B104	7B-8			1B154	7A-30		
1B005	7B-64			1B055	8A-44			1B105	7B-7			1B155	7A-29		
1B006	7B-65			1B056	8A-45			1B106	7B-6			1B156	7A-28		
1B007	7B-66			1B057	8A-46			1B107	7B-5			1B157	7A-27		
1B008	7B-67			1B058	8A-48			1B108	7A-80			1B158	7A-26		
1B009	7B-69			1B059	8A-49			1B109	7A-79			1B159	7A-24		
1B010	7B-70			1B060	8A-50			1B110	7A-78			1B160	7A-23		
1B011	7B-71			1B061	8A-51			1B111	7A-77			1B161	7A-22		
1B012	7B-72			1B062	8A-52			1B112	7A-76			1B162	7A-21		
1B013	7B-73			1B063	8A-53			1B113	7A-75			1B163	7A-20		
1B014	7B-74			1B064	8A-54			1B114	7A-74			1B164	7A-19		
1B015	7B-75			1B065	8A-55			1B115	7A-73			1B165	7A-18		
1B016	7B-76			1B066	8A-56			1B116	7A-72			1B166	7A-17		
1B017	7B-77			1B067	8A-57			1B117	7A-71			1B167	7A-16		
1B018	7B-78			1B068	8A-59			1B118	7A-69			1B168	7A-14		
1B019	8A-5			1B069	8A-60			1B119	7A-68			1B169	7A-13		
1B020	8A-6			1B070	8A-61			1B120	7A-67			1B170	7A-12		
1B021	8A-7			1B071	8A-62			1B121	7A-66			1B171	7A-11		
1B022	8A-8			1B072	8A-63			1B122	7A-65			1B172	7A-10		
1B023	8A-9			1B073	8A-64			1B123	7A-64			1B173	7A-9		
1B024	8A-10			1B074	8A-65			1B124	7A-63			1B174	7A-8		
1B025	8A-11			1B075	8A-66			1B125	7A-62			1B175	7A-7		
1B026	8A-12			1B076	8A-67			1B126	7A-61			1B176	7A-6		
1B027	8A-13			1B077	8A-68			1B127	7A-60			1B177	7A-5		
1B028	8A-14			1B078	8A-70			1B128	7A-58			1B178	7B-37		
1B029	8A-16			1B079	7B-35			1B129	7A-57			1B179	7B-36		
1B030	8A-17			1B080	7B-34			1B130	7A-56			1B180	7B-35		
1B031	8A-18			1B081	7B-33		2	1B131	7A-55			1B181	7B-34		4
1B032	8A-19			1B082	7B-32		3	1B132	7A-54			1B182	7B-33		4
1B033	8A-20			1B083	7B-31		4	1B133	7A-53			1B183	7B-32		4
1B034	8A-21			1B084	7B-30			1B134	7A-52			1B184	7B-31		4
1B035	8A-22			1B085	7B-29			1B135	7A-51			1B185	7B-30		
1B036	8A-23			1B086	7B-28			1B136	7A-50			1B186	7B-29		
1B037	8A-24			1B087	7B-27			1B137	7A-49			1B187	7B-28		
1B038	8A-26			1B088	7B-26			1B138	7A-47			1B188	7B-27		
1B039	8A-27			1B089	7B-24			1B139	7A-46			1B189	7B-26		
1B040	8A-28			1B090	7B-23			1B140	7A-45			1B190	7B-25		
1B041	8A-29		1	1B091	7B-22			1B141	7A-44			1B191	7B-24		
1B042	8A-30		2	1B092	7B-21			1B142	7A-43		5	1B192	7B-23		
1B043	8A-31		4	1B093	7B-20			1B143	7A-42		4	1B193	7B-22		
1B044	8A-32			1B094	7B-19			1B144	7A-41		1	1B194	7B-21		
1B045	8A-33			1B095	7B-18			1B145	7A-40			1B195	7B-20		
1B046	8A-34			1B096	7B-17			1B146	7A-39			1B196	7B-19		
1B047	8A-35			1B097	7B-16			1B147	7A-38			1B197	7B-18		
1B048	8A-37			1B098	7B-14			1B148	7A-36			1B198	7B-17		
1B049	8A-38			1B099	7B-13			1B149	7A-35			1B199	7B-16		
1B050	8A-39			1B100	7B-12			1B150	7A-34			1B200	7B-15		
												1B201	6A-2		3

Film	Data
Roll No	Film Type
7A	104-06-04
7B	104-06-04
8A	104-06-04
6A	104-06-04
3	101-06-04

* Appendix C compiled at NRL by Warren H. Funk.

Camera No. B2

Sequence Log

ATM	Film	Dev	ATM	Film	Dev	ATM	Film	Dev	ATM	Film	Dev
No.	Roll	Strips	No.	Roll	Strips	No.	Roll	Strips	No.	Roll	Strips
2B001	3	1	2B051	1-49		2B101	2-47		2B151	2-101	
2B002	2-25	A	2B052	1-47		2B102	2-48		2B152	3-5	
2B003	2-24	1	2B053	1-46		2B103	2-49	3	2B153	3-6	
2B004	2-23		2B054	1-45		2B104	2-50	5	2B154	3-7	
2B005	2-22		2B055	1-44		2B105	2-51		2B155	3-8	
2B006	2-21		2B056	1-43		2B106	2-52		2B156	3-9	
2B007	2-20		2B057	1-42		2B107	2-53		2B157	3-10	
2B008	2-19		2B058	1-41		2B108	2-54		2B158	3-11	
2B009	2-18		2B059	1-40		2B109	2-55		2B159	3-12	
2B010	2-17		2B060	1-39		2B110	2-56		2B160	3-13	
2B011	2-16		2B061	1-38		2B111	2-57		2B161	3-14	
2B012	2-15		2B062	1-37		2B112	2-58		2B162	3-15	
2B013	2-14		2B063	1-36		2B113	2-59		2B163	3-16	
2B014	2-13		2B064	1-35		2B114	2-60		2B164	3-17	
2B015	2-12		2B065	1-34		2B115	2-61		2B165	3-18	
2B016	2-11		2B066	1-33		2B116	2-62		2B166	3-19	
2B017	2-10		2B067	1-32		2B117	2-63		2B167	3-20	
2B018	2-9		2B068	1-31		2B118	2-64		2B168	3-21	
2B019	2-8		2B069	1-30		2B119	2-65		2B169	3-22	
2B020	2-7		2B070	1-29		2B120	2-66		2B170	3-23	
2B021	2-6		2B071	1-28		2B121	2-67		2B171	3-24	
2B022	2-5		2B072	1-27		2B122	2-68		2B172	3-25	
2B023	1-80		2B073	1-26		2B123	2-69		2B173	3-26	
2B024	1-79		2B074	1-25		2B124	2-70		2B174	3-27	
2B025	1-78		2B075	1-24		2B125	2-71		2B175	3-28	
2B026	1-77		2B076	1-23		2B126	2-72		2B176	3-29	
2B027	1-76		2B077	1-22		2B127	2-73		2B177	3-30	
2B028	1-75		2B078	1-21		2B128	2-74		2B178	3-31	
2B029	1-74		2B079	1-20		2B129	2-75		2B179	3-32	
2B030	1-73		2B080	1-19		2B130	2-76		2B180	3-33	
2B031	1-72		2B081	1-18		2B131	2-77		2B181	3-34	
2B032	1-71		2B082	1-17		2B132	2-78		2B182	3-35	
2B033	1-70		2B083	1-16		2B133	2-79		2B183	3-36	
2B034	1-69		2B084	1-15		2B134	2-80		2B184	3-37	
2B035	1-68		2B085	1-14		2B135	2-81		2B185	3-38	
2B036	1-67		2B086	1-13		2B136	2-82		2B186	3-39	
2B037	1-66		2B087	1-12		2B137	2-83		2B187	3-40	
2B038	1-65		2B088	1-11		2B138	2-84		2B188	3-41	
2B039	1-64		2B089	1-10		2B139	2-85		2B189	3-42	
2B040	1-63		2B090	1-9		2B140	2-86		2B190	3-43	
2B041	1-62		2B091	1-8		2B141	2-87		2B191	3-44	
2B042	1-61		2B092	1-7		2B142	2-88		2B192	3-45	
2B043	1-60		2B093	1-6		2B143	2-89		2B193	3-46	
2B044	1-59		2B094	1-5		2B144	2-90		2B194	3-47	
2B045	1-58		2B095	2-37		2B145	2-91		2B195	3-48	
2B046	1-57		2B096	2-38		2B146	2-92		2B196	3-49	
2B047	1-56		2B097	2-39		2B147	2-93		2B197	3-50	
2B048	1-55		2B098	2-40		2B148	2-94		2B198	3-51	
2B049	1-54		2B099	2-41		2B149	2-95		2B199	3-52	
2B050	1-53		2B100	2-42		2B150	2-96		2B200	3-53	
									2B201	3-54	

Film Data	
Roll No	Film Type
1	104-06-06
2	104-06-06
3	104-06-06
3	101-06-05

Camera No. B3 Sequence Log

ATM	Film	Dev	ATM	Film	Dev	ATM	Film	Dev	ATM	Film	Dev
No.	Roll	Stamp Cut	No.	Roll	Stamp Cut	No.	Roll	Stamp Cut	No.	Roll	Stamp Cut
28301	3-56		28351	18-14		28401	17-6	3	28451	16-36	
28302	3-57		28352	18-16		28402	17-5	5	28452	16-34	
28303	3-58		28353	18-17		28403	16-88		28453	16-33	
28304	3-(101)		28354	18-18		28404	16-87		28454	16-32	
28305	17-52		28355	18-19		28405	16-86		28455	16-31	
28306	17-53		28356	18-20		28406	16-85		28456	16-30	
28307	17-54		28357	18-21		28407	16-84		28457	16-29	
28308	17-55		28358	18-22		28408	16-83		28458	16-28	
28309	17-56		28359	18-23		28409	16-82		28459	16-27	
28310	17-57		28360	18-24		28410	16-81		28460	16-26	
28311	17-58		28361	18-25		28411	16-80		28461	16-25	
28312	17-60		28362	18-27		28412	16-79		28462	16-23	
28313	17-61		28363	18-28		28413	16-77		28463	16-22	
28314	17-62		28364	18-29		28414	16-76		28464	16-21	
28315	17-63		28365	18-30		28415	16-75		28465	16-20	
28316	17-64		28366	18-31		28416	16-74		28466	16-19	
28317	17-65		28367	18-32		28417	16-73		28467	16-18	
28318	17-66		28368	18-33		28418	16-72		28468	16-17	
28319	17-67		28369	18-34		28419	16-71		28469	16-16	
28320	17-68		28370	18-35		28420	16-70		28470	16-14	
28321	17-69		28371	18-36		28421	16-69		28471	16-13	
28322	17-71		28372	18-38		28422	16-68		28472	16-12	
28323	17-72		28373	18-39		28423	16-66		28473	16-11	
28324	17-73		28374	18-40		28424	16-65		28474	16-10	
28325	17-74		28375	18-41		28425	16-64		28475	16-9	
28326	17-75		28376	18-42		28426	16-63		28476	16-8	
28327	17-76		28377	17-94		28427	16-62		28477	16-7	
28328	17-77		28378	17-95		28428	16-61		28478	16-6	
28329	17-78		28379	17-96		28429	16-60		28479	16-5	
28330	17-79		28380	17-97	2	28430	16-59		28480	17-26	4
28331	17-80		28381	17-98	3	28431	16-58		28481	17-27	1
28332	17-82		28382	17-99		28432	16-56		28482	17-28	
28333	17-83		28383	17-102		28433	16-55		28483	17-29	
28334	17-84		28384	17-24		28434	16-54		28484	17-30	
28335	17-85		28385	17-23		28435	16-53		28485	17-31	
28336	17-86		28386	17-22		28436	16-52		28486	17-32	
28337	17-87		28387	17-21		28437	16-51		28487	17-33	
28338	17-88		28388	17-20		28438	16-50		28488	17-34	
28339	17-89		28389	17-19		28439	16-49		28489	17-35	
28340	17-90		28390	17-18		28440	16-48		28490	17-36	
28341	17-91		28391	17-17		28441	16-47		28491	17-37	
28342	18-5		28392	17-16		28442	16-45		28492	17-37	
28343	18-6		28393	17-15		28443	16-44		28493	17-40	
28344	18-7		28394	17-13		28444	16-43		28494	17-41	
28345	18-8		28395	17-12		28445	16-42		28495	17-42	
28346	18-9		28396	17-11		28446	16-41		28496	17-43	
28347	18-10		28397	17-10		28447	16-40		28497	17-44	
28348	18-11		28398	17-9		28448	16-39		28498	17-45	
28349	18-12		28399	17-8		28449	16-38		28499	17-47	3
28350	18-13		28400	17-7		28450	16-37		28500	17-48	A
									28501	17-49	1

Film Data	
Roll No.	Film Type
16	109-06-05
17	104-06-05
18	104-06-05
3	104-06-05
3(101)	101-06-05

Camera No. B 4 Sequence Log

ATM	Film	Dev	ATM	Film	Dev	ATM	Film	Dev	ATM	Film	Dev
No.	Roll	Stop cut	No.	Roll	Stop cut	No.	Roll	Stop cut	No.	Roll	Stop cut
38001	8-55	4	38051	9-8		38101	9-C3	4	38151	4-54	
38002	8-54		38052	9-9		38102	9-C4		38152	4-53	
38003	8-53		38053	9-10		38103	9-C5		38153	4-52	
38004	8-52		38054	9-11		38104	9-C6		38154	4-51	
38005	8-51		38055	9-12		38105	9-C7		38155	4-50	
38006	8-50		38056	9-13		38106	9-C8		38156	4-49	
38007	8-49		38057	9-14		38107	9-C9		38157	4-48	
38008	8-47		38058	9-16		38108	9-70		38158	4-47	
38009	8-46		38059	9-17		38109	4-3		38159	8-102	
38010	8-45		38060	9-18		38110	4-4		38160	8-101	
38011	8-44		38061	9-19		38111	4-5		38161	8-100	
38012	8-43		38062	9-20		38112	4-6		38162	8-99	
38013	8-42		38063	9-21		38113	4-7		38163	8-98	
38014	8-41		38064	9-22		38114	4-8		38164	8-97	5
38015	8-40		38065	9-23		38115	4-9		38165	8-96	1
38016	8-39		38066	9-24		38116	4-10		38166	8-95	3
38017	8-38	4	38067	9-25		38117	4-11		38167	8-94	
38018	8-36	3	38068	9-27		38118	4-13		38168	8-93	
38019	8-35	4	38069	9-28		38119	4-14		38169	8-91	
38020	8-34		38070	9-29		38120	4-15		38170	8-90	
38021	8-33		38071	9-30		38121	4-16		38171	8-89	
38022	8-32		38072	9-31		38122	4-17	4	38172	8-88	
38023	8-31		38073	9-32		38123	4-18	5	38173	8-87	
38024	8-30		38074	9-33		38124	4-19		38174	8-86	
38025	8-29		38075	9-34		38125	4-20		38175	8-85	
38026	8-28		38076	9-35		38126	4-21		38176	8-84	
38027	8-27		38077	9-36	1	38127	4-22		38177	8-83	
38028	8-25		38078	9-38	2	38128	4-24		38178	8-82	
38029	8-24		38079	9-39		38129	4-25		38179	8-80	
38030	8-23		38080	9-40		38130	4-26		38180	8-79	
38031	8-22		38081	9-41		38131	4-27		38181	8-78	
38032	8-21		38082	9-42		38132	4-28		38182	8-77	
38033	8-20		38083	9-43		38133	4-29		38183	8-76	3
38034	8-19		38084	9-44		38134	4-30		38184	8-75	2
38035	8-18		38085	9-45		38135	4-31		38185	8-74	
38036	8-17	3	38086	9-46		38136	4-32		38186	8-73	
38037	8-16	1	38087	9-47		38137	4-33		38187	8-72	
38038	8-14		38088	9-49		38138	4-35		38188	8-70	
38039	8-13		38089	9-50		38139	4-36		38189	8-69	
38040	8-12		38090	9-51		38140	4-37		38190	8-68	
38041	8-11		38091	9-52		38141	4-38		38191	8-67	
38042	8-10		38092	9-53		38142	4-39		38192	8-66	
38043	8-9		38093	9-54		38143	4-40		38193	8-65	
38044	8-8		38094	9-55		38144	4-41		38194	8-64	
38045	8-7		38095	9-56		38145	4-42		38195	8-63	
38046	8-6		38096	9-57		38146	4-43		38196	8-62	
38047	8-5		38097	9-58		38147	4-44		38197	8-61	
38048	9-5		38098	9-60		38148	4-45		38198	8-60	
38049	9-6		38099	9-61		38149	4-56		38199	8-58	
38050	9-7		38100	9-62	2	38150	4-55		38200	8-57	2
									38201	8-56	

Film Data	
Roll No	Film Type
8	104-06-08
9	104-06-08
4	101-06-10

Appendix D. ATM BIBLIOGRAPHY

1 May 1977

(Commences with the initiation of the ATM Project and includes all publications and papers based on S082A and B material up to the present.)

- I. Professional Publications Published or in Press
- II. Professional Publications - Submitted
- III. Abstracts
- IV. Professional Talks - Invited
- V. Professional Talks - Contributed
- VI. Colloquia
- VII. Other Publications

I. PROFESSIONAL PUBLICATIONS - PUBLISHED OR IN PRESS

- 1457 "Apollo Solar Experiments - Paving the Way for Advanced Space Observatories", Winter, T. C., Jr. 1969, *Astronautics and Aeronautics*, March, p. 64.
- 1481 "Observations of the Extreme Ultraviolet Solar Spectrum", Tousey, R. 1971, in 'A Discussion on Solar Studies with Special Reference to Space Observations', *Phil. Trans. Roy. Soc. Lond. A* 270, 59. (Invited)
- 1489 "Semi-Automatic Acquisition of Extreme Ultraviolet Reflectance Data for Calculating Optical Constants", Hunter, W. R. 1970, *Rev. Sci. Instr.* 41, 1419.
- 1502 "Spectral Radiance of the Carbon Arc Between 2500 Å and 1900 Å", Pitz, E. E. 1971, *Appl. Opt.* 10, 813.
- 1515 "Survey of New Solar Results", Tousey, R. 1971, in 'New Techniques in Space Astronomy', *IAU Symp.* 41, 223, ed. F. Labuhn and R. Lust, Reidel, Dordrecht.
- 1517 "High Angular Resolution Absolute Intensity of the Solar Continuum from 1400 Å to 1790 Å", Brueckner, G. E., and Moe, O. K. 1972, *Space Research XII*, Vol. 2, 1595, ed. S. A. Bowhill, L. D. Jaffe, and M. J. Rycroft, Akademie-Verlag, Berlin.
- 1518 "Solar Spectroscopy from Space Vehicles", Tousey, R. 1972, in 'Developments in Applied Spectroscopy', Vol. 10, 191, ed. A. J. Perkins, E. L. Grove, E. F. Kaelble and J. E. Westermeyer, Plenum, New York. (Invited)
- 1522 "High Angular Resolution Observations from Rockets: Solar XUV Observations", Tousey, R. 1972, *Space Research XII*, Vol. 2, 1719, ed. S. A. Bowhill, L. D. Jaffe, and M. J. Rycroft, Akademie-Verlag, Berlin. (Invited)
- 1529 "On the Classification of Some Highly Ionized Iron and Nickel Lines in the 200-400 Å Region of the Solar Spectrum", Widing, K. G., Sandlin, G. D., and Cowan, R. D. 1971, *Astrophys. J.* 169, 405.
- 1548 "Simultaneous Optical Monitoring of Angular and Translational Alignment", Bohlin, J. D. 1972, *Appl. Opt.* 11, 961.
- 1549 "Extreme Ultraviolet Solar Images Televised In-Flight with a Rocket-Borne SEC Vidicon System", Tousey, R. and Limansky, I. 1972, *Appl. Opt.* 11, 1025.
- 1566 "Rocket Observation of Ar XII-XVI and Ca XIV-XVIII in the XUV Spectrum of a Solar Flare", Purcell, J. D. and Widing, K. G. 1972, *Astrophys. J.* 176, 239.
- 1570 "Cleaning of Contaminated Channel Electron Multiplier Arrays", Harlow, F. E. and Hunter, W. R. 1972, *Appl. Opt.* 11, 2719.

- 1573 "Comparison of an Aluminum-Coated Phosphor Layer and a Channel-tron Electron Multiplier Array as Extreme Ultraviolet-to-Visible Image Converters for Use in Space Applications", Hunter, W. R., and Harlow, F. E. 1973, Appl. Opt. 12, 968.
- 1579 "The Extreme-Ultraviolet Spectrum of Fe XV in a Solar Flare", Cowan, R. D. and Widing, K. G. 1973, Astrophys. J. 180, 285.
- 1603 "New Stigmatic, Coma-free, Concave Grating Spectrograph", Bartoe, J. -D. F. and Brueckner, G. E., 1975, JOSA 65, 13.
- 1606 "The Increase in Transmittance of Unbacked Aluminum Filters Exposed to RF and DC Discharge in Oxygen", Hunter, W. R., Steele, G. N. and Gillette, R. B. 1973, Appl. Opt. 12, 2800.
- 1620 "A Preliminary Study of the Extreme Ultraviolet Spectroheliograms from Skylab", Tousey, R., Bartoe, J. -D. F., Bohlin, J. D., Brueckner, G. E., Purcell, J. D., Scherrer, V. E., Sheeley, N. R., Jr., Schumacher, R. J. and Van Hoosier, M. E. 1973, Solar Phys. 33, 265.
- 1642 "The Extreme Ultraviolet Spectrograph", Bartoe, J. -D. F., Brueckner, G. E., Purcell, J. D., and Tousey, R. 1974, SPIE 44, 153.
- 1647 "On the Fe XXIV Emission in the Solar Flare on June 15, 1973", Widing, K. G. and Cheng, C. C. 1974, Astrophys. J. Lett. 194, L111.
- 1650 "Structure of the Sun's Polar Cap in the Wavelengths 240-600 Å", Bohlin, J. D., Sheeley, N. R., Jr., and Tousey, R., 1975 Space Research XV, 651, ed. Akademie-Verlag, Berlin.
- 1652 "Preliminary Results from the NRL/ATM Instruments from Skylab 2", Tousey, R., Bartoe, J. -D. F., Bohlin, J. D., Brueckner, G. E., Purcell, J. D., Scherrer, V. E., Schumacher, R. J., Sheeley, N. R., Jr., and Van Hoosier, M. E. 1974, in 'Coronal Disturbances', p. 491, ed. G. Newkirk, Jr., Reidel, Dordrecht.
- 1655 "Implications of NRL/ATM Solar Flare Observations on Flare Theories", Cheng, C. C. and Spicer, D. S. 1975, in 'Solar Gamma-, X-, and EUV Radiation', p. 423, ed. S. R. Kane, Reidel, Dordrecht.
- 1666 "Some Reflections on the Use of Conventional and Holographic Diffraction Gratings in the Vacuum Ultraviolet Spectral Region", Hunter, W. R. 1974, Proc. IV International Conf. on Vacuum-Ultraviolet Radiation Physics, p. 683.
- 1671 "Diffraction Gratings for the XUV - Conventional vs. Holographic", Hunter, W. R. 1974, Japanese J. of Spectroscopical Soc. 23, 37.

- 1673 "Flare-Like Ultraviolet Spectra of Active Regions", Brueckner, G. E. 1975, in 'Solar Gamma-, X-, and EUV Radiation', 105, ed. S. R. Kane, Reidel, Dordrecht.
- 1675 "Ultraviolet Emission Line Profiles of Flares and Active Regions", Brueckner, G. E. 1975, in 'Solar Gamma-, X-, and EUV Radiation', 135, ed. S. R. Kane, Reidel, Dordrecht.
- 1676 "The Fine Structure of the Solar Atmosphere in the Far Ultraviolet", Brueckner, G. E., and Bartoe, J. -D. F. 1974, Solar Phys. 38, 133.
- 1677 "Fe XXIV Emission in Solar Flares Observed with the NRL/ATM XUV Slitless Spectrograph", Widing, K. G. 1975, 'Solar Gamma-, X-, and EUV Radiation', 153, ed. S. R. Kane, Reidel, Dordrecht.
- 1678 "Flares Observed by the NRL/ATM Spectrograph and Spectroheliogram During the Skylab Missions", Scherrer, V. E. and Tousey, R. 1975, Proc. International Conf. on 'X-rays in Space', Vol. II, 986, Univ. of Calgary.
- 1683 "Observations of the Hydrogen Ly- α (1216 Å) Emission Line of Comet Kohoutek (1973f) by the Skylab/ATM S082B Spectrograph", Keller, H. U., Bohlin, J. D., and Tousey, R. 1975, Proc. Comet Kohoutek Workshop, NASA SP-355, ed. G. A. Gary.
- 1684 "High Resolution Ly- α Observations of Comet Kohoutek by Skylab and Copernicus", Bohlin, J. D., Drake, J. F., Jenkins, E. B., and Keller, H. U., Proc. IAU Colloq. 25, 'The Study of Comets', Part 1, NASA SP-393, 315.
- 1686 "XUV Observations of Coronal Magnetic Fields", Sheeley, N. R., Jr., Bohlin, J. D., Brueckner, G. E., Purcell, J. D., Scherrer, V. E., and Tousey, R. 1975, Solar Phys. 40, 103.
- 1688 "Selected Tables of Atomic Spectra; Atomic Energy Levels and Multiplet Tables; NI, NII, NIII", Moore-Sitterly, C. E. 1975, NSRDS-NBS 3, Section 5.
- 1687 "Observed Heights of EUV Lines Formed in the Transition Zone and Corona", Simon, G. W., Seagraves, P. H., Tousey, R., Purcell, J. D., Noyes, R. W. 1974, Solar Phys. 39, 121.
- 1689 "Ultraviolet Solar Identifications Based on Extended Absorption Series Observed in the Laboratory Spectra of Si I", Moore, C. E., Tousey, R., Sandlin, G. D., Brown, C. M., Ginter, M. L., and Tilford, S. G., 1975, Astrophys. and Sp. Sci., 38, 359.

- 1691 "Eruptive Prominences Recorded by the XUV Spectroheliograph on Skylab", Tousey, R. 1976, 'A Discussion on the Physics of the Solar Atmosphere', Phil. Trans. Roy. Soc. Lond. A 281, 359.
- 1692 "High Resolution Ly α Observations of Comet Kohoutek Near Perihelion", Keller, H. U., Bohlin, J. D., and Tousey, R. 1975, Astron. and Astrophys. 38, 413.
- 1695 "A Comparison of Spicules in the H α and He II (304 Å) Lines", Moe, O. K., Engvold, E. and Beckers, J. 1975, Solar Phys. 40, 65.
- 1709 "The Reconnection of Magnetic Field Lines in the Solar Corona", Sheeley, N.R., Jr., Bohlin, J. D., Brueckner, G. E., Purcell, J. D., Scherrer, V. E., and Tousey, R. 1975, Astrophys. J. Lett. 196, L129.
- 1713 "Forbidden Lines of Highly Ionized Iron in Solar Flare Spectra", Doschek, G. A., Feldman, U., Dere, K. P., Sandlin, G. D., Van Hoosier, M. E., Brueckner, G. E., Purcell, J. D., and Tousey, R. 1975, Astrophys. J. Lett. 196, L83.
- 1715 "XUV Results from Skylab", Tousey, R. 1975, Proc. International Conf. on 'X-Rays in Space', Vol. I, 472, Univ. of Calgary. (Invited)
- 1716 "The XUV Sun as Observed by ATM S082", Tousey, R., Proc. of AIAA/AGU Space Science Conf. on 'Scientific Experiments of Project Skylab', in press.
- 1718 "Classification of Flares and Flare-Like Events Observed by the ATM XUV Spectroheliograph S082A and Spectrograph S082B During the Skylab Missions", Scherrer, V. E. and Tousey, R., Proc. of AIAA/AGU Space Science Conf. on 'Scientific Experiments of Project Skylab', in press.
- 1720 "The Stark Broadening Mechanism in an Unstable Plasma", Spicer, D. S. and Davis, J. 1975, Solar Phys. 43, 107.
- 1721 "On the Fe XXIV Emission in the Solar Flare of 1973 June 15", Widing, K. G. and Cheng, C. C. 1974, Astrophys. J. Lett. 194, L115.
- 1724 "Fe XXIII 263 Å and Fe XXIV 255 Å Emission in Solar Flares", Widing, K. G. 1975, Astrophys. J. Lett. 197, L133.
- 1727 "A Newly Observed Solar Feature: Macro-Spicules in He II 304 Å", Bohlin, J. D., Vogel, S. N., Purcell, J. D., Sheeley, N. R., Jr., Tousey, R., and Van Hoosier, M. E. 1975, Astrophys. J. Lett. 197, L133.
- 1729 "The 1640.4 Å H α Line of He II Observed from Skylab", Feldman, U., Doschek, G. A., Van Hoosier, M. E., and Tousey, R. 1975, Astrophys. J. Lett. 199, L67.

- 1733 "XUV Emission from Above the West Limb Near 20:00 U.T., January 17, 1974", Tousey, R. 1975, *Astrophys. and Sp. Sci.*, Vol. 38, 327.
- 1741 "ATM Observations of the XUV Emission from Solar Flares," Brueckner, G. E. 1976, 'A Discussion on the Physics of the Solar Atmosphere', *Phil. Trans. Roy. Soc. Lond. A* 281, 443.
- 1745 "Spatial Distribution of XUV Emission in Solar Flares", Cheng, C.C. and Widing, K. G. 1975, *Astrophys. J.* 201, p. 735.
- 1748 "The Interpretation of Ultraviolet Solar Spectra", Moore-Sitterly, C. E., *Proc. Twentieth Liege International Astrophysical Symp.*, 1975, *Mem. de la Societe Royale de Liege* 9, p. 59.
- 1749 "Coronal Changes Associated with a Disappearing Filament," Sheeley, N. R., Jr., Bohlin, J. D., Brueckner, G. E., Purcell, J. D., Scherer, V. E., Tousey, R., Smith, J. B., Jr., Speich, D. M., Tandberg-Hanssen, E., Wilson, R. M., de Loach, A. C., Hoover, R. B., and McGuire, J. P., *Solar Physics* 45, p. 377.
- 1760 "Absolute Solar Intensities 1750 Å-2100 Å and their Variations with Solar Activity", Brueckner, G. E., Bartoe, J.-D. F., Moe, O. K., Van Hoosier, M. E. 1975, *Proc. of the Workshop: The Solar Constant and the Earth's Atmosphere*, p. 71.
- 1762 "Selected Tables of Atomic Spectra, Atomic Energy Levels and Multiplet Tables 0I", Moore-Sitterly, C. E. 1976, *NSRDS-NBS* 3, Sec. 7.
- 1765 "Limb Brightening Curves of XUV Transition Zone Lines in the Quiet Sun and in a Polar Coronal Hole Observed from Skylab", Doschek, G. A., Feldman, U. and Tousey, R. *Astrophys. J. Lett.* 202, L147.
- 1766 "The Intensities and Profiles of XUV Transition Lines in a Quiet Sun Region Compared to a Polar Coronal Hole", Feldman, U., Doschek, G. A. and Tousey, R. *Astrophys. J. Lett.* 202, L151.
- 1773 "Advances in X-Ray and EUV Spectroscopy of Solar Flares and Laboratory Plasmas", Doschek, G. A. 1975, *Proc. International Conf. on 'X-Rays in Space'*, Vol. I, p. 306.
- 1783 "The Calculation of Force-Free Fields from Discrete Flux Distributions," Sheeley, N. R., Jr., and Harvey, J. W., *Solar Physics* 45, p. 275.
- 1789 "Energy Released by the Interaction of Coronal Magnetic Fields," Sheeley, N. R., Jr., *Solar Physics* 47, p. 173.
- 1795 "Synoptic Maps of Coronal Hole Boundaries Derived from He II 304 Å Spectroheliograms from the Manned Skylab Missions," Bohlin, J. D. and Rubenstein, D. M. 1975, *World Center A for Solar-Terrestrial Physics*, NOAA, Report UAG-51.

- 1796 "The Emission Line Spectrum Above the Limb of the Quiet Sun: 1100-1940 Angstroms," Doschek, G. A., Feldman, U., Van Hoosier, M. E. and Bartoe, J. -D. F. 1976, *Astrophys. J. Supp. Series* 31, 417.
- 1797 "The Emission Line Spectrum Above the Limb of a Solar Coronal Hole: 1100-1940 Angstroms." Feldman, U., Doschek, G. A., Van Hoosier, M. E. and Purcell, J. D. 1976, *Astrophys. J. Supp. Series* 31, 445.
- 1799 "The Lithium-Like $2s^2 S-2p^2 P$ Transition in Solar Flares," Widing, K. G. and Purcell, J. D. 1976, *Astrophys. J. Lett.* 204, L151.
- 1800 "High Temperature Flare Lines in the Solar Spectrum 171-630Å," Sandlin, G. D., Brueckner, G. E., Tousey, R. and Scherrer, V. E. 1976, *Astrophys. J. Lett.* 205, L47.
- 1804 "Space-Resolved Spectra of Laser-Produced Plasmas in the XUV," Feldman, U., Doschek, G. A., Prinz, D. K. and Nagel, D. J. 1976, *J. of Appl. Phys.* 47, No. 4, 1341.
- 1806 "The Profile of the Solar Lyman Beta Line of Hydrogen," Nicolas, K. R., Moe, O. K., Bartoe, J. -D. F. and Tousey, R. 1976, *J. of Geophys. Res. - Space Physics* 81, 3465.
- 1807 "Effects of Plasma Microfields on Radiative Transients from Atomic Levels Above the Ionization Threshold," Davis, J. and Jacobs, V. L., *Phys. Rev. A* 12, 2017.
- 1808 "High Latitude Observations of Solar Wind Streams and Coronal Holes," Rickett, B. J., Sime, D. G., Sheeley, N. R., Jr., Crockett, W. R. and Tousey, R. 1976, *J. of Geophys. Res.* 81, 3845.
- 1810 "The Sources of Material Comprising a Mass Ejection Coronal Transient," Hildner, E., Gosling, J. T., Hansen, R. T. and Bohlin, J. D. 1975, *Solar Physics* 45, 363.
- 1812 "Doppler Wavelength Shifts of Transition Zone Lines Measured in Skylab Solar Spectra," Doschek, G. A., Feldman, U. and Bohlin, J. D. 1976, *Astrophys. J. Lett.* 205, L177.
- 1813 "Polar Faculae During the Interval 1906-1975," Sheeley, N. R., Jr. 1976, *J. of Geophys. Res.* 81, 3462.
- 1814 "Spectroscopic Far Ultraviolet Observations of Transition Zone Instabilities and Their Possible Role in a Pre-Flare Energy Build-up," Brueckner, G. E., Patterson, N. P. and Scherrer, V. E. *Solar Physics* 47, 127.

- 1817 "Absolute Solar Ultraviolet Intensities and Their Variations with Solar Activity Part I: The Wavelength Region 1750Å - 2100Å," Brueckner, G. E., Bartoe, J.-D. F., Moe, O. K., and Van Hoosier, M. E., *Astrophys. J.* 209, 935.
- 1820 "Observation of a Kink Instability in a Solar Flare," Cheng, C. C., *Astrophys. J.* 213, 558.
- 1822 "Thin Aluminum Filters for Use on the Apollo Television Monitor Flown on Skylab," Schumacher, R. J. and Hunter, W. R., *Appl. Opt.* 16, 904.
- 1824 "Density Sensitive Lines of Highly Ionized Iron," Doschek, G. A., Feldman, U., Davis, J. and Cowan, R. D., *Phys. Rev. A* 12, 980.
- 1826 "Transitions of Zn XXII, Zn XXIII, ZnXXIV, Ge XXIV and Ge XXV Observed in Laser-Produced Plasmas," Behring, W. E., Cohen, Leonard, Doschek, G. A. and Feldman, U., *JOSA* 66, 376.
- 1827 "NRL/ATM Extreme Ultraviolet Solar Image Television Monitor Flown on Skylab," Crockett, W. R., Patterson, N. P., Purcell, J. D., Schumacher, R. J. and Tousey, R., *Appl. Opt.* 16, 893.
- 1837 "The Emission Line Spectrum of a Sunspot in the Far Ultraviolet," Cheng, C. C., Doschek, G. A. and Feldman, U., *Astrophys. J.* 210, 836.
- 1844 "The XUV Spectrum of C I Observed from Skylab During a Solar Flare," Feldman, U., Brown, C. M., Doschek, G. A., Moore, C. E. and Rosenberg, F. D. 1976, *J. Opt. Soc. Am.* 66, 853.
- 1846 "Coronal Holes, Solar Wind Streams and Recurrent Geomagnetic Disturbances: 1973-1976," Sheeley, N. R., Jr., Harvey, J. W. and Feldman, W. C., *Solar Physics* 49, 271.
- 1850 "Emission Measures, Electron Densities and Nonthermal Velocities from Optically Thin UV-Lines Near a Quiet Solar Limb," Kjeldseth Moe, O. and Nicolas, K. R., *Astrophys. J.* 211, 579.
- 1851 "The Quiet Sun Chromospheric Network Observed from Skylab," Feldman, U., Doschek, G. A. and Patterson, N. P. 1976, *Astrophys. J.* 209, 270.
- 1866 "The Influence of Autoionization Accompanied by Excitation on Dielectronic Recombination and Ionization Equilibrium," Jacobs, V. L., Davis, J., Kepple, P. C. and Blaha, M., *Astrophys. J.* 211, 605.
- 1869 "The Emission Spectrum of the Hydrogen Balmer Series Observed Above the solar Limb from Skylab I. A Quiet-Sun and Polar Coronal Hole," Rosenberg, F. D., Feldman, U. and Doschek, G. A. *Astrophys. J.* 212, 905

- 1872 "The Profile of the 977 Å Line of C III," Moe, O. K., Nicolas, K. R. and Bartoe, J. -D. F. Contribution to the NASA Workshop on the Physical Output of the Sun, 1976, in press.
- 1875 "The Apollo Telescope Mount of Skylab - An Overview," Tousey, R. Appl. Opt. 16, 825.
- 1876 "The Solar XUV Grazing Incidence Spectrograph on Skylab," Garrett, D. L. and Tousey, R., Appl. Opt. 16, 898.
- 1880 "The Emission Spectrum of the Hydrogen Balmer Series Observed Above the Solar Limb from Skylab II. Active Regions," Feldman, U. and Doschek, G. A., Astrophys. J. 212, 913.
- 1883 "Exploring the Earth's Atmosphere by Photography from Skylab," Packer, D. M. and Packer, I. G., Appl. Opt. 16, 983.
- 1885 "The Extreme Ultraviolet Spectrograph ATM Experiment S082B," Bartoe, J. -D. F., Brueckner, G. E., Purcell, J. D. and Tousey, R., Appl. Opt. 16, 879.
- 1897 "The 3s-3p and 3p-3d Lines of Mg II Observed Above the Solar Limb from Skylab," Feldman, U. and Doschek, G. A., Astrophys. J. Lett. 212, L 147.
- 1899 "Observing and Recording Instantaneous Images on ATM Television Monitors," Patterson, N. P., Tousey, R. and Delamere, W. A., Appl. Opt. 16, 922.
- 1900 "Experience with Schumann-Type XUV Film on Skylab," Van Hoosier, M. E., Bartoe, J. -D. F., Brueckner, G. E., Patterson, N. P. and Tousey, R., Appl. Opt. 16, 887.
- 1901 "The Extreme Ultraviolet Spectroheliograph ATM Experiment S082A," Tousey, R., Bartoe, J. -D. F., Brueckner, G. E. and Purcell, J. D., Appl. Opt. 16, 870.
- 1904 "Chromospheric Limb Spectra from Skylab: 200 to 3200 Å," Doschek, G. A. and Feldman, U., Astrophys. J. Supp. Series 33, 101.
- 1906 "Enhancement of Dielectronic Reombination by Plasma Electric Microfields," Jacobs, V. L., Davis, J. and Kepple, P. C., Phys. Rev. Lett. 37, 1390.
- 1922 "Electron Impact Excitation Coefficients for Laboratory and Astrophysical Plasmas," Davis, J., Kepple, P. C. and Blaha, M., J. Quant. Spectrosc. Radiat. Transfer, Vol. 16, 1043.

II. PROFESSIONAL PUBLICATIONS - SUBMITTED

- 1873 "A Comment on the Acceleration of Charged Particles in the Presence of Micro-Turbulence as Related to Solar Flares," Spicer, D. S. Research Note submitted to Solar Physics.
- 1882 "Extreme-Ultraviolet Observations of Coronal Holes: I. Locations, Sizes and Evolution of Coronal Holes June 1973 - January 1974," Bohlin, J. D. Submitted to Solar Physics.
- 1884 "Emission Measures and Structure of the Transition Region of a Sunspot from Emission Lines in the Far Ultraviolet," Cheng, C. C. and Moe, O. K. Submitted to Solar Physics.
- 1886 "Observations of the O Column Density Between 120 km and 70 km and Absorption Cross Section in the Vicinity of H-Lyman Alpha," Prinz, D. K. and Brueckner, G. E. Submitted to J. of Geophys. Res.
- 1887 "Multiple Loop Activations and Continuous Energy Release in the Solar Flare of 1973 June 15," Widing, K. G. and Dere, K. P. Submitted to Solar Physics.
- 1894 "Solar XUV Emission Line Profiles of Si II and Si III and Their Center to Limb Variations," Nicolas, K. R., Brueckner, G. E., Tousey, R., Tripp, D. A., White, O. R. and Athay, R. G. Submitted to Solar Physics.
- 1898 "Comparison of Flare Bremsstrahlung Resulting from Energetic Thermal and Non-Thermal Electrons," Davis, J. and Rogerson, J. E. Submitted to Solar Physics.
- 1902 "The Thermal and Non-Thermal Flare: A Result of Non-Linear Threshold Phenomena During Magnetic Field Line Reconnection," Spicer, D. S. Submitted to Solar Physics.
- 1905 "Forbidden Lines of the Solar Corona and Transition Zone $\lambda\lambda 955 \text{ \AA} - 3000 \text{ \AA}$," Sandlin, G. D., Brueckner, G. E. and Tousey, R. Submitted to Astrophys. J.
- 1908 "Structure and Dynamics of a Solar Flare: X-Ray and XUV Observations," Dere, K. P., Horan, D. M. and Kreplin, R. W. Submitted to Astrophys. J.
- 1917 "A Pictorial Comparison of Interplanetary Magnetic Field Polarity, Solar Wind Speed and Geomagnetic Disturbance Index During the Sunspot Cycle," Sheeley, N. R., Jr., Asbridge, J. R., Bame, S. J., and Harvey, J. W. Submitted to Solar Physics.
- 1918 "Plasma Diagnostics Using High Resolution Spectroscopic Techniques," Feldman, U and Doschek, G. A. Submitted J. Opt. Soc. of Am.

- 1919 "XUV Spectra of the 15 June 1973 Solar Flare Observed from Skylab I. Allowed Transition in Chromospheric and Transition Zone Ions," Doschek, G. A., Feldman, U. and Rosenberg, F. D. Submitted to Astrophys. J.
- 1920 "XUV Spectra of the 15 June 1973 Solar Flare Observed from Skylab II. Intersystem and Forbidden Transitions in Transition Zone and Coronal Ions," Feldman, U., Doschek, G. A. and Rosenberg, F. D. Submitted to Astrophys. J.
- 1936 "High Resolution Spectra of the Solar Mg II h and k Lines," Doschek, G. A. and Feldman, U. Submitted to Astrophys. J. Suppl.
- 1937 "A Search for a Turbulent Free Region in the Solar Transition Zone," Feldman U. and Doschek, G. A. Submitted to Astrophys. J.
- 1938 "On the Problem of Density Diagnostics for the EUV Spectrum for the EUV Spectrum of the Solar Transition Zone," Doschek, G. A. and Feldman, U. Submitted to Astronomy and Astrophys. Lett.
- 1941 "Electrostatically Unstable Heat Flow During Solar Flares and its consequences," Spicer, D. S. Submitted to Solar Physics.
- 1946 "A Survey of Coronal Holes and Their Solar Wind Associations Throughout Sunspot Cycle 20," Broussard, R. M., Sheeley, N. R., Jr., Tousey, R. and Underwood, J. H. Submitted to Solar Physics.

III. ABSTRACTS

- 1509 "Absolute Intensity of the Continuum in the Ultraviolet Spectrum of the Sun Between 1650-1800 Å", Brueckner, G. E., Moe, O. K., and Pitz, E., BAAS 3, 260 (1971).
- 1510 "High Spectral and Spatial Resolution Ultraviolet Spectroscopy of the Sun in the Region 1170-1800 Å", Brueckner, G. E., BAAS 3, 259 (1971).
- 1529 "On the Classification of Some Highly Ionized Iron and Nickel Lines in the 200-400 Å Region of the Solar Spectrum", Widing, K. G. and Sandlin, G. D., Cowan, R. D., Sp. Sci. Rev. 13, 665 (1972).
- 1544 "Extreme Ultraviolet Spectroheliograms of a Solar Flare", Purcell, J. D. and Tousey, R., BAAS 3, 448 (1971).
- 1545 "Preliminary Results of Identifications in the XUV Spectrum of a Solar Flare", Purcell, J. D., Tousey, R., and Widing, K. G., BAAS 3, 448 (1971).
- 1565 "The Coronal Origin of a Solar Flare", Brueckner, G. E., BAAS 4, 378 (1972).
- 1572 "A Recalibration of Spectral Radiance of Mercury and Deuterium Arc Standard Lamps in the Near UV", Bartoe, J. -D. F. and Ott, W. R., J. Opt. Soc. Am. 62, 1372 (1972).
- 1623 "The 1175 Å to 1900 Å Ultraviolet Spectrum of Solar Flares", Brueckner, G. E., Bohlin, J. D., Moe, O. K., Nicolas, K. R., Purcell, J. D., Scherrer, V. E., Sheeley, N. R., Jr., and Tousey, R., BAAS 6, 285 (1974).
- 1624 "Electron Density from Line Ratios in the XUV Spectrum of a Solar Flare", Widing, K. G., Purcell, J. D., and Tousey R., BAAS 6, 297 (1974).
- 1625 "The Screw Pinch and the Solar Flare", Spicer, D. S. and Cheng, C. C., BAAS 6, 294 (1974).
- 1626 "A Preliminary Study of Coronal Structures by Means of Time-Lapse Photography", Sheeley, N. R., Jr., Bohlin, J. D., Brueckner, G. E., Purcell, J. D., Scherrer, V. E., and Tousey, R., BAAS 6, 294 (1974).
- 1628 "Rocket Spectroheliogram Observations of the Heights of Formation and Sizes of Bright Features in the Transition Zone", Simon, G. W., Seagraves, P. H., and Tousey, R., BAAS 6, 294 (1974).
- 1629 "Cinematographic Observations for ATM and Their Comparison with Some ATM Results", Zirin, H., Holt, J., Brueckner, G. E., Bohlin, J. D., Purcell, J. D., Scherrer, V. E., Sheeley, N. R., Jr., and Tousey, R., BAAS 6, 298 (1974).

- 1637 "Studies of Atmospheric Extinction from Skylab", Brown, C. M., Tousey, R., Tilford, S. G., and Prinz, D. K., EOS 55, 371 (1974).
- 1640 "Coronal Extreme Ultraviolet Spectroheliograph and Chromospheric Extreme Ultraviolet Spectrograph", Tousey., BAAS 6, 297 (1974).
- 1642 "The Extreme Ultraviolet Spectrograph", Bartoe, J. -D. F., Brueckner, G. E., Purcell, J. D., and Tousey, R., SPIE. 'Instrumentation in Astronomy - II', 1974, SPIE 44, 153.
- 1657 "Skylab Observation of the White Light Corona and the He II 304 Å Chromosphere During the Eruptive Prominence Event of August 21, 1973", Bohlin, J. D., Brueckner, G. E., Purcell, J. D., Scherrer, V. E., Sheeley, N. R., Jr., Tousey, R., Poland, A. I., EOS 55, 409 (1974).
- 1657 "The Eruptive Prominence of August 21, 1973, Observed from Skylab in the White Light Corona and in the He II 304 Å Chromosphere", Poland, A. I., Bohlin, J. D., Brueckner, G. E., Purcell, J. D., Scherrer, V. E., Sheeley, N. R., Jr., and Tousey, R., BAAS 6, 219 (1974).
- 1658 "Preliminary Results from the Extreme Ultraviolet Spectroheliograph and Ultraviolet Spectrograph on ATM", Tousey, R., EOS 55, 408 (1974).
- 1668 "Skylab Observations of the Sun (170-630 Å) with the NRL Objective Grating Spectroheliograph", Widing, K. G., J. Opt. Soc. Am. 64, 1375 (1974).
- 1674 "Spectrophotometry of the Solar Ultraviolet Line Spectrum with the NRL Spectrograph onboard Skylab", Brueckner, G. E., J. Opt. Soc. Am. 64, 1375 (1974).
- 1685 "ATM Observations on the XUV Emission from Flares", Brueckner, G. E., Astrophys. and Sp. Sci., in press.
- Ibid., Stanford Univ. Inst. for Plasma Res. Report No. 594 (1974).
- 1696 "A Catalog and Classification of Flares and Flare-Like Events Observed by the ATM XUV Spectrograph S082A and Spectroheliograph S082B", Scherrer, V. E., Tousey, R., and Sandlin, G. D., BAAS 7, 356 (1975).
- 1697 "Polar Plumes in XUV Emission-Line Corona", Bohlin, J. D., Purcell, J. D., Sheeley, N. R., Jr., and Tousey, R., BAAS 7, 356 (1975).
- 1698 "Macro-Spicules in He II 304 Å Over the Sun's Polar Cap", Bohlin, J. D., Vogel, S. N., Purcell, J. D., Sheeley, N. R., Jr., Tousey, R. and Van Hoosier, M. E., BAAS 7, 354 (1975).

- 1699 "Flare Mechanisms Based on the Current Limitation Concept", Spicer, D. S., BAAS 7, 352 (1975).
- 1700 "Absolute Solar UV Intensities 1680 Å to 2100 Å", Moe, O. K., Brueckner, G. E., Bartoe, J. -D. F., and Van Hoosier, M. E., EAAS 7, 360 (1975).
- 1701 "On the XUV Emissions in Solar Flares Observed with the ATM/NRL Spectroheliograph", Cheng, C. C. and Widing, K. G., BAAS 7, 356 (1975).
- 1703 "Observations from Skylab of the Density Dependent C III Multiplet at 1175 Å in Active and Quiet Regions and Above the Limb", Nicolas, K. and Brueckner, G. E., BAAS 7, 353 (1975).
- 1705 "The High-Energy Limb Event of January 17, 1974", Tousey, R., Bohlin, J. D., Moe, O. K., Purcell, J. D., and Sheeley, N. R., Jr., BAAS 7, 348 (1975).
- 1706 "Interpreting XUV Spectroheliograms in Terms of Coronal Magnetic Field Structures", Sheeley, N. R., Jr., Bohlin, J. D., Brueckner, G. E., Purcell, J. D., Scherrer, V. E., and Tousey, R., BAAS 7, 346 (1975).
- 1707 "Line Profiles of the Fe XXIV Emission at 192 Å and 255 Å in Solar Flares", Brueckner, G. E., Moe, O. K., and Van Hoosier, M. E., BAAS 7, 356 (1975).
- 1712 "The Superheating Instability as a Trigger for Solar Flares", Tidman, D. A., Spicer, D. S., and Davis, J., BAAS 7, 352 (1975).
- 1716 "The XUV Sun as Observed by ATM S082", Tousey, R., AIAA Bulletin 11, 344 (1974).
- 1718 "Classification of Flares and Flare-Like Events Observed by the ATM XUV Spectroheliograph S082A and Spectrograph S082B During the Skylab Missions", Scherrer, V. E. and Tousey, R., AIAA Bulletin 11, 345 (1974).
- 1726 "Structure and Temperature of Solar Flare Plasma", Scherrer, V. E. and Sandlin, G. D., BAPS 20, 659 (1974).
- 1750 "A Resistive Screw Instability Model of a Solar Flare", Spicer, D. S., BAAS 7, 397 (1975).
- 1751 "A Time Dependent Study of Conductive Heat Flow in a Flaring Arch", Kepple, P. C. and Spicer, D. S., BAAS 7, 397 (1975).
- 1752 "The Sun's Polar Caps as Coronal Holes; Their Sizes, Evolution, and Phenomenology During the Skylab Mission", Bohlin, J. D., Rubenstein, D. M., and Sheeley, N. R., Jr., BAAS 7, 457 (1975).

- 1753 "Energy Release and Thermal Structure in Solar Flares" Cheng, C. C. and Widing, K. G., BAAS 7, 424 (1975).
- 1754 "X-Ray Event of August 13-15, 1973", Scherrer, V. E., Sandlin, G. D., Sheeley, N. R., Jr., and Tousey, R., BAAS 7, 430 (1975).
- 1756 "Skylab/ATM Observations of Transient Events Having the GRF X-Ray and Microwave Character", Sheeley, N. R., Jr., Bohlin, J. D., Scherrer, V. E., and Tousey, R., BAAS 7, 429 (1975).
- 1757 "Measured Variation of the XUV Line Widths and Intensities Near the Solar Limb", Moe, O. K. and Nicolas, K. R., BAAS 7, 460 (1975).
- 1758 "Evolution of XUV Plasmas in Solar Flares", Widing, K. G. and Cheng, C. C., BAAS 7, 424 (1975).
- 1763 "Spectroscopic Study of Plasmas Preceding and During Solar Flares", Scherrer, V. E. and Sandlin, G. D., BAPS 10, 1325 (1975).
- 1768 "Solar Flare Collision Excitation Rate Coefficients", Tousey, R., Kepple, P. C., and Davis, J. BAAS 7, 398 (1975).
- 1769 "Plasma Heating and Flare X-Rays", Davis, J., Kepple, P., Strickland, D., and Brueckner, G., BAAS 7, 398 (1975).
- 1770 "Hydrodynamics of Electron Beam Deposition in Solar Flares", Bloomberg, H., Kepple, P. C., Davis, J., Boris, J., Brueckner, G., BAAS 7, 398 (1975).
- 1771 "Results from the NRL XUV Experiment on Skylab", Tousey, R., J. Opt. Soc. Am. 64, 523 (1974).
- 1772 "Maximum Efficiency of Ruled Concave Diffraction Gratings in the Ultraviolet", Mikes, T. L., J. Opt. Soc. Am. 64, 1371 (1974).
- 1776 "Time Dependent Ionization Equilibrium and Line Emission from Ionized Iron Under Flare-Like Conditions", Kepple, P. and Davis, J., EOS 56, 1183 (1974).
- 1777 "Transient Line Emission from Ionized Iron Under Flare-Like Conditions", Davis, J., Kepple, P., and Tousey, R., BAAS 7, 357 (1975).
- 1778 "Absolute Calibrated Solar UV Intensities 1700 - 2100 Å", Moe, O. K., J. Opt. Soc. 64, 1375 (1974).
- 1779 "The Source of Material Comprising a Mass Ejection Coronal Transient", Hildner, E., Gosling, J. T., Hansen, R. T., and Bohlin, J. D., BAAS 7, 473 (1975).
- 1781 "Evidence for Non-Hydrostatic Equilibrium Conditions in the Transition Region", Brueckner, G. E., Stanford Univ. Inst. for Plasma Res. Report No. 594 (1974).

- 1782 "Evidence for Magnetic Field Line Reconnection in the Lower Corona", Sheeley, N. R., Jr., EOS Transactions, Vol. 56, 1049.
- 1794 "Extreme Ultraviolet Spectroheliograph for Plasma Diagnostics," Scherrer, V. E., Purcell, J. D. and Sandlin, G. D. First Topical Conference on Diagnostics of High Temperature Plasmas, American Physical Society, 7-9 January 1976, Knoxville, Tennessee.
- 1796 "The Emission Line Spectrum Above the Limb of the Quiet Sun: 1175-1940 Angstroms," Doschek, G. A., Feldman, U., Van Hoosier, M. E. and Bartoe, J. -D. F. Astrophys. J. 206, 964 (1976).
- 1797 "The Emission Line Spectrum Above the Limb of a Solar Coronal Hole: 1175-1940 Angstroms," Feldman, U., Doschek, G. A., Van Hoosier, M. E. and Purcell, J. D. Astrophys. J. 206, 965 (1976).
- 1825 "Diagnostics for Plasma Temperatures in the Spectrum 171 - 630Å," Scherrer, Victor E. and Sandlin, G. D., 1976 Spring Meeting of APS, 26-29 April 1976, Washington, D. C., BAPS 21, 598 (1976).
- 1829 "High Spatial Resolution UV Spectra of the Sun: The Dynamics of the Transition Zone," Brueckner, G. E., Bartoe, J. -D. F., Kjeldseth Moe, O., Nicolas, K. R. and Van Hoosier, M. E., XIX COSPAR Meeting, 8-19 June 1976, Philadelphia, PA.
- 1831 "Spectrophotometry of the Photospheric and Chromospheric Granulation in the UV Region 1240-1650Å," Bartoe, J. -D. F., Brueckner, G. E., Kjeldseth Moe, O., Nicolas, K. R. and Van Hoosier, M. E., XIX COSPAR Meeting, 8-19 June 1976, Philadelphia, PA.
- 1836 "Amplitude Instability and Stochastic Behavior During Magnetic Field Line Reconnection," Spicer, D. S., Solar Physics Div. of 148th A.A.A. Meeting, 21-24 June 1976, Haverford, PA., BAAS 8, 373 (1976).
- 1839 "Final Report on Coronagraph Feasibility Studies for an Out-of-Ecliptic Mission," Bohlin, J. D., Howard, R. A., Koomen, M. J., and Michels, D. J. 'Phase A Final Review of a Joint ESA/NASA Out-of-Ecliptic Mission,' ESA Headquarters, 6-7 April 1976, Paris, France.
- 1847 "Multiple Loop Activations and Continuous Energy Release in a Solar Flare," Widing, K. G., Solar Physics Div. of 148th A.A.S. Meeting, 21-24 June 1976, Haverford, PA., BAAS 8, 375 (1976).
- 1853 "Identification of H α Macrospicules with EUV Macrospicules and with Flares in X-Ray Bright Points," Moore, R. L., Tang, F., Bohlin, J. D. and Golub, L., Solar Physics Div. of 148th A.A.S. Meeting, 21-24 June 1976, Haverford, PA., BAAS 8, 333 (1976).

- 1854 "Observation of a Kink Instability in a Solar Flare," Cheng, C. C., Solar Physics Div. of 148th A.A.S. Meeting, 21-24 June 1976, BAAS 8, 373 (1976).
- 1855 "Preliminary Analysis of NRL Skylab Spectroheliograms in Lines of He I and He II," Mango, S., Bohlin, J. D., Glackin, D. and Linsky, J., Solar Physics Div. of 148th A.A.S. Meeting, 21-24 June 1976, Haverford, PA., BAAS 8, 332 (1976).
- 1856 "Pre-flare Observations During the Evolution of McMath Region 12474 August 7-9, 1973," Scherrer, V., Brueckner, G., Sandlin, G. and Tousey, R., Solar Physics Div. of 148th A.A.S. Meeting, 21-24 June 1976, Haverford, PA., BAAS 8, 373 (1976).
- 1857 "Time Dependent Ionization and Radiation of a Gas Moving through the Solar Transition Zone," Kjeldseth Moe, O., Solar Physics Div. of 148th A.A.S. Meeting, 21-24 June 1976, Haverford, PA., BAAS 8, 331 (1976).
- 1858 "Coronal Lines in ATM Spectra 1100 - 3000 Å," Sandlin, G. D., Brueckner, G. E. and Tousey, R., Solar Physics Div. of 148th A.A.S. Meeting, 21-24 June 1976, Haverford, PA., BAAS 8, 339 (1976).
- 1859 "Spectrophotometry of the Photospheric and Chromospheric Granulation in the UV Region 1240-1650Å," Bartoe, J. -D. F., Brueckner, G. E., Kjeldseth Moe, O., Nicolas, K. R. and Van Hoosier, M. E., Solar Physics Div. of 148th A.A.S. Meeting, 21-24 June 1976, Haverford, PA., BAAS 8, 312 (1976).
- 1860 "The UV Spectrum of a Sunspot (1175 to 1700 Å) Observed with High Spatial and Spectral Resolution," Brueckner, G. E., Nicolas, K. R., Bartoe, J. -D. F. and Van Hoosier, M. E., Solar Physics Div. of 148th A.A.S. Meeting, 21-24 June 1976, Haverford, PA., BAAS 8, 345 (1976).
- 1861 "Densities in the Solar Chromosphere above the Quiet Sun and a Coronal Hole Derived from the Hydrogen Balmer Lines," Rosenberg, F. D., Feldman, U. and Doschek, G. A., Solar Physics Div. of 148th A.A.S. Meeting, 21-24 June 1976, Haverford, PA., BAAS 8, 338 (1976).
- 1865 "Preliminary Analysis of NRL Rocket Spectra of the La Line Wings," Basri, G., Bartoe, J. -D. F., Brueckner, G., Linsky, J. and Van Hoosier, M. E., Solar Physics Div. of 148th A.A.S. Meeting, 21-24 June 1976, Haverford, PA., BAAS 8, 331 (1976).
- 1868 "The Presence of Si I Series in the Ultraviolet Solar Spectrum: 3000Å - 1200Å", Moore, C. E., Brown, C. M., Sandlin, G. D., Tilford, S. G. and Tousey, R., Ap. J. 212, 310 (1977).

- 1904 "Chromospheric Limb Spectra from Skylab: 2000 to 3200Å", Doschek, G. A., Feldman, U. and Cohen, L., Ap. J. 210, 890 (1976).
- 1909 "The Origin of Coronal Holes and a Hypothesis for Their Occurrence During the Solar Cycle", Bohlin, J. D., Topical Conference on Solar and Interplanetary Physics, 12-15 January 1977, Tucson, Arizona, to be published in Bull. of A.A.S.
- 1912 "ATM Skylab Observations of Flare Lyman- α Line Profiles", Canfield, R. C. and Van Hoosier, M. E., Topical Conf. on Solar and Interplanetary Physics, 12-15 January 1977, Tucson, Arizona, to be published in Bull. of A.A.S.
- 1926 "Observations of Coronal Holes Throughout Sunspot Cycle 20", Broussard, R. M., Underwood, J. H., Tousey, R., and Sheeley, N. R., Jr., 149th A.A.S. Meeting, 16-19 Honolulu, Hawaii, BAAS 8, 557 (1976).
- 1927 "Enhancement of Dielectronic Recombination by Plasmas", Jacobs, V. L., Davis, J. and Kepple, P. C., Topical Conf. on Atomic Processes in High Temperature Plasmas of Am. Physical Soc., 16-18 February 1977, Knoxville, Tennessee, to be published in Bull. of A.P.S.
- 1928 "The Influence of Metastable Levels on the Oxygen Impurity Radiation from Flare-like Plasmas", Rogerson, J. E., Davis, J. and Jacobs, V. L., Topical Conf. on Atomic Processes in High Temperature Plasmas of Am. Physical Soc., 16-18 February 1977, Knoxville, Tennessee, to be published in Bull. of A.P.S.
- 1945 "Models of Solar Chromosphere Structures Implied by Lyman- α Rocket Spectra", Basri, G., Linsky, J. L., Bartoe, J. -D. F., Brueckner, G. E. and Van Hoosier, M. E., 149 A.A.S. Meeting, 16-19 January, 1977, Honolulu, Hawaii, BAAS 8, 534 (1976).

IV. PROFESSIONAL TALKS - INVITED

- "The ATM Project", Tousey, R., Symp. on 'Calibration Methods in the UV and X-Ray Regions of the Spectrum', Institut für extra-terrestrische Physik, Max Planck Institut für Physik und Astrophysik, Munich, Germany, 27-30 May 1968.
- 1514 "Identifications in the Solar XUV Spectrum", Tousey, R., 14th Gen. Assembly IAU, Commission 44, University of Sussex, Brighton, England, 20 August 1970.
- "Solar Astronomy, Some Highlights of the Past Year", Tousey, R., 14th Gen. Assembly IAU, IAU Commission 44, University of Sussex, Brighton, England, 20 August 1970.
- 1515 "Survey of New Solar Results", Tousey, R., IAU Symp. 41, 'New Techniques in Space Astronomy', Munich, Germany, 10-14 August 1970.
- 1518 "Solar Spectroscopy from Space Vehicles", Tousey, R., Tenth National Meeting of the Society for Applied Spectroscopy, St. Louis, Missouri, 18-22 October 1971.
- 1522 "High Angular Observations from Rockets: Solar XUV Observations", Tousey, R., COSPAR XII, Seattle, Washington, 17 June - 2 July 1971.
- 1565 "The Coronal Origin of a Solar Flare", Brueckner, G. E., COSPAR XV, Madrid, Spain, 10-24 May 1972.
- Ibid., AAS, Solar Phys. Div., University of Maryland, College Park, Maryland, 4-6 April 1972.
- 1641 "The Extreme Ultraviolet Spectroheliograph and the Extreme Ultraviolet TV Monitor", Tousey, R., Bartoe, J. -D. F., Brueckner, G. E., and Purcell, J. D., Soc. Photo-Optical Instr. Eng., 'Instrumentation in Astronomy - II', Tucson, Arizona, 4-6 March 1974.
- 1642 "The Extreme Ultraviolet Spectrograph", Bartoe, J. -D. F., Brueckner, G. E., Purcell, J. D., and Tousey, R., Soc. Photo-Optical Instr. Eng., 'Instrumentation in Astronomy - II', Tucson, Arizona, 4-6 March 1974.
- 1651 "The Sun as Observed by the ATM XUV Spectroheliograph and Spectrograph, S082A and B", Tousey, R., COSPAR XVII, Sao Paulo, Brazil, 25 June - 1 July 1974.
- 1652 "Preliminary Results from the NRL/ATM Instruments from Skylab 2", Tousey, R., Bartoe, J. -D. F., Bohlin, J. D., Brueckner, G. E., Purcell, J. D., Scherrer, V. E., Schumacher, R. J., Sheeley, N. R., Jr., and Van Hoosier, M. E., IAU Symp. 57, 'Coronal Disturbances', Surfers Paradise, Queensland, Australia, 19 August - 11 September 1973.
- 1658 "Preliminary Results from the Extreme Ultraviolet Spectroheliograph and Ultraviolet Spectrograph on ATM", Tousey, R., AGU, 55th Annual Meeting, Washington, D. C., 8-12 April 1974.

- "Results from the NRL Experiments on Skylab", Tousey, R., Opt. Soc. Am., Washington, D. C., 22 April 1974.
- 1662 "Some NRL/ATM Observations of a Coronal Hole at the Solar Limb", Sheeley, N. R., Jr., 3rd Solar Wind Conf., Asilomar, California, 25-29 March 1974.
- 1668 "Skylab Observations of the Sun (170-630 Å) with the NRL Objective Grating Spectroheliograph", Widing, K. G., Opt. Soc. Am., Houston, Texas, 15-18 October 1974.
- 1671 "Diffraction Gratings for the XUV - Conventional vs. Holographic" Hunter, W. R., Symp. on 'Diffraction Gratings and Grating Instruments', Tokyo, Japan, 31 August 1974.
- 1675 "Ultraviolet Emission Line Profiles of Flares and Active Regions", Brueckner, G. E., IAU/COSPAR Symp. 68, 'Solar Extreme UV, X and Radiation', Buenos Aires, Argentina, 11-14 June 1974.
- 1677 "Fe XXIV Emission in Solar Flares Observed with the NRL/ATM XUV Slitless Spectrograph", Widing, K. G., IAU/COSPAR Symp. 68, 'Solar Extreme UV, X and Radiation', Buenos Aires, Argentina, 11-14 June 1974.
- 1679 "XUV Observations of Coronal Magnetic Fields", Sheeley, N. R., Jr., Bohlin, J. D., Brueckner, G. E., Purcell, J. D., Scherrer, V. E., and Tousey, R., Conf. on 'Flare-Related Magnetic Field Dynamics', Boulder, Colorado, 23 September 1974.
- 1683 "Observations of the Hydrogen Ly- α (1216 Å) Emission Line of Comet Kohoutek (1973f) by the Skylab/ATM S082B Spectrograph", Keller, H. U., Bohlin, J. D., and Tousey, R., Comet Kohoutek Workshop, MSFC, Huntsville, Alabama, 13-14 June 1974.
- 1685 "ATM Observations on the XUV Emission from Flares", Brueckner, G. E., IAU Colloq. 27, 'Fourth Conf. on Ultraviolet and X-Ray Spectroscopy of Astrophysical and Laboratory Plasmas', Harvard University, Cambridge, Massachusetts, 9-11 September 1974.
- Ibid., 'Solar Physics - Plasma Physics Workshop', Stanford University, Stanford, California, 17-20 September 1974.
- 1690 "Ultraviolet Observations of Solar Flares from Skylab", Brueckner, G. E., Royal Society Discussion Meeting 'The Physics of the Solar Atmosphere', London, England, 14-15 January 1975.
- 1691 "Eruptive Prominences Recorded by the XUV Spectroheliograph on Skylab", Tousey, R., Royal Society Discussion Meeting, 'The Physics of the Solar Atmosphere', London, England, 14-15 January 1975.
- 1715 "XUV Results from Skylab", Tousey, R., International Conf. on 'X-Rays in Space', University of Calgary, Calgary, Alberta, Canada, 14-21 August 1974.

- 1733 "XUV Emission from Above the West Limb Near 20:00 U. T., January 17, 1974", Tousey, R., IAU Colloq. 27, 'Fourth Conf. on Ultraviolet and X-Ray Spectroscopy of Astrophysical and Laboratory Plasmas', Cambridge, Massachusetts, 9-11 September 1974.
- 1734 "A Review of Skylab/ATM Observations and Analyses of Coronal Transients", Gosling, J. T., Bohlin, J. D., Krieger, A. S., Schmahl, E. J., Tandberg-Hanssen, E., COSPAR XVIII, Varna, Bulgaria, 29 May - 7 June 1975.
- 1748 "The Interpretation of Ultraviolet Solar Spectra", Moore-Sitterly, C. E., Twentieth Liege International Astrophysical Symp., Liege, Belgium, 17-20 June 1975.
- 1749 "Coronal Changes Associated With a Disappearing Filament", Sheeley, N. R., Jr., Bohlin, J. D., Brueckner, G. E., Purcell, J. D., Scherrer, V. E., Tousey, R., Smith, J. B., Jr., Speich, D. M., Tandberg-Hanssen, E., Wilson, R. M., de Loach, A. C., Hoover, R. B., and McGuire, J. P., Annual Meeting of HAO, SPO, KPNO, Santa Fe, New Mexico, 23 May 1975.
- 1760 "Absolute Solar Intensities 1750 Å - 2100 Å and Their Variations with Solar Activity", Brueckner, G. E., Bartoe, J.-D. F., Moe, O. K., Van Hoosier, M. E., 'Workshop on the Solar Constant and the Earth's Atmosphere', Big Bear Solar Observatory, Big Bear City, California, 19-21 May 1975.
- 1774 "First Results from Skylab", Tousey, R., AAS, Tucson, Arizona, 2-6 December 1973.
- 1778 "Absolute Calibrated Solar UV Intensities 1700 to 2100 Å", Moe, O. K., Opt. Soc. Am., Houston, Texas, 15-18 October 1974.
- 1781 "Evidence for Non-Hydrostatic Equilibrium Conditions in the Transition Region", Brueckner, G. E., 'Solar Physics - Plasma Physics Workshop', Stanford University, Stanford, California, 17-20 September 1974.
- 1784 "Spectroscopic Far Ultraviolet Observations of Active Regions Prior to and During Flares", Brueckner, G. E., Patterson, N. P., Scherrer, V. E., 'Flare Build-up Study Workshop', Falmouth, Cape Cod, Massachusetts, 8-11 September 1975.
- 1786 "Solar Research with Diffraction Gratings in the Far Ultraviolet", Brueckner, G. E., U. S. -Japan Seminar on Diffraction Gratings, Washington, D. C., 14-17 October 1975.
- "Photospheric Magnetic Field and Its Coronal Extension", Sheeley, N. R., Jr., AAS, Solar Physics Div., 20 January 1975.

- 1838 "Mechanisms for Particle Acceleration in Solar Flares," Spicer, D. S., Goddard Space Flight Center/University of Maryland High Energy Astrophysics Seminar, 15 March 1976.
- 1840 "Resistive Kink Model of a Solar Flare," Spicer, D. S., Bartol Institute, Swarthmore, Pennsylvania, 17 February 1976.
- 1841 "The Morphology and Evolution of Coronal Holes," Bohlin, J. D., Coll. at Observatoire de Paris, Paris, France, 9 April 1976.
- 1862 "Spectroscopic Ultraviolet Observations of Flares from Skylab," Brueckner, G. E., U. S. -Japan Cooperative Seminar on "High Energy Phenomena in Solar Flares," 10-13 May 1976, Tokyo, Japan.
- 1863 "Skylab Spectroheliograph Observations of the Double Ribbon Flare of 1973 June 15," Widing, K. G., U. S. -Japan Cooperative Seminar on "High Energy Phenomena in Solar Flares," 10-13 May 1976, Tokyo, Japan.
- 1870 "The Physical Properties of Coronal Holes," Bohlin, J. D., AGU International Sym. on Solar-Terrestrial Physics, 7-18 June 1976, Boulder, Colorado.
- 1878 "The Thermal and Non-Thermal Flare: A Result of Non-Linear Threshold Phenomena," Spicer, D. S., I.A.U. Commission #14, 25 August 1976, Grenoble, France.
- 1891 "Multiple Loop Activations and Continuous Energy Release in a Solar Flare", Widing, K. G., XVI General Assembly, I.A.U., 24 August - 2 September 1976, Grenoble, France.
- 1895 "Analyses of Laboratory Spectra of Special Interest for the Interpretation of Ultraviolet Stellar Spectra," Moore-Sitterly, C. and Widing, K., I.A.U. Commission #14, 25 August 1976, Grenoble, France.
- "The Prime Energy Release and Subsequent Flare Development", Brueckner, G. E., I.A.U. Commission #10, 24 August - 2 September 1976, Grenoble, France.
- "High Spatial Resolution UV Spectroscopy of the Sun", Brueckner, G. E., I.A.U. Commission #44, 24 August - 2 September 1976, Grenoble, France.
- 1907 "Detecting Ultraviolet Radiation from and through the Atmosphere", Prinz, D. K., 20th Annual Technical Symposium of the Society of Photo-Optical Instrumentation Engineers, 26 August 1976, San Diego, California.
- 1915 "A Random Walk Through the Results of the Solar Experiments of the Skylab Mission", Bohlin, J. D., National Capital Section of Opt. Soc. of Am., 25 January 1977, Washington, D. C.

- 1923 "The Phenomenon of 'Overlapping of Resonances' as Applied to Magnetic Reconnection Problems in Space", Spicer, D. S., N. C. Christophilos International Summer School and Conference on Laboratory and Space Plasmas, 20-30 July 1977, Spetses, Greece.
- 1925 "A Survey of Coronal Holes and Their Solar Wind Associations Throughout Sunspot Cycle 20", Sheeley, N. R., Jr., Topical Conf. on Solar and Interplanetary Physics, 12-15 January 1977, Tucson, Arizona.
- 1929 "An Arch Model of a Solar Flare", Spicer, D. S., High Altitude Observatory, 3 March 1977, Boulder, Colorado.

V. PROFESSIONAL TALKS - CONTRIBUTED

- 1420 "Some Recent XUV Spectroheliograms and Heliograms from Rockets," Purcell, J. D., Bartoe, J. -D. F., Snider, C. B., and Tousey, R., Second International Conf. on 'Vacuum Ultraviolet and X-Ray Spectroscopy of Laboratory and Astrophysical Plasmas', University of Maryland, 24-28 March 1968.
- 1469 "Radiation Light Sources for Stellar Telescope Calibration from 700 Å to 7000 Å," Hunter, W. R., Workshop on Optical Telescope Technology, MSFC, Huntsville, Alabama, May 1969.
- 1471 "Some Experiments on the Corona Surrounding a Spacecraft - Past, Planned and Proposed," Tousey, R., Opt. Soc. Am. Symp. on 'Optical Contamination in Space', Aspen, Colorado, 13-15 August 1969.
- 1479 "A Photographic Spectrum of a Flare in the XUV," Purcell, J. D. and Tousey, R., International Symp. on Solar Terrestrial Physics, Leningrad, U.S.S.R., 13 May 1970.
- 1481 "Observations of the Sun in the Extreme Ultraviolet," Tousey, R., Meeting of the Royal Society, London, England, 21-22 April 1970.
- 1499 "Observation of Stark-Effect in a Far UV Flare Spectrum," Brueckner, G. E., 14th Gen. Assembly IAU, University of Sussex, Brighton, England, 18-27 August 1970.
- 1509 "Absolute Intensity of the Continuum in the Ultraviolet Spectrum of the Sun Between 1650-1800 Å," Brueckner, G. E., Moe, O. K., Pitz, E., AAS, Solar Phys. Div., Huntsville, Alabama, 17 November 1970.
- 1510 "High Spectral and Spatial Resolution Ultraviolet Spectroscopy of the Sun in the Region 1170-1800 Å," Brueckner, G. E., AAS, Solar Phys. Div., Huntsville, Alabama, 17 November 1970.
- 1529 "On the Classification of Some Highly Ionized Iron and Nickel Lines in the 200-400 Å Region of the Solar Spectrum," Widing, K. G., Sandlin, G. D., and Cowan, R. D., Third Symp. on 'Ultraviolet and X-Ray Spectroscopy of Astrophysical and Laboratory Plasmas', Utrecht, The Netherlands, 24-26 August 1971.
- 1536 "XUV Television of a Solar Image from a Rocket," Tousey, R., Symp. on 'The Processing of Telescopic Images', Laval University, Quebec, Quebec, Canada, 1-2 October 1971.
- 1538 "Possibilities for Measuring Atmospheric Extinction and Absorption with the ATM Solar Experiments in Skylab," Tousey, R., Informal Conf. on 'The Uses of Astronomy in the Study of Air Pollution' Project, Seattle, Washington, 19 August 1971.
- 1544 "Extreme Ultraviolet Spectroheliograms of a Solar Flare," Purcell, J. D. and Tousey, R., AAS, 136th meeting, San Juan, Puerto Rico, 6-8 December 1971.

- 1545 "Preliminary Results of Identifications in the XUV Spectrum of a Solar Flare," Purcell, J. D., Tousey, R., and Widing, K. G., AAS, San Juan, Puerto Rico, 6-8 December 1971.
- 1572 "A Recalibration of Spectral Radiance of Mercury and Deuterium Arc Standard Lamps in the Near UV," Bartoe, J. -D. F. and Ott, W. R., Opt. Soc. Am., San Francisco, California, 17-20 October 1972.
- 1606 "The Increase in Transmittance of Unbacked Aluminum Filters Exposed to RF and DC Discharge in Oxygen," Hunter, W. R., Steele, G. N., and Gillette, R. B., Opt. Soc. Am., Rochester, New York, 9-12 October 1973.
- 1623 "The 1175 Å to 1900 Å Ultraviolet Spectrum of Solar Flares," Brueckner, G. E., Bohlin, J. D., Moe, C. K., Nicolas, K. R., Purcell, J. D., Scherrer, V. E., Sheeley, N. R., Jr., and Tousey, R., AAS, Solar Phys. Div., Honolulu, Hawaii, 9-11 January 1974.
- 1624 "Electron Density from Line Ratios in the XUV Spectrum of a Solar Flare," Widing, K. G., Purcell, J. D., and Tousey, R., AAS, Solar Phys. Div., Honolulu, Hawaii, 9-11 January 1974.
- 1625 "The Screw Pinch and the Solar Flare," Spicer, D. S. and Cheng, C. C., AAS, Solar Phys. Div., 9-11 January 1974.
- 1626 "A Preliminary Study of Coronal Structures by Means of Time-Lapse Photography," Sheeley, N. R., Jr., Bohlin, J. D., Brueckner, G. E., Purcell, J. D., Scherrer, V. E., and Tousey, R., AAS, Solar Phys. Div., 9-11 January 1974.
- 1628 "Rocket Spectroheliogram Observations of the Heights of Formation and Sizes of Bright Features in the Transition Zone," Simon, G. W., Seagraves, P. H., and Tousey, R., AAS, Solar Phys. Div., Honolulu, Hawaii, 9-11 January 1974.
- 1629 "Cinematographic Observations for ATM and their Comparison with some ATM Results," Zirin, H., Holt, J., Brueckner, G. E., Bohlin, J. D., Purcell, J. D., Scherrer, V. E., Sheeley, N. R., Jr., and Tousey, R., AAS, Solar Phys. Div., Honolulu, Hawaii, 9-11 January 1974.
- 1637 "Studies of Atmospheric Extinction from Skylab," Brown, C. M., Tousey, R., Tilford, S. G., and Prinz, D. K., AGU, 55th Annual Meeting, Washington, D. C., 8-12 April 1974.
- 1640 "Coronal Extreme Ultraviolet Spectroheliograph and Chromospheric Extreme Ultraviolet Spectrograph," Tousey, R., AAS, Solar Phys. Div., Honolulu, Hawaii, 9-11 January 1974.
- 1643 "Oxygen Densities at Altitudes Between 70 and 129 km," Brueckner, G. E., Bartoe, J. -D. F., Brown, C. M., Prinz, D. K., Tilford, S. G., and Van Hoosier, M. E., COSPAR XVII, Sao Paulo, Brazil, 25 June - 1 July 1974.

- 1646 "Ultraviolet Emission Line Profiles of Flares and Flare-Like Events Observed from Skylab," Brueckner, G. E., Moe, O. K., and Nicolas, K. R., COSPAR XVII, Sao Paulo, Brazil, 25 June - 1 July 1974.
- 1647 "On the Fe XXIV Emission in the Solar Flare of June 15, 1973," Widing, K. G. and Cheng, C. C., COSPAR XVII, Sao Paulo, Brazil, 25 June - 1 July 1974.
- 1650 "Structure of the Sun's Polar Cap in the Wavelengths 240-600 Å," Bohlin, J. D., Sheeley, N. R., Jr., and Tousey, R., COSPAR XVII, Sao Paulo, Brazil, 25 June - 1 July 1974.
- 1655 "Implications of NRL/ATM Solar Flare Observations on Flare Theories," Cheng, C. C. and Spicer, D. S., IAU/COSPAR Symp. 68, 'Solar Extreme UV, X and γ Radiation', Buenos Aires, Argentina, 11-14 June 1974.
- 1657 "Skylab Observation of the White Light Corona and the He II 304 Å Chromosphere During the Eruptive Prominence Event of August 21, 1973," Bohlin, J. D., Brueckner, G. E., Purcell, J. D., Scherrer, V. E., Sheeley, N. R., Jr., Tousey, R., and Poland, A. I., AGU, 55th Annual Meeting, Washington, D. C., 8-12 April 1974.
- 1657 "The Eruptive Prominence of August 21, 1973, Observed from Skylab in the White Light Corona and in the He II 304 Å Chromosphere," Poland, A. I., Bohlin, J. D., Brueckner, G. E., Purcell, J. D., Scherrer, V. E., Sheeley, N. R., Jr., and Tousey, R., AAS, Lincoln, Nebraska, 26-29 March 1974.
- 1666 "Some Reflections on the Use of Conventional and Holographic Diffraction Gratings in the Vacuum Ultraviolet Spectral Region," Hunter, W. R., IV International Conf. on Vacuum-Ultraviolet Radiation Physics, Hamburg, Germany, 22-26 July 1974.
- 1673 "Flare-Like Ultraviolet Spectra of Active Regions," Brueckner, G. E., IAU/COSPAR Symp. 68, 'Solar Extreme UV, X and γ Radiation', Buenos Aires, Argentina, 11-14 June 1974.
- 1678 "Flares Observed by the NRL/ATM Spectrograph and Spectroheliograph During the Skylab Missions," Scherrer, V. E. and Tousey, R., International Conf. on 'X-Rays in Space', University of Calgary, Calgary, Alberta, Canada, 14-21 August 1974.
- 1681 "The Impact of ATM/NRL Flare Data on Flare Theory," Spicer, D. S., Cheng, C. C., Widing, K. G., and Tousey, R., Second European Conf. on Cosmic Plasma Physics, Culham, England, 1 July 1974.
- "Diffraction Gratings in Space Research - Problems and Accomplishments," Hunter, W. R., Informal meeting on Diffraction Gratings, Kyoto, Japan, 6 September 1974.

- 1684 "High Resolution Ly- α Observations of Comet Kohoutek by Skylab and Copernicus," Bohlin, J. D., Drake, J. F., Jenkins, E. B., and Keller, H. U., IAU Colloq. 25, Goddard Space Flight Center, Greenbelt, Maryland, 28 October - 1 November 1974.
- 1689 "Ultraviolet Solar Identifications Based on Extended Absorption Series Observed in the Laboratory Spectra of Si I," Moore, C. E., Tousey, R., Sandlin, G. D., Brown, C. M., Ginter, M. L., and Tilford, S. G., IAU Colloq. 27, 'Fourth Conf. on Ultraviolet and X-Ray Spectroscopy of Astrophysical and Laboratory Plasmas', Harvard University, Cambridge, Massachusetts, 9-11 September 1974.
- 1696 "A Catalog and Classification of Flares and Flare-Like Events Observed by the ATM XUV Spectrograph S082A and Spectroheliograph S082B," Scherrer, V. E., Tousey, R., and Sandlin, G. D., AAS, Solar Phys. Div., Boulder, Colorado, 20-22 January 1975.
- 1697 "Polar Plumes in XUV Emission-Line Corona," Bohlin, J. D., Purcell, J. D., Sheeley, N. R., Jr., and Tousey, R., AAS, Solar Phys. Div., Boulder, Colorado, 20-22 January 1975.
- 1698 "Macro-Spicules in He II 304 Å Over the Sun's Polar Cap," Bohlin, J. D., Vogel, S. N., Purcell, J. D., Sheeley, N. R., Jr., Tousey, R., and Van Hoosier, M. E., AAS, Solar Phys. Div., Boulder, Colorado, 20-22 January 1975.
- 1699 "Flare Mechanisms Based on the Current Limitation Concept," Spicer, D. S., AAS, Solar Phys. Div., Boulder, Colorado, 20-22 January 1975.
- 1700 "Absolute Solar UV Intensities 1680 Å to 2100 Å," Moe, O. K., Brueckner, G. E., Bartoe, J. -D. F., and Van Hoosier, M. E., AAS, Solar Phys. Div., Boulder, Colorado, 20-22 January 1975.
- 1701 "On the XUV Emissions in Solar Flares Observed with the ATM/NRL Spectroheliograph," Cheng, C. C. and Widing, K. G., AAS, Solar Phys. Div., Boulder, Colorado, 20-22 January 1975.
- 1703 "Observations from Skylab of the Density Dependent C III Multiplet at 1175 Å in Active and Quiet Regions and Above the Limb," Nicolas, K. and Brueckner, G. E., AAS, Solar Phys. Div., Boulder, Colorado, 20-22 January 1975.
- 1705 "The High-Energy Limb Event of January 17, 1974," Tousey, R., Bohlin, J. D., Moe, O. K., Purcell, J. D., and Sheeley, N. R., Jr., AAS, Solar Phys. Div., Boulder, Colorado, 20-22 January 1975.
- 1706 "Interpreting XUV Spectroheliograms in Terms of Coronal Magnetic Field Structures," Sheeley, N. R., Jr., Bohlin, J. D., Brueckner, G. E., Purcell, J. D., Scherrer, V. E., and Tousey, R., AAS, Solar Phys. Div., Boulder, Colorado, 20-22 January 1975.

- 1707 "Line Profiles of the Fe XXIV Emission at 192 Å and 255 Å in Solar Flares," Brueckner, G. E., Moe, O. K., and Van Hoosier, M. E., AAS, Solar Phys. Div., Boulder, Colorado, 20-22 January 1975.
- 1712 "The Super Heating Instability as a Trigger for Solar Flares," Tidman, D. A., Spicer, D. S., and Davis, J., AAS, Solar Phys. Div., Boulder, Colorado, 20-22 January 1975.
- 1714 "Forbidden Lines of Highly Ionized Iron in Solar Flare Spectra," Döschek, G. A., Sandlin, G. D., Brueckner, G. E., Van Hoosier, M. E., and Tousey, R., IAU Colloq. 27, 'Fourth Conf. on Ultra-violet and X-Ray Spectroscopy of Astrophysical and Laboratory Plasma', Harvard University, Cambridge, Massachusetts, 9-11 September 1974.
- 1716 "The XUV Sun as Observed by ATM S082," Tousey, R., AIAA/AGU Space Science Conf. on 'Scientific Experiments of Project Skylab', MSFC, Huntsville, Alabama, 30 October- 1 November 1974.
- 1718 "Classification of Flares and Flare-Like Events Observed by the ATM XUV Spectroheliograph S082A and Spectrograph S082B During the Skylab Missions," Scherrer, V. E. and Tousey, R., AIAA/AGU Space Science Conf. on 'Scientific Experiments of Project Skylab', MSFC, Huntsville, Alabama, 30 October-1 November 1974.
- 1726 "Structure and Temperature of Solar Flare Plasma," Scherrer, V. E. and Sandlin, G. D., Am. Phys. Soc., Washington, D. C., 28 April - 1 May 1975.
- 1731 "The Character and Temperature of a Coronal Transient: I. The Event of 25-27 August 1973," Bohlin, J. D., Hildner, E., and Hansen, R. T., COSPAR XVIII, Varna, Bulgaria, 29 May - 7 June 1975.
- 1738 "Experience with Schumann Type UV Film on Skylab," Van Hoosier, M. E., Bartoe, J.-D. F., Brueckner, G. E., Moe, O. K., Nicolas, K. R., and Tousey, R., Topical Meeting on 'Imaging in Astronomy', Harvard University, Cambridge, Massachusetts, 18-20 June 1975.
- 1739 "Limitations of Imaging Capabilities of Schumann Type UV Film," Bartoe, J.-D., Brueckner, G. E., and Van Hoosier, M. E., Topical Meeting on 'Imaging in Astronomy', Harvard University, Cambridge, Massachusetts, 18-20 June 1975.
- 1750 "A Resistive Screw Instability Model of a Solar Flare," Spicer, D. S., AAS, San Diego, California, 17-20 August 1975.

- 1752 "The Sun's Polar Caps as Coronal Holes; Their Sizes, Evolution, and Phenomenology During the Skylab Mission," Bohlin, J. D., Rubenstein, D. M., and Sheeley, N. R., Jr., AAS, San Diego, California, 17-20 August 1975.
- 1753 "Energy Release and Thermal Structure in Solar Flares," Cheng, C. C. and Widing, K. G., AAS, San Diego, California, 17-20 August 1975.
- 1754 "X-Ray Event of August 13-15, 1973," Scherrer, V. E., Sandlin, G. D., Sheeley, N. R., Jr., and Tousey, R., AAS, San Diego, California, 17-20 August 1975.
- 1756 "Skylab/ATM Observations of Transient Events Having the GRF X-Ray and Microwave Character," Sheeley, N. R., Jr., Bohlin, J. D., Scherrer, V. E., and Tousey, R., AAS, San Diego, California, 17-20 August 1975.
- 1757 "Measured Variation of the XUV Line Widths and Intensities Near the Solar Limb," Moe, O. K. and Nicolas, K. R., AAS, San Diego, California, 17-20 August 1975.
- 1758 "Evolution of XUV Plasmas in Solar Flares," Widing, K. G. and Cheng, C. C., AAS, San Diego, California, 17-20 August 1975.
- 1768 "Solar Flare Collisional Excitation Rate Coefficients," Tousey, R., Kepple, P. C., and Davis, J., AAS, San Diego, California, 17-20 August 1975.
- 1769 "Plasma Heating and Flare X-Rays," Davis, J., Kepple, P., Strickland, D., and Brueckner, G., AAS, San Diego, California, 17-20 August 1975.
- 1770 "Hydrodynamics of Electron Beam Deposition in Solar Flares," Bloomberg, H., Kepple, P. C., Davis, J., Boris, J. and Brueckner, G., AAS, San Diego, California, 17-20 August 1975.
- 1771 "Results from the NRL XUV Experiments on Skylab," Tousey, R., Opt. Soc. Am., Washington, D. C., 21-25 April 1974.
- 1772 "Maximum Efficiency of Ruled Concave Diffraction Gratings in the Ultraviolet," Mikes, T. L., Opt. Soc. Am., Houston, Texas, 15-18 October 1974.
- 1776 "Time Dependent Ionization Equilibrium and Line Emission from Ionized Iron Under Flare-Like Conditions," Kepple, P. and Davis, J., AGU, San Francisco, California, December 1974.
- 1777 "Transient Line Emission from Ionized Iron Under Flare-Like Conditions," Davis, J., Kepple, P., and Tousey, R., AAS, Solar Phys. Div., Boulder, Colorado, 20-22 January 1975.

VI. COLLOQUIA

- 1465 "Apollo Telescope Mount Project", Winter, T. C., National Bureau of Standards, Washington, D. C., 27 February 1969.
- 1635 "The Sun in Lyman-Alpha", Prinz, D. K., National Capitol Section of the Amateur Astronomers of America, 2 February 1974.
- 1661 "NRL/ATM Observations with the XUV Spectroheliograph", Sheeley, N. R., Jr., Sacramento Peak Observatory, Sunspot, New Mexico, 15 March 1974.
- 1708 "Observations of the Sun in XUV with ATM", Tousey, R., Goddard Space Flight Center, Greenbelt, Maryland, 6 December 1974.
- "Observations of the Sun in XUV with ATM", Tousey, R., University of Michigan, Ann Arbor, Michigan, 12 February 1975.
- 1728 "Preliminary Results from the NRL XUV Spectroheliograph and Spectrograph", Bohlin, J. D., University of Maryland, College Park, Maryland, 26 February 1975.
- 1737 "Behavior of Coronal Magnetic Fields as Deduced from Skylab Observations", Sheeley, N. R., Jr. High Altitude Observatory, Boulder, Colorado, 14 March 1975.
- 1767 "Macrospicules, Polar Plumes, Coronal Holes, and Other Assorted Phenomena of the Sun's Polar Cap", Bohlin, J. D., National Capital Astronomers, Washington, D.C., 6 September 1975.
- "The Structure and Development of Coronal Magnetic Fields as Deduced from Skylab Observations", Sheeley, N. R., Jr., Los Alamos Scientific Laboratory, Los Alamos, New Mexico, 21 March 1975.

VII. OTHER PUBLICATIONS

- 1438 "Effects of High-Energy Protons on Photographic Film", Winter, T. C., Jr. and Brueckner, G. E. 1969, NRL Report No. 6797.
- 1455 "DOD Solar Experiments in NASA Prototype Space Station", Winter, T. C., Jr. 1970, Military Review, February, p. 58.
- 1469 "Radiation Light Sources for Stellar Telescope Calibration from 700 Å to 7000 Å", Hunter, W. R. 1969, NRL Progress Report, September, p. 1.
- 1476 "Spectroscopy in the Space Science Division of the Naval Research Laboratory", Hunter, W. R. and Winter, T. C., Jr. 1969, ONR Reviews.
- 1500 "Schumann-Type Photographic Film: Preliminary Environment Test Results", Winter, T. C. and Van Hoosier, M. E. 1970, Report of NRL Progress, May.
- 1504 "Schumann-Type Photographic Film: Preliminary Environment Test Results", Winter, T. C. and Van Hoosier, M. E. 1970, NRL Report No. 7072.
- 1764 "The NRL Solar Experiments in the Apollo Telescope Mount of Skylab", Tousey, R. 1975, Report of NRL Progress, April, p. 1.
- 1823 "Electron Impact Excitation Rate Coefficients for Ions of Solar Interest", Kepple, P. C., Davis, J. and Blaha, M. 1975, NRL Memorandum Report 3171, Nov.
- 1890 "A Spectral Atlas of the Sun Between 1175Å and 2100Å", Kjeldseth Moe, O., Van Hoosier, M. E., Bartoe, J. -D. F. and Brueckner, G. E. 1976, NRL Report No. 8057.
- 1896 "Holes in the Corona", Bohlin, J. D. 1976, Natural History 85, pp. 69-70.
- 1903 "An Unstable Arch Model of a Solar Flare", Spicer, D. S. 1976, NRL Report No. 8036.
- "NRL/ATM User's Guide to Experiment S082A", Packer, I. G. Patterson, N. P., Mango, S. A. and Tousey, R. NRL Memorandum Report No. 3410, Nov. 1976.
- "Flare Atlas and User's Instruction Guide for NRL Flare Data of 15 June, 5 and 7 September 1973", Scherrer, V. E. and Sandlin, G. D., NRL Instruction Book No. 161, May 1976.

VII. OTHER PUBLICATIONS

- 1438 "Effects of High-Energy Protons on Photographic Film", Winter, T. C., Jr. and Brueckner, G. E. 1969, NRL Report No. 6797.
- 1455 "DOD Solar Experiments in NASA Prototype Space Station", Winter, T. C., Jr. 1970, Military Review, February, p. 58.
- 1469 "Radiation Light Sources for Stellar Telescope Calibration from 700 Å to 7000 Å", Hunter, W. R. 1969, NRL Progress Report, September, p. 1.
- 1476 "Spectroscopy in the Space Science Division of the Naval Research Laboratory", Hunter, W. R. and Winter, T. C., Jr. 1969, ONR Reviews.
- 1500 "Schumann-Type Photographic Film: Preliminary Environment Test Results", Winter, T. C. and Van Hoosier, M. E. 1970, Report of NRL Progress, May.
- 1504 "Schumann-Type Photographic Film: Preliminary Environment Test Results", Winter, T. C. and Van Hoosier, M. E. 1970, NRL Report No. 7072.
- 1764 "The NRL Solar Experiments in the Apollo Telescope Mount of Skylab", Tousey, R. 1975, Report of NRL Progress, April, p. 1.
- 1823 "Electron Impact Excitation Rate Coefficients for Ions of Solar Interest", Kepple, P. C., Davis, J. and Blaha, M. 1975, NRL Memorandum Report 3171, Nov.
- 1890 "A Spectral Atlas of the Sun Between 1175Å and 2100Å", Kjeldseth Moe, O., Van Hoosier, M. E., Bartoe, J.-D. F. and Brueckner, G. E. 1976, NRL Report No. 8057.
- 1896 "Holes in the Corona", Bohlin, J. D. 1976, Natural History 85, pp. 69-70.
- 1903 "An Unstable Arch Model of a Solar Flare", Spicer, D. S. 1976, NRL Report No. 8036.
- "NRL/ATM User's Guide to Experiment S082A", Packer, I. G. Patterson, N. P., Mango, S. A. and Tousey, R. NRL Memorandum Report No. 3410, Nov. 1976.
- "Flare Atlas and User's Instruction Guide for NRL Flare Data of 15 June, 5 and 7 September 1973", Scherrer, V. E. and Sandlin, G. D., NRL Instruction Book No. 161, May 1976.

Appendix E. Line Lists for SO82B Data

The following tables have been extracted from the references given. Additional data concerning the measurements or theoretical techniques involved may be obtained from the published papers. References to studies of specific ions or solar phenomena may be found in the Bibliography, Appendix D.

E.1.1 (DFVB)

"The Emission Line Spectrum Above the Limb of the Quiet Sun: 1175-1940 Angstroms," G. A. Doschek, U. Feldman, M. E. VanHoosier and J.-D. F. Bartoe. Ap. J. Supp. Series 31, p. 417 (1976).

TABLE 2 (DFV13)
STRONG SOLAR LINES 4 ARC SECONDS ABOVE THE LIMB

Ion	λ (Å) (Lab)	λ (Å) (Solar)	Int.*	Ion	λ (Å) (Lab)	λ (Å) (Solar)	Int.*
C III.....	1174.933	1174.94	1.1	S IV.....	1404.77	1404.79	1.8
C III.....	1175.263	1175.27	0.90	O IV.....	1404.812		
C III.....	1175.590	1175.64	B2.0	S IV.....	1406.00	1406.04†	0.73
C III.....	1175.711	1175.73	B2.0	O IV.....	1407.386	1407.38	0.66
C III.....	1175.987	1175.99	B0.83	Ni II.....	1411.071	1411.05	0.14
C III.....	1176.370	1176.37	0.95	Fe II.....	1412.834	1412.83	0.14
S III.....	1190.17	1190.20†	0.088	S IV.....	1416.94	1416.92	0.36
		1190.49	0.046			1423.86	0.088
S III.....	1194.02	1194.07†	0.12	Fe II.....	1424.716	1424.71	0.13
S III.....	1194.40	1194.39	0.063	Fe II.....	1434.994	1434.98	0.10
Fe II.....	1194.66	1194.63**	0.063	Fe II.....	1442.746	1442.75	0.051
		1199.17	0.28	Si III.....	1447.196	1447.23	0.056
S III.....	1200.97	1200.97	0.43	Ni II.....	1454.852	1454.84	0.20
S III.....	1201.71	1201.73	0.056	C I.....	1459.032	1459.03	0.036
		1204.31†	0.17	C I.....	1463.336	1463.34	0.11
Si III.....	1206.510	1206.52	2.5	Ni II.....	1467.265	1467.27	0.094
La.....	1215.67	1215.64	42	C I.....	1467.402	1467.40	0.075
O V.....	1218.406	1218.35§	2.9	Ni II.....	1467.762	1467.75	0.11
N V.....	1238.821	1238.82	3.6	S I.....	1472.972	1472.96	0.069
N V.....	1242.804	1242.81	2.0	S I.....	1473.995	1473.99	0.059
C III.....	1247.383	1247.38	0.14	C I.....	1481.763	1481.76	0.10
S II.....	1250.50	1250.58†	0.18	N IV.....	1486.496	1486.51	1.54
S II.....	1253.79	1253.81	0.35	N I.....	1492.625	1492.63	0.069
C I.....	1256.498	1256.47	0.034	Ni II.....	1500.437	1500.44	0.16
S II.....	1259.53	1259.52	0.43			1501.81	0.094
Si II.....	1260.421	1260.41	0.13	Ni II.....	1502.150	1502.15	0.094
Si II.....	1264.737	1264.74	0.33	Ni II.....	1510.859	1510.86	0.11
Si II.....	1265.001	1265.08	B0.16	Si II.....	1526.708	1526.71	0.58
C I.....	1274.984	1274.98	0.041	Si II.....	1533.432	1533.44	0.58
C I.....	1288.422	1288.42	0.041	Ni II.....	1536.746	1536.74	0.081
Si III.....	1294.543	1294.55	0.40	P II.....	1542.29	1542.31	0.056
Si III.....	1296.726	1296.73	0.28	C IV.....	1548.185	1548.19	21.6
Si III.....	1298.891			Fe II.....	1550.260	1550.29	B
	1298.960}	1298.94	1.2	C IV.....	1550.774	1550.79	14.1
		1300.90	0.046	Fe II.....	1551.933	1551.93	0.088
Si III.....	1301.146	1301.15	0.11	Fe II.....	1558.690	1558.62	B0.40
O I.....	1302.169	1302.17	1.24	Fe II.....	1559.084	1559.09	1.3
Si III.....	1303.320	1303.32	0.35	C I.....	1560.309	1560.30	0.34
Si II.....	1304.372	1304.37	0.24	C I.....	1560.69	1560.69	B0.35
O I.....	1304.857	1304.86	1.3	C I.....	1561.438	1561.42	0.39
Si II.....	1305.590	1305.58	0.063	Fe II.....	1563.788	1563.79	1.2
O I.....	1306.029	1306.03	1.3	Fe II.....	1565.374	1565.35	0.088
Si II.....	1309.277	1309.29	0.27	Fe II.....	1566.819	1566.82	0.81
C I.....	1311.363	1311.35	0.046	Fe II.....	1568.016	1568.02	0.31
Si III.....	1312.590	1312.58	0.16	Fe II.....	1569.674	1569.67	0.61
Ni II.....	1317.220	1317.21	0.25	Fe II.....	1570.242	1570.24	0.88
C II.....	1323.93	1323.92	B0.25	Fe II.....	1573.825	1573.83	0.35
C I.....	1328.833	1328.81	0.038	Fe II.....	1574.03	1574.02**	0.23
C I.....	1329.10	1329.14	B0.045	Fe II.....	1574.768	1574.78	B
C I.....	1329.59	1329.55	B0.048	Fe II.....	1574.923	1574.91	1.1
C II.....	1334.532	1334.53	4.0			1576.65	0.15
Ni II.....	1335.203	1335.21	B0.16	Fe II.....	1577.166	1577.16	0.28
C II.....	1335.707	1335.71	5.0	Fe II.....	1578.497	1578.49	0.088
P III.....	1344.34	1344.32	0.051	Fe II.....	1580.625	1580.62	0.77
O I.....	1355.598	1355.58	0.78	Fe II.....	1584.949	1584.95	0.81
C I.....	1355.844	1355.83	0.069			1586.53	0.088
O I.....	1358.512	1358.49	0.18	Fe II.....	1588.286	1588.29	0.58
Fe II.....	1360.18	1360.16**	0.12	Fe II.....	1600.02	1600.01	0.088
Fe II.....	1361.372	1361.36	0.15	Fe II.....	1602.51	1602.51**	0.19
Fe II.....	1368.098	1368.07	0.075	Fe II.....	1605.318	1605.32	0.063
Ni II.....	1370.136	1370.12	0.21	Fe II.....	1608.456	1608.46	0.39
O V.....	1371.292	1371.29	0.70	Fe II.....	1610.921	1610.92	0.61
Fe II.....	1379.60	1379.60**	0.059	Fe II.....	1611.21	1611.19	0.28
Ni II.....	1381.295	1381.28	0.11	Fe II.....	1612.802	1612.81	1.0
Fe II.....	1387.22	1387.20	0.046	Fe II.....	1616.65	1616.65	0.069
Fe II.....	1392.82	1392.80	0.094	Fe II.....	1618.470	1618.47	0.28
Ni II.....	1393.330	1393.33	B	Fe II.....	1621.24	1621.25**	0.081
Si IV.....	1393.755	1393.76	15.6	Fe II.....	1621.685	1621.69	0.21
O IV.....	1397.20	1397.20	0.24	Fe II.....	1621.85	1621.83**	B
O IV.....	1399.774	1399.77	0.68	Fe II.....	1623.091	1623.09	0.49
O IV.....	1401.156	1401.16	4.6	Fe II.....	1623.715	1623.71	0.094
Si IV.....	1402.770	1402.78	10.8	Fe II.....	1625.520	1625.52	1.12

TABLE 2—Continued (DFVB)

Ion	λ (Å) (Lab)	λ (Å) (Solar)	Int.*	Ion	λ (Å) (Lab)	λ (Å) (Solar)	Int.*
Fe II.....	1625.909	1625.90	0.081	Fe II.....	1716.577	1716.57	0.55
Fe II.....	1627.401	1627.37	0.16	Fe II.....	1718.123	1718.09	0.25
Fe II.....	1629.154	1629.16	0.18	N IV.....	1718.551	1718.56	0.06?
Fe II.....	1629.376	1629.36	B0.075	Fe II.....	1720.042	1720.03	0.08?
Fe II.....	1631.120	1631.12	0.15	Fe II.....	1720.616	1720.61	1.37
Fe II.....	1632.668	1632.66	0.32	Al II.....	1721.26	1721.27	0.091
Fe II.....	1633.908	1633.90	0.82	Fe II.....	1722.425	1722.42	0.055
Fe II.....	1634.345	1634.34	0.094	Fe II.....	1724.854	1724.87	0.89
Fe II.....	1635.398	1635.39	0.10	Fe II.....	1726.391	1726.39	1.0
Fe II.....	1636.321	1636.34	0.12			1728.94	0.39
Fe II.....	1637.397	1637.40	1.0	Fe II.....	1731.038	1731.05	0.064
Fe II.....	1639.403	1639.40	0.10	Ni II.....	1741.547	1741.55	0.71
Fe II.....	1640.150	1640.14	0.8	Fe II.....	1746.818		
He II.....	1640.4	1640.39#	4.8	N III.....	1746.82P	1746.82	0.20
Fe II.....	1641.759	1641.77	0.059	Ni II.....	1748.285	1748.28	0.44
Fe II.....	1643.576	1643.58	0.79	N III.....	1748.61	1748.63	0.15
C III.....	1645.03	1645.01	0.088	Fe II.....	1749.136	1749.12	0.045
Fe II.....	1649.423	1649.42	0.49	N III.....	1749.674	1749.67	0.70
Fe II.....	1654.26	1654.26**	0.19	Ni II.....	1751.911	1751.91	0.52
Fe II.....	1654.476	1654.47	0.39	N III.....	1752.16P	1752.12	B0.11
C I.....	1656.267	1656.27	0.44	N III.....	1753.986	1753.98	0.15
C I.....	1656.928			Ni II.....	1754.808	1754.80	0.10
C I.....	1657.008	1656.99	0.43	Fe II.....	1761.379	1761.36	0.21
C I.....	1657.380	1657.39	0.42	Al II.....	1763.952	1763.95	0.10
C I.....	1657.907	1657.92	B0.41	Fe II.....	1764.117	1764.07	B
C I.....	1658.122	1658.13	0.43	Fe II.....	1772.509	1772.50	0.34
Fe II.....	1658.771	1658.77	0.81	Ni II.....	1773.949	1773.94	0.11
Fe II.....	1659.483	1659.48	1.5	Fe II.....	1785.262	1785.27	0.059
O III.....	1660.803	1660.81	1.2	Fe II.....	1788.072	1788.04	0.094
Fe II.....	1661.347	1661.32	0.091	Ni II.....	1788.485	1788.48	0.26
Fe II.....	1663.221	1663.22	0.76	Fe II.....	1793.367	1793.36	0.21
O III.....	1666.153	1666.15	2.94	Fe II.....	1798.156	1798.15	0.12
Fe II.....	1669.68	1669.66**	0.18	Ni II.....	1804.473	1804.48	0.069
Fe II.....	1670.742			Si II.....	1808.012	1808.01	5.6
Al II.....	1670.787	1670.80	1.24	Si II.....	1816.928	1816.93	9.5
Fe II.....	1671.010			Si II.....	1817.451	1817.44	0.92
Fe II.....	1673.462	1673.46	0.31	Fe II.....	1818.509	1818.51	0.10
Fe II.....	1674.254	1674.25	0.44	Fe II.....	1822.150	1822.13	0.063
Fe II.....	1674.716	1674.71	0.37	Fe II.....	1823.888	1823.89	0.056
Fe II.....	1676.853	1676.85	0.30	Fe II.....	1835.874	1835.86	0.12
Fe II.....	1679.381	1679.39	0.28	Fe II.....	1841.701	1841.65	0.081
Fe II.....	1681.12	1681.10	0.41	Fe II.....	1846.573	1846.57	0.063
Fe II.....	1685.954	1685.95	0.40	Fe II.....	1848.771	1848.76	0.056
Fe II.....	1686.455	1686.45	0.40	Al III.....	1854.716	1854.72	1.4
Fe II.....	1686.692	1686.68	0.47	Fe II.....	1859.741	1859.74	0.14
Fe II.....	1688.401	1688.39	0.17	Fe II.....	1860.055	1860.04	0.36
Fe II.....	1689.828	1689.83	0.073	Al III.....	1862.790	1862.79	0.70
Fe II.....	1690.759	1690.77	0.069	Fe II.....	1864.743	1864.72	0.16
Fe II.....	1691.271	1691.27	0.47	Fe II.....	1876.838	1876.83	0.25
Ni III?.....	1692.514			Fe II.....	1877.467	1877.46	0.11
Fe II.....	1692.516	1692.52	0.059	Fe II.....	1880.976	1880.97	0.081
Fe II.....	1693.936	1693.93	0.16	Fe II.....	1888.733	1888.73	0.12
Fe II.....	1694.68	1694.67**	0.071	Si III.....	1892.030	1892.04	15.2
Fe II.....	1696.794	1696.78	0.65	Fe III?.....	1895.457	1895.48	0.34
Fe II.....	1698.190	1698.13	0.05	Fe II.....	1898.538	1898.54	0.050
Fe II.....	1699.190	1699.19	0.059	Fe II.....	1901.76	1901.76**	0.088
Fe II.....	1702.043	1702.04	1.65	Fe II.....	1904.784	1904.79	0.045
Ni II.....	1703.408	1703.41	0.084	C III.....	1908.734P	1908.74	4.05
Fe II.....	1704.652	1704.63	0.25	Fe III.....	1914.071	1914.07††	0.29
Fe II.....	1706.142	1706.14	0.26	Fe III.....	1915.095	1915.09††	0.088
Fe II.....	1707.399	1707.40	0.069	Fe II.....	1917.337	1917.31	0.053
Fe II.....	1707.66	1707.66**	0.071	Fe II.....	1925.983	1925.99	0.13
Fe II.....	1708.250	1708.25	0.05	Fe III.....	1926.323	1926.31††	0.22
Fe II.....	1708.621	1708.62	0.59	C I.....	1930.905	1930.91	0.55
Ni II.....	1709.598	1709.59	0.52	Fe II.....	1935.296	1935.30	0.081
Fe II.....	1712.997	1713.00	1.65	Fe II.....	1936.799	1936.80	0.069
Fe II.....	1715.503	1715.50	0.12				

NOTES TO TABLE 2

NOTE.—B = blend. P = predicted wavelength.

* Peak intensity of the line. The units are the same as used in Table 1.

Notes to Table 2 (DFVB)

* The differences between our measured wavelengths and the wavelengths given in Kelly and Palumbo (1973) for these lines are considerable. We feel that the laboratory wavelengths are in error.

+ Burton and Ridgeley (1970) identify this line as S V ($3s^2 1S_0 - 3s3p^3 P_1$). However, the limb brightening curve for this line is suggestive of a lower temperature ion.

**The wavelength difference between the laboratory and solar wavelength is considerable, and the difference is unexplained.

*+We tentatively identify these weak lines as transitions in phosphorus ions.

++The 1640.39 Å He II line is actually composed of seven components, e.g., see Feldman et al. (1975b).

‡ Int ≡ photographic density measured by a densitometer. Values near 90 correspond to saturated lines.

B = blend.

70 Be typed

E.2 The Long Wavelength Spectra

E.2.1 (DFC) "Chromospheric Limb Spectra from Skylab: 2000 to 3200 A," G. A. Doschek, U. Feldman and L. Cohen. Ap. J. Supp. Series 33, 101, 1977.

TABLE 1 (DFC)
THE SOLAR SPECTRUM 4" ABOVE THE WHITE LIGHT LIMB: 2000–3200 Å

λ (Å) Solar (air)	λ (Å) Lab	Ion	Mul*	Flux† $\pi(\text{photons cm}^{-2}$ $\text{s}^{-1} \text{sr}^{-1})$	λ (Å) Solar (air)	λ (Å) Lab	Ion	Mul*	Flux† $\pi(\text{photons cm}^{-2}$ $\text{s}^{-1} \text{sr}^{-1})$
1986.88.....	0.907	Fe III	(50)	...	2177.06.....	{0.025	Fe II	(106)	1.3(13)
1991.03.....	0.016	Fe III	(50)	...		{0.080	Ni II	(40)	
2000.36.....	0.368	Fe II	(122)	7.4(13)	2179.37.....	0.36	Ni II	(40)	9.7(12)
2010.69.....	0.688	Fe II	(122)	4.1(13)	2180.48.....	0.46	Ni II	(40)	1.5(13)
2015.48.....	0.500	Fe II	(83)	4.3(13)	2184.60.....	0.61	Ni II	(13)	6.9(13)
2018.78.....	0.772	Fe II	(94)	1.0(14)	2185.51.....	0.51	Ni II	(40)	2.2(13)
2020.75.....	0.739	Fe II	(83)	5.5(13)	2186.84.....	0.89	Fe II†	...	9.7(12)
2025.53.....	0.58	Cr II	(2)	3.7(13)	2187.71.....	0.678	Fe II?	(89)	1.2(13)
2029.20.....	0.182	Fe II	(93)	2.2(13)	2188.02.....	0.05	Ni II	(12)	6.9(12)
2032.40.....	0.407	Fe II	(94)	8.8(13)	2189.03.....	8.999	Co II	(11)	1.1(13)
2036.44.....	0.435	Fe II	(137)	3.2(13)	2192.31.....	0.26	Cu II	(14)	9.2(12)
2039.90.....	0.90	Cr II	(2)	2.4(13)	2201.41.....	0.41	Ni II	(13)	5.5(13)
2040.68.....	0.687	Fe II	(93)	1.9(14)	2206.71.....	0.71	Ni II	(13)	8.3(13)
2051.04.....	0.028	Fe II	(93)	1.1(14)	2210.38.....	0.38	Ni II	(13)	5.1(13)
2055.59.....	0.59	Cr II	(1)	1.8(14)		{0.952	Fe II	(118)	
2057.34.....	0.332	Fe II	(82)	2.0(13)	2211.08.....	{0.090	Ni II	(52)	6.9(12)
	{0.54	Cr II	(1)	1.5(14)		{0.112	Fe II	{(168)	
2061.58.....	{0.552	Fe III	(48)	...				{(289)	
2062.00.....	0.00	Fe II†	...	2.7(13)	2213.22.....	0.19	Ni II	(30)	9.7(12)
2063.69.....	0.672	Fe II	(92)	6.5(13)	2213.65.....	0.679	Fe II	(168)	4.2(13)
2065.50.....	0.460	Cr II	(1)	1.2(14)	2216.48.....	0.479	Ni II	(12)	1.3(14)
2067.96.....	0.917	Fe II	(137)	3.0(13)	2219.90.....	0.889	Fe II	(168)	2.8(13)
2068.24.....	0.243	Fe III	(48)	1.9(13)	2220.38.....	{0.388	Fe II	(118)	1.1(14)
2079.00.....	0.989	Fe III	(48)	2.6(13)		{0.40	Ni II	(28)	
2080.25.....	0.246	Fe II	(92)	4.6(13)	2221.16.....	0.160	Fe II	(168)	2.2(13)
2087.56.....	0.527	Fe II	(108)	2.1(13)	2222.96.....	0.948	Ni II	(12)	9.7(13)
2090.14.....	0.14	Ni II	(15)	7.9(12)	2223.48.....	0.481	Fe II	(168)	2.1(13)
2093.53.....	0.55	Ni II	(15)	9.7(12)	2224.40.....	0.351	Ni II	(21)	1.7(13)
2097.10.....	0.08	Ni II	(31)	1.1(13)	2224.86.....	0.88	Ni II	(12)	1.1(14)
			{(80)		2226.33.....	0.34	Ni II	(12)	8.8(13)
2097.57.....	0.512	Fe II	{(120)}	1.6(13)	2227.22.....	0.18	Fe II†	...	7.9(12)
2103.85.....	0.799	Fe III	(66)	...	2229.88.....	0.85	Ni II†
2107.41.....	0.324	Fe III	(66)	...	2232.08.....	0.05	Co II	(10)	2.3(13)
2108.00.....	{7.94	Ni II	(60)	1.0(13)	2233.91.....	0.917	Fe II	(118)	8.3(13)
	{0.139	Fe II	(81)		2236.66.....	0.680	Fe II	(4)	7.9(12)
2110.74.....	0.724	Fe II	(108)	1.4(13)	2240.34.....	0.33	Fe II†	...	9.7(12)
2118.17.....	0.195	Fe II	(120)	8.3(12)	2241.78.....	0.81	Fe II†	...	7.9(12)
2119.03.....	0.050	Fe II	(120)	1.0(13)	2243.59.....	0.578	Fe II	(118)	8.3(12)
2125.14.....	0.12	Ni II	(14)	1.0(13)	2244.03.....
2128.58.....	0.57	Ni II	(15)	2.0(13)	2244.65.....	0.60	Fe II†	...	1.2(13)
2130.24.....	0.259	Fe II	(80)	1.2(13)	2245.13.....	0.11	Co II	(10)	1.8(13)
2131.28.....	0.27	Ni II	(14)	7.9(12)	2246.93.....	0.995	Cu II	(13)	4.2(13)
2132.67.....	0.72	Cr II	(24)	7.9(12)	2249.17.....	0.18	Fe II	(5)	1.4(14)
2133.50.....	0.49	Cr II	(23)	1.6(13)	2250.17.....	0.171	Fe II	(4)	5.5(13)
	{0.52	Cr II	(23)	1.6(13)	2250.93.....	0.937	Fe II	(4)	9.2(13)
2134.56.....	{0.62	Cr II	(23)	...	2251.55.....	0.556	Fe II	(5)	3.8(13)
					2253.13.....	0.119	Fe II	(4)	1.4(14)
2135.37.....	0.34	Cr II	(23)	1.2(13)	2254.37.....	0.401	Fe II	(5)	1.2(13)
2137.71.....	0.735	Fe II	(6)	7.4(12)	2255.14.....	0.16	Fe II†	...	1.6(13)
2138.61.....	0.60	Ni II	(13)	1.2(13)	2255.77.....	0.759	Fe II	(133)	6.5(13)
2139.01.....	2.6(13)	2255.94.....	0.979	Fe II	(4)	BL
2139.62.....	0.676	Fe II	(6)	1.1(13)	2256.43.....	0.43	Fe II†	...	2.2(13)
2142.77.....	6.0(13)	2257.91.....	0.96	7.4(12)
2146.05.....	0.058	Fe II	(6)	1.2(13)					2.0(14)
2147.68.....	0.719	Fe II	(213)	...	2260.11.....	{0.078	Fe II	(4)	
	{0.618	Fe II	(135)	1.5(13)		{0.228	Fe II	(5)	
2150.65.....	{0.762	Fe II	(248)	...	2260.85.....	0.853	Fe II	(4)	6.9(13)
2151.10.....	0.095	Fe II	(106)	1.2(13)	2262.68.....	0.686	Fe II	(5)	4.6(13)
2152.38.....	{0.373	Fe II	(106)	1.4(13)	2263.21.....	0.224	Fe II	(246)	1.2(13)
	{0.488	Fe II	(151)	...	2264.47.....	0.456	Ni II	(12)	1.2(14)
2158.75.....	0.73	Ni II	(13)	1.3(13)	2265.99.....	0.991	Fe II	(5)	4.3(13)
	{0.161	Fe II	(213)	...	2267.58.....	0.584	Fe II	(4)	1.4(14)
2161.21.....	{0.21	Ni II	(14)	2.8(13)	2268.11.....	0.14	Fe II†	...	1.0(13)
2162.01.....	0.023	Fe II	(90)	1.2(14)	2268.58.....	0.562	Fe II	(5)	2.1(13)
2164.34.....	0.339	Fe II	(79)	2.7(13)	2268.76.....	0.844	Fe II	(5)	1.5(13)
	{0.555	Fe II	(185)	...	2270.21.....	0.209	Ni II	(12)	1.2(14)
2165.55.....	{0.55	Ni II	(13)	1.3(14)	2274.73.....	0.75	Ni II	(38)	6.9(12)
					2275.68.....	0.70	Ni II	(39)	1.1(13)
2169.10.....	0.10	Ni II	(13)	7.9(13)	2276.03.....	0.02	Fe II†	...	1.4(13)
2172.95.....	0.989	Fe II	(134)	6.9(12)	2277.28.....	0.282	Ni II†	...	3.6(13)
2174.68.....	0.67	Ni II	(14)	9.2(13)	2278.76.....	0.771	Ni II	(22)	1.4(14)
2175.15.....	0.16	Ni II	(13)	7.4(13)	2279.91.....	0.918	Fe II	(4)	2.6(14)
2175.42.....	0.445	Fe II	(90)	7.4(13)					

TABLE 1—Continued (D F C)

λ (Å) Solar (air)	λ (Å) Lab	Ion	Mul*	Flux† π (photons cm^{-2} $\text{s}^{-1} \text{sr}^{-1}$)	λ (Å) Solar (air)	λ (Å) Lab	Ion	Mul*	Flux† π (photons cm^{-2} $\text{s}^{-1} \text{sr}^{-1}$)
2283.99.....	0.991	Fe II	(132)	4.0(13)	2352.69.....
2286.14.....	0.165	Co II	(9)	4.6(13)	2353.42.....	0.446	Co II	(8)	2.6(13)
2287.08.....	0.08	Ni II	(22)	6.9(13)	2354.50.....	0.473	Fe II	(165)	1.0(14)
2287.61.....	0.66	Ni II	(38)	1.2(13)	2354.90.....	0.884	Fe II	(35)	3.9(14)
2293.76.....	0.765	Fe II	(184)	1.2(13)	2356.40.....	0.41	Ni II	(22)	2.5(13)
2294.60.....	0.605	Fe II	(184)	1.3(13)	2357.00.....	0.005	Fe II	(333)	1.6(13)
2296.58.....	0.55	Ni II	(21)	1.7(14)	2359.12.....	0.111	Fe II	(3)	4.8(14)
2297.12.....	{0.140	Ni II	(11)	2.3(14)	2359.97.....	0.999	Fe II	{(35)	6.5(14)
	{0.17	Cr II	(19)	...				{(165)	...
2297.44.....	0.486	Ni II	(11)	1.4(14)	2360.28.....	0.287	Fe II	(36)	6.5(14)
2298.26.....	{0.225	Fe II	(133)	...	2362.00.....	0.014	Fe II	(35)	3.3(14)
	{0.269	Ni II	(21)	8.8(13)	2363.80.....	0.838	Co II	(8)	5.9(13)
2298.91.....	0.95	Mn II	(2)	9.2(12)	2364.83.....	0.825	Fe II	(3)	5.2(14)
2299.64.....	0.65	Ni II	(27)	2.6(13)	2366.61.....	0.591	Fe II	(35)	2.8(14)
2300.07.....	0.10	Ni II	(27)	3.0(13)	2367.38.....	0.395	Ni II	(11)	2.7(13)
2301.38.....	0.424	Fe II	(184)	8.3(12)	2368.60.....	0.593	Fe II	(36)	5.2(14)
2302.48.....	0.465	Ni II	(59)	1.4(13)	2369.19.....	0.232	Fe II	(182)	2.5(13)
2302.99.....	0.98	Ni II	(11)	2.1(14)	2370.50.....	0.494	Fe II	(35)	3.1(14)
2303.23.....	0.238	V II?	(26)	BL	2372.63.....	0.631	Fe II	(333)	1.8(13)
2304.75.....	0.736	Fe II	(184)	1.5(13)	2373.74.....	0.733	Fe II	(2)	4.8(14)
2304.95.....	5.001	Mn II	(2)	1.5(13)	2375.23.....	0.192	Fe II	(36)	5.2(14)
2307.15.....	0.19	Cr II	(19)	2.3(13)	2378.61.....	0.636	Co II	(7)	4.8(13)
2307.84.....	0.84	Co II	(9)	5.1(13)	2379.26.....	0.275	Fe II	(36)	4.3(14)
2311.23.....	0.224	Fe II	(245)	1.1(13)	2380.77.....	0.757	Fe II	(3)	3.7(14)
2311.61.....	0.602	Co II	(9)	4.6(13)	2382.08.....	0.034	Fe II	(2)	1.0(15)
2312.02.....	0.028	Fe II	(105)	4.6(13)	2383.15.....	{0.060	Fe II	{(2)	9.6(14)
2312.91.....	0.91	Ni II	(58)	2.4(13)		{0.242	Fe II	{(36)	...
2314.04.....	0.036	Co II	(9)	2.1(13)	2384.40.....	0.386	Fe II	(36)	4.8(14)
2314.75.....	{0.71	Cr II	(19)	1.8(13)	2384.99.....	0.999	Fe II	(35)	1.4(14)
	{0.81	Cr II	(19)	...	2386.35.....	0.367	Co II	(7)	3.2(13)
2314.93.....	0.97	Co II	(9)	2.8(13)	2387.43.....	0.424	Fe II	(286)	1.6(13)
2316.04.....	0.034	Ni II	(11)	3.3(14)	2387.77.....	0.77	Ni II	(19)	2.2(13)
2318.52.....	0.534	Fe II	(132)	3.3(13)	2388.58.....	0.629	Fe II	(2)	4.2(14)
2319.36.....	0.38	Cr II?	(34)	1.8(13)	2389.53.....	0.565	Co II	(7)	1.6(13)
2319.74.....	0.73	Ni II	(37)	9.2(12)	2391.47.....	0.475	Fe II	(35)	2.2(14)
2320.06.....	0.08	Cr II	(11)	1.4(13)	2394.53.....	0.518	Ni II	(20)	1.8(14)
2321.68.....	0.687	Fe II	(183)	1.3(13)	2394.85.....	{0.892	Fe II	{(116)	8.6(13)
2322.34.....	0.326	Fe II	(183)	1.0(13)		{0.843	Ni II	{(36)	BL
2323.52.....	0.500	C II§	(0.01)	1.5(13)	2395.59.....	{0.416	Fe II	{(2)	5.2(14)BL
2324.39.....	0.317	Co II	(8)	...		{0.627	Fe II	{(2)	5.2(14)
2324.72.....	0.689	C II§	(0.01)	1.9(14)	2395.71.....	0.714	Fe II	(211)	4.4(13)
2325.40.....	0.398	C II§	(0.01)	3.8(14)	2397.39.....	0.423	Co II?	(16)	2.1(13)
2326.16.....	0.15	Co II	(8)	...	2399.25.....	0.237	Fe II	{(2)	4.3(14)
2326.46.....	{0.44	Ni II	(11)	4.2(13)				{(36)	...
	{0.493	Co II	(8)	...	2400.33.....	{0.274	Fe II	{(181)	1.7(14)
2326.98.....	0.930	C II§	(0.01)	5.7(13)		{0.338	Fe II	{(244)	...
2327.39.....	0.391	Fe II	(2)	4.6(14)	2402.28.....	0.255	Fe II	(181)	...
2328.14.....	0.122	C II§	(0.01)	2.2(14)	2402.59.....	0.597	Fe II	(36)	1.6(14)
2330.35.....	0.37	Co II	(8)	1.6(13)	2404.40.....	0.430	Fe II	(2)	2.8(14)
2331.30.....	0.308	Fe II	(35)	4.6(14)	2404.90.....	0.882	Fe II	(2)	4.7(14)
2332.81.....	0.798	Fe II	(3)	5.1(14)	2406.68.....	0.660	Fe II	(2)	4.7(14)
2334.55.....	{0.590	Ni II	(20)	...	2407.92.....	0.940	Fe II	(116)	5.0(13)
	{0.606	Si II	(0.01)	5.5(14)	2408.73.....	0.770	Co II	(7)	1.8(13)
2335.44.....	0.42	Fe II†	2409.37.....	0.377	Fe II	(150)	1.3(13)
2336.21.....	0.246	Co II	(8)	1.4(13)	2409.70.....	0.708	Fe II	(224)	1.5(13)
2336.70.....	0.70	Ni II	(50)	1.7(13)	2410.54.....	0.521	Fe II	(2)	4.3(14)
2338.01.....	0.005	Fe II	(3)	5.1(14)	2411.05.....	0.062	Fe II	(2)	4.0(14)
2339.40.....	0.408	Fe II	(105)	7.4(13)	2413.32.....	0.308	Fe II	(2)	4.3(14)
2340.46.....	0.459	Fe II	(166)	3.9(13)	2414.08.....	{0.069	Co II	{(7)	2.4(13)
2341.12.....	{0.939	Fe II	(166)	...		{0.080	Fe II	{(164)	...
	{1.18	Ni II	(50)	2.9(13)	2415.06.....	0.068	Fe II	(181)	5.3(13)
2342.22.....	0.238	Fe II	(104)	3.0(13)	2416.14.....	0.134	Ni II	(20)	2.5(14)
2343.41.....	0.495	Fe II	(3)	5.5(14)	2416.82.....	0.705	Fe II	(286)	1.5(13)
2343.90.....	0.958	Fe II	(35)	5.5(14)	2417.85.....	0.859	Fe II	(244)	2.2(14)
2344.24.....	0.278	Fe II	(3)	5.5(14)	2420.74.....	0.735	Co II	?	1.1(13)
2345.34.....	0.327	Fe II	(165)	1.2(14)	2421.92.....	0.898	Fe II	(116)	1.3(13)
2347.40.....	0.406	Co II	(8)	2.0(13)	2422.70.....	0.688	Fe II	(301)	5.0(13)
2348.21.....	{0.118	Fe II	(36)	6.5(14)	2423.20.....	0.204	Fe II	(301)	3.3(13)
	{0.300	Fe II	(3)	...	2424.16.....	0.141	Fe II	(180)	...
2350.17.....	0.174	Si II	(0.01)	2.5(14)	2424.47.....	{0.380	Fe II	{(149)	2.6(14)
2351.19.....	0.198	Fe II	(165)	1.0(14)		{0.585	Fe II	{(180)	...
2352.09.....	2425.36.....	0.362	Fe II	(210)	1.7(13)

TABLE 1—Continued (D FC)

λ (Å) Solar (air)	λ (Å) Lab	Ion	Mul*	Flux† π (photons cm^{-2} $\text{s}^{-1} \text{sr}^{-1}$)	λ (Å) Solar (air)	λ (Å) Lab	Ion	Mul*	Flux† π (photons cm^{-2} $\text{s}^{-1} \text{sr}^{-1}$)
2425.72.....	0.677	Fe II	(224)	2.4(13)	2486.35.....	0.343	Fe II	(208)	1.8(14)
2427.18.....	0.197	Fe II	(114)	1.6(13)	2488.14.....	0.143	Fe I	(9)	3.4(13)
2428.34.....	0.367	Fe II	(300)	7.9(13)	2489.51.....	0.485	Fe II	(161)	1.8(14)
2429.40.....	{0.382	Fe II	(148)	7.2(13)	2489.81.....	0.826	Fe II	(207)	2.8(14)
	{0.497	Fe II	(180)		2490.84.....	0.856	Fe II	(179)	1.7(14)
2430.09.....	0.073	Fe II	(180)	2.8(14)	2491.38.....	0.392	Fe II	(207)	9.6(13)
2432.26.....	0.259	Fe II	(180)	2.3(14)	2492.35.....	0.341	Fe II	(243)	4.0(13)
2433.50.....	{0.495	Fe II	(164)	1.1(14)					
	{0.57	Ni II	(19)	...	2493.25.....	{0.174	Fe II	{(161)	8.5(14)
	{0.733	Fe II	(321)	...		{0.269	Fe II	{(207)	
2434.85.....	{0.942	Fe II	(180)	1.4(14)		{0.111	Fe II	{(161)	2.5(13)
	{0.816	Fe II	(164)	1.5(13)	2494.11.....	{0.709	Fe II	{(242)	...
2435.80.....	0.222	Fe II	(209)	1.8(13)		{0.817	Fe II	{(175)	1.4(14)
2436.20.....	0.157	Fe II	(210)	2.0(13)		{0.897	Fe II	{(207)	
2437.18.....	0.892	Ni II	(19)	8.6(13)	2498.90.....	0.897	Fe II	(161)	4.5(14)
2437.89.....	0.301	Fe II	(209)	3.0(14)	2500.93.....	0.919	Fe II	(357)	2.7(13)
2439.30.....	0.416	Fe II	(300)	4.2(13)	2502.39.....	0.388	Fe II	(207)	1.3(14)
2440.42.....	0.515	Fe II	(148)	4.0(14)		{0.323	Fe II	{(206)	2.4(14)
2444.52.....	0.569	Fe II	(148)	3.3(14)		{0.560	Fe II	{(161)	...
2445.58.....	0.203	Fe II	(209)	2.0(14)	2503.38.....	{0.870	Fe II	{(175)	
2446.16.....	0.462	Fe II	(164)	...		{0.217	Fe II	{(285)	1.2(14)
2446.47.....	{0.203	Fe II	(300)	4.4(13)	2503.82.....	0.217	Fe II	(33)	4.6(13)
	{0.320	Fe II	(299)	...	2505.21.....	0.091	Fe II	(207)	1.0(14)
2447.25.....	{0.753	Fe II	(320)	4.0(13)	2506.09.....	0.429	Fe II	(128)	3.4(13)
2447.74.....	0.185	Fe II	(129)	1.5(13)	2506.38.....	0.896	Si I	(1)	1.8(13)
2449.20.....	0.739	Fe II	(34)	...	2506.94.....	0.117	Fe II	(242)	3.1(13)
2449.75.....	{9.961	Fe II	(300)	6.0(13)	2509.12.....	0.87	Ni II	(18)	9.5(13)
	{0.022	Co II?	(16)	...	2510.88.....	0.375	Fe II	(33)	...
2450.04.....	{0.106	Fe II	(34)	5.7(13)	2511.44.....	0.759	Fe II	(161)	6.8(14)
	{0.208	Fe II	(209)	...	2511.77.....	0.513	Fe II	(343)	2.4(13)
2451.14.....	0.794	Fe II	(163)	8.6(13)	2512.52.....	0.383	Fe II	(285)	8.8(13)
2453.79.....	0.574	Fe II	(320)	5.7(13)	2514.38.....	0.912	Fe II	{(175)	5.0(13)
2454.57.....	0.816	Fe II	(209)	1.9(13)		{0.108	Si I	{(206)	
2456.81.....	0.782	Fe II	(209)	...	2516.10.....	0.124	Fe II	(147)	2.6(13)
2458.79.....	{0.964	Fe II	(299)	2.9(14)	2517.13.....	0.100	Fe I	(7)	2.0(14)
	{9.097	Fe II	(163)	...	2518.08.....	0.044	Fe II	(268)	1.4(13)
2458.99.....	0.282	Fe II	(209)	1.9(14)	2519.05.....	0.829	Co II?	(15)	1.1(14)
2461.29.....	0.855	Fe II	(209)	2.6(14)	2519.80.....	0.669	Fe II	(242)	1.8(13)
2461.83.....	0.280	Fe II	(208)	8.1(13)	2520.67.....	0.089	Fe II	(268)	2.1(13)
2463.29.....	0.007	Fe II	(208)	1.0(14)	2521.09.....	0.810	Fe II	(330)	7.4(13)
2464.01.....	0.903	Fe II	(208)	1.1(14)	2521.82.....	0.189	Fe II	(159)	4.8(13)
2464.96.....	0.194	Fe II	(148)	1.2(14)	2522.18.....	0.848	Fe I	(7)	3.5(13)
2465.15.....	0.911	Fe II	(208)	1.0(14)	2522.86.....	0.108	Si I	(1)	5.7(13)
2465.91.....	{0.670	Fe II	(179)	1.6(14)	2524.15.....	0.386	Fe II	(159)	1.3(13)
	{0.811	Fe II	(179)	...	2525.41.....	{0.071	Fe II	{(159)	5.1(14)
	{(145)			9.0(13)		{0.292	Fe II	{(145)	
2468.29.....	0.292	Fe II	{(163)	...	2526.22.....	0.107	Fe II	{(159)	3.7(14)
				5.2(13)	2527.11.....	0.433	Fe I	(7)	1.4(14)
2469.49.....	0.512	Fe II	(299)	...	2527.43.....	0.51	Si I	(1)	6.7(13)
2470.47.....	0.406	Fe II	(208)	2.3(14)	2528.59.....	0.221	Fe II	(241)	3.2(13)
2470.68.....	{0.661	Fe II	(179)	...		{0.071	Fe II	{(145)	...
	{0.752	Fe II	(223)	...	2529.24.....	0.545	Fe II	{(175)	5.3(14)
2472.10.....	0.075	Fe II	(162)	2.1(13)		0.103	Fe II	(178)	2.3(14)
2472.42.....	0.426	Fe II	(179)	6.0(13)	2530.09.....	{0.082	Fe II	{(33)	4.5(13)
2472.91.....	0.910	Fe I	(9)	...	2531.20.....	{0.266	Ti II?	{(4)	
2473.30.....	0.314	Fe II	(148)	8.5(13)		0.626	Fe II	(159)	1.6(13)
2474.75.....	0.762	Fe II	(208)	7.1(13)	2532.68.....	0.413	Fe II	(159)	7.5(14)
2476.26.....	0.264	Fe II	(163)	8.2(13)	2533.64.....	0.480	Fe II	(177)	6.0(14)
2476.66.....	4.8(13)	2535.47.....	0.880	Ti II?	(4)	2.6(14)
2477.35.....	0.342	Fe II	(162)	6.0(13)		{0.673	Fe II	{(241)	
	{0.115	Fe II	(224)	...	2536.81.....	{0.882	Fe II	{(159)	6.0(14)
2478.19.....	{0.206	Fe II	(149)	1.8(14)		{0.205	Fe II	{(319)	
	{0.449	Fe II	(161)	...	2538.32.....	{0.500	Fe II	{(160)	2.9(14)
	{0.568	Fe II	(179)	...		{0.794	Fe II	{(158)	
2478.56.....	0.775	Fe I	(9)	2.6(14)		{0.898	Fe II	{(158)	6.5(14)
2479.86.....	0.155	Fe II	(179)	...	2538.95.....	{9.003	Fe II	{(177)	9.0(13)
2480.15.....	0.044	Fe II	(243)	3.5(13)		{0.205	Fe II	{(343)	
2481.04.....	0.117	Fe II	(161)	2.8(14)		0.094	Fe II	(177)	1.6(14)
2482.12.....	0.654	Fe II	(207)	1.4(14)	2541.83.....	0.831	Fe II	(158)	3.3(14)
2482.64.....	0.270	Fe I	(9)	3.2(13)					
2483.25.....	0.721	Fe II	(331)	1.8(13)					
2483.73.....	0.243	Fe II	(243)	1.8(14)					
2484.23.....	0.076	Fe II	(34)	2.0(13)					

TABLE 1—Continued (DFC)

λ (Å) Solar (air)	λ (Å) Lab	Ion	Mul*	Flux† π (photons cm^{-2} $\text{s}^{-1} \text{sr}^{-1}$)	λ (Å) Solar (air)	λ (Å) Lab	Ion	Mul*	Flux† π (photons cm^{-2} $\text{s}^{-1} \text{sr}^{-1}$)
2542.74.....	0.733	Fe II	(223)	5.4(13)	2623.74.....	0.721	Fe II	(171)	8.0(13)
2543.38.....	{0.382	Fe II	(159)	3.8(14)	2625.66.....	{0.489	Fe II	(318)	...
	0.431	Fe II	(177)	...		0.664	Fe II	(1)	1.6(15)
2545.15.....	4.992	Fe II	(147)	3.2(14)	2626.46.....	0.499	Fe II	(173)	1.5(14)
	0.215	Fe II	(159)	...	2628.30.....	0.291	Fe II	(1)	1.5(15)
2545.87.....	0.903	Ni II	(18)	3.5(13)	2629.58.....	0.590	Fe II	(171)	2.4(14)
2546.67.....	0.667	Fe II	(177)	2.8(14)	2630.05.....	0.068	Fe II	(171)	1.8(14)
2547.32.....	0.330	Fe II	(158)	6.6(13)					
2548.37.....	0.325	Fe II	(146)	8.7(13)	2631.21.....	{0.045	Fe II	{(1) (171)}	3.9(15)
2548.72.....	0.741	Fe II	(145)	2.3(14)		0.321	Fe II	(1)	...
2549.40.....	{0.399	Fe II	(177)	3.1(14)	2632.31.....	0.353	Mn II	(19)	4.7(13)
	0.453	Fe II	(177)	...	2633.20.....	0.200	Fe II	(356)	3.2(13)
2550.02.....	0.023	Fe II	(240)	4.0(14)	2637.62.....	0.643	Fe II	(221)	1.1(14)
	0.575	Fe II	(158)	...	2638.13.....	0.173	Mn II	(19)	7.6(13)
2550.67.....	0.680	Fe II	(240)	3.4(14)	2639.60.....	0.560	Fe II	(221)	6.9(13)
2553.71.....	0.738	Fe II	(127)	2.7(13)	2641.98.....	2.015	Fe II	(309)	4.3(13)
2555.06.....	0.066	Fe II	(177)	8.5(13)	2653.56.....	0.57	Cr II	(8)	1.8(14)
2555.42.....	0.447	Fe II	(177)	5.6(13)	2658.58.....	0.59	Cr II	(8)	2.3(14)
2555.96.....	0.988	Ti II?	(9)	2.2(13)	2661.70.....	0.73	Cr II	(8)	7.4(13)
2557.52.....	0.500	Fe II	(175)	9.9(13)	2663.49.....	0.42	Cr II	(8)	1.6(14)
2558.60.....	0.605	Mn II	(20)	4.6(13)	2664.66.....	0.665	Fe II	(263)	7.0(14)
2559.80.....	0.774	Fe II	(205)	1.1(14)	2666.00.....	0.02	Cr II	(8)	2.8(14)
2560.26.....	0.278	Fe II	(221)	2.5(14)	2666.63.....	0.631	Fe II	(203)	5.0(14)
2562.16.....	0.094	Fe II	(221)	1.9(15)	2668.70.....	0.71	Cr II	(8)	2.9(14)
2562.54.....	0.535	Fe II	(64)	...	2669.14.....	0.17	Al II	(1)	7.1(14)
2563.48.....	0.472	Fe II	(64)	1.2(15)	2671.78.....	0.80	Cr II	(8)	3.9(14)
2566.26.....	5.6(13)	2672.80.....	0.83	Cr II	(8)	2.8(14)
2566.91.....	0.908	Fe II	(64)	1.2(15)	2677.15.....	{0.13	Cr II	{(8) (8)}	7.6(14)
2567.51.....	2.2(13)		0.19	Cr II	(8)	...
2568.39.....	0.405	Fe II	(145)	1.0(14)	2678.77.....	0.79	Cr II	(7)	4.3(14)
2569.76.....	0.775	Fe II	(266)	2.3(13)	2684.73.....	0.752	Fe II	(282)	2.8(14)
2570.84.....	0.843	Fe II	(284)	1.5(14)	2687.06.....	0.09	Cr II	(7)	2.3(14)
2571.50.....	0.542	Fe II?	(174)	3.1(13)	2687.94.....	0.960	V II?	(3)	5.3(13)
2571.90.....	0.78	Cr II	(89)	2.4(13)	2688.20.....	0.28	Cr II	(84)	4.9(13)
2572.58.....	1.6(13)	2689.15.....	0.20	Cr II	(35)	3.2(13)
2573.20.....	0.206	Fe II	(205)	8.6(13)	2691.02.....	0.03	Cr II	(8)	1.6(14)
2574.36.....	0.363	Fe II	(144)	6.0(14)	2692.63.....	0.601	Fe II	(283)	3.2(14)
2576.11.....	0.107	Mn II	(1)	6.5(14)	2697.44.....	{0.330	Fe II	{(341) (341)}	5.5(13)
2576.87.....	0.859	Fe II	(326)	7.5(13)		0.453	Fe II	(341)	...
2577.92.....	0.920	Fe II	(64)	1.0(15)	2698.52.....	0.40	Cr II	(7)	3.6(14)
2579.42.....	0.406	Fe II	(266)	4.4(13)	2701.67.....	0.693	Mn II	(18)	1.1(14)
2580.30.....	0.372	Co II?	(14)	9.5(13)	2703.98.....	0.988	Fe II	(261)	4.3(14)
2581.32.....	2.6(13)	2705.70.....	0.727	Mn II	(18)	1.0(14)
2582.59.....	0.582	Fe II	(64)	9.4(14)	2708.40.....	0.445	Mn II	(18)	7.5(13)
2585.88.....	0.876	Fe II	(1)	2.5(15)	2709.06.....	0.051	Fe II	(218)	1.1(14)
2587.19.....	0.225	Co II	...	3.0(13)	2710.28.....	0.332	Mn II	(18)	5.5(13)
2587.94.....	0.945	Fe II	(326)	8.5(13)	2711.84.....	0.842	Fe II	(201)	2.9(14)
2590.59.....	0.548	Fe II	(145)	4.7(13)	2712.31.....	0.300	Cr II	(7)	2.2(14)
2591.55.....	0.542	Fe II	(64)	1.2(15)	2714.41.....	0.414	Fe II	(63)	1.1(15)
2592.77.....	0.781	Fe II	(318)	4.4(14)	2716.21.....	0.216	Fe II	(261)	3.2(14)
	0.722	Fe II	(64)	...	2717.51.....	{0.51	Cr II	{(7) (32)}	8.1(13)
2593.72.....	0.731	Mn II	(1)	8.8(14)		0.533	Fe II	(32)	...
2595.21.....	0.285	Fe II	(172)	2.6(13)	2718.99.....	9.027	Fe II	(5)	4.2(13)
2598.39.....	0.369	Fe II	(1)	> 2.5(15)	2722.72.....	0.74	Cr II	(7)	1.6(14)
2599.40.....	0.395	Fe II	(1)	> 2.5(15)	2724.86.....	0.879	Fe II	(62)	3.8(14)
2605.63.....	0.697	Mn II	(1)	6.5(14)	2726.47.....	0.509	Fe II	(261)	...
2606.56.....	0.514	Fe II	(342)	...	2727.50.....	{0.382	Fe II	{(200) (63)}	1.2(15)
2607.01.....	0.084	Fe II	(1)	> 2.5(15)		0.538	Fe II	(63)	...
2608.86.....	0.852	Fe II	(171)	...	2730.72.....	0.735	Fe II	(62)	5.9(14)
2609.07.....	0.122	Fe II	(310)	3.9(13)	2732.41.....	0.441	Fe II	(32)	7.6(13)
2609.87.....	0.859	Fe II	(204)	7.1(13)	2736.96.....	0.968	Fe II	(63)	1.1(15)
2610.16.....	0.202	Mn II	(19)	7.5(13)	2739.56.....	0.545	Fe II	(63)	2.3(15)
2611.08.....	0.075	Fe II	(64)	3.0(14)	2741.37.....	0.395	Fe II	(260)	4.3(13)
2611.88.....	0.873	Fe II	(1)	> 2.5(15)	2742.00.....	0.02	Cr II	(6)	6.6(13)
2613.83.....	0.820	Fe II	(1)	> 2.5(15)	2743.22.....	0.196	Fe II	(62)	1.9(15)
2617.62.....	0.618	Fe II	(1)	> 2.5(15)	2746.42.....	0.487	Fe II	(62)	1.9(15)
2619.07.....	0.071	Fe II	(171)	1.0(14)	2747.03.....	6.978	Fe II	(63)	1.7(15)
	0.408	Fe II	(1)	3.2(14)		0.178	Fe II	(63)	...
2620.45.....	0.693	Fe II	(171)	...	2749.30.....	{0.324	Fe II	{(62) (63)}	2.0(15)
2621.66.....	0.669	Fe II	(1)	8.0(14)		0.482	Fe II	(63)	...
2623.11.....	0.129	Fe II	(318)	2.6(13)	2750.70.....	0.72	Cr II	(6)	1.8(14)

TABLE 1—Continued (D Fc)

λ (Å) Solar (air)	λ (Å) Lab	Ion	Mul*	Flux† $\pi(\text{photons cm}^{-2}$ $\text{s}^{-1} \text{sr}^{-1})$	λ (Å) Solar (air)	λ (Å) Lab	Ion	Mul*	Flux† $\pi(\text{photons cm}^{-2}$ $\text{s}^{-1} \text{sr}^{-1})$
2751.07.....	0.121	Fe II	(217)	1.0(14)	2873.41.....	{0.399	Fe II	(279)	1.7(14)
2751.85.....	0.85	Cr II	(6)	1.2(14)	2873.74.....	{0.46	Cr II	(5)	...
2753.27.....	0.289	Fe II	(235)	1.1(15)	2875.35.....	0.81	Cr II	(11)	7.5(13)
2755.74.....	0.733	Fe II	(62)	2.3(15)	2875.35.....	0.342	Fe II	(258)	6.9(13)
2756.97.....	7.029	Fe II	(199)	4.0(13)	2876.00.....	{5.97	Cr II	(11)}	2.4(14)
2757.69.....	0.72	Cr II	(6)	1.3(14)	2877.95.....	{0.24	Cr II	(5)}	6.0(13)
2759.29.....	0.336	Fe II	(32)	6.4(13)	2880.79.....	0.97	Cr II	(5)	1.6(14)
2761.79.....	0.813	Fe II	(63)	4.0(14)	2889.18.....	{0.750	Fe II	(61)}	8.0(13)
2762.56.....	0.58	Cr II	(6)	2.1(14)	2889.52.....	{0.828	Fe II	(258)}	8.5(13)
2766.52.....	0.55	Cr II	(6)	3.4(14)	2898.58.....	0.190	Cr II	(11)	7.3(13)
2767.50.....	0.50	Fe II	(235)	9.9(14)	2926.56.....	1.5(14)
2768.93.....	0.940	Fe II	(63)	2.1(14)	2933.06.....	0.584	Fe II	(60)	8.5(14)
2769.26.....	{0.153	Fe II	(200)	...	2936.49.....	0.051	Mn II	(5)	1.2(14)
2774.62.....	0.686	Fe II	(218)	1.3(14)	2939.31.....	0.496	Mg II	(2)	8.8(14)
2779.29.....	0.302	Fe II	(234)	4.7(13)	2944.39.....	0.302	Mn II	(5)	3.4(14)
2779.78.....	0.832	Mg I?	(6)	3.9(14)	2947.65.....	0.399	Fe II	(78)	2.9(14)
2783.68.....	0.690	Fe II	(234)	7.7(13)	2949.22.....	0.658	Fe II	(78)	1.0(15)
2790.75.....	{0.768	Mg II	(3)}	5.8(14)	2953.74.....	0.201	Mn II	(5)	1.1(14)
2793.90.....	{0.752	Fe II?	(32)}	1.5(14)	2984.84.....	0.774	Fe II	(60)	4.0(14)
2795.55.....	0.887	Fe II	(198)	5.1(13)	2985.54.....	0.831	Fe II	(78)	2.0(14)
2795.55.....	0.523	Mg II	(1)	S	3002.63.....	0.545	Fe II	(78)	2.0(14)
2797.96.....	{0.914	Fe II	(234)}	2.4(14)	3066.26.....	0.650	Fe II	(78)	1.2(14)
2799.29.....	{0.989	Mg II	(3)}	5.4(13)	3072.96.....	{0.220	Ti II	(5)}	1.7(14)
2802.72.....	0.292	Fe II	(233)	S	3075.22.....	0.364	Ti II	(5)}	1.7(14)
2818.30.....	0.698	Mg II	(1)	3.7(13)	3078.66.....	0.971	Ti II	...	2.1(14)
2822.34.....	0.38	Cr II	(82)	7.9(13)	3088.04.....	0.225	Ti II	(5)	3.0(14)
2828.60.....	0.622	Fe II	(231)	4.9(13)	3095.57.....	0.645	Ti II	(5)	3.3(14)
2830.45.....	0.46	Cr II	(82)	8.5(13)	3100.68.....	0.027	Ti II	(5)	...
2831.54.....	0.562	Fe II	(217)	2.9(14)	3102.32.....	...	OH	...	2.2(14)
2835.64.....	0.630	Cr II	(5)	4.5(14)	3110.67.....	0.295	V II	(1)	1.1(14)
2839.99.....	4.01	Cr II	(82)	7.1(13)	3118.61.....	0.708	V II	(1)	2.8(14)
2840.64.....	0.644	Fe II	(217)	1.5(14)	3120.36.....	0.652	Cr II	(5)	2.8(14)
2843.24.....	0.24	Cr II	(5)	4.8(14)	3124.98.....	0.371	Cr II	(5)	3.5(14)
2848.03.....	0.046	Fe II	(196)	4.9(13)	3128.70.....	0.978	Cr II	(5)	1.3(14)
2849.81.....	0.83	Cr II	(5)	4.0(14)	3132.07.....	0.699	Cr II	(5)	6.7(14)
2852.11.....	0.120	Mg I	(1)	3.4(14)	3136.70.....	0.058	Cr II	(5)	1.2(14)
2855.67.....	{0.67	Cr II	(5)}	3.8(14)	3147.98.....	0.680	Cr II	(5)	1.2(14)
2856.74.....	{0.676	Fe II	(196)}	7.6(13)	3154.20.....	8.033	Ti II	(4)	1.6(14)
2857.37.....	0.77	Cr II	(11)	6.3(13)	3161.18.....	0.195	Ti II	(10)	1.3(14)
2858.36.....	0.40	Cr II	(11)	1.3(14)	3161.75.....	0.205	Ti II	(10)	1.3(14)
2858.88.....	0.340	Fe II	{(195) (279)}	1.9(14)	3162.59.....	0.775	Ti II	(10)	1.8(14)
2860.92.....	0.910	Cr II	(5)	2.1(14)	3168.51.....	0.570	Ti II	(10)	2.3(14)
2862.55.....	0.92	Cr II	(5)	2.5(14)	3179.32.....	0.519	Ti II	(10)	1.2(14)
2865.10.....	0.57	Cr II	(5)	3.9(14)	3180.68.....	0.332	Ca II	(4)	2.3(14)
2866.73.....	0.10	Cr II	(5)	3.6(14)	3186.72.....	0.73	Cr II	(9)	1.7(14)
2867.63.....	0.72	Cr II	(5)	2.6(14)	3187.76.....	0.740	Fe II	(6)	5.1(14)
2868.81.....	0.65	Cr II	(5)	5.0(13)	3190.87.....	0.743	He I	(3)	2.0(14)
2870.43.....	0.874	Fe II	(61)	1.6(14)	3192.93.....	0.874	Ti II	(26)	1.1(14)
	0.430	Cr II	(11)	1.6(14)	3193.78.....	0.917	Fe II	(6)	1.6(14)
						0.809	Fe II	(6)	1.6(14)

NOTES TO TABLE 1

NOTE.—BL = blend, S = very strong line. Slightly more accurate wavelengths for the Ni II lines are given by Shenstone (1970).

* Multiplet from cited references to Moore's compilations.

† Fluxes are values at the Sun. True intensities in photons $\text{cm}^{-2} \text{s}^{-1} \text{sr}^{-1}$ are obtained by dividing the numbers in the table by $\pi/1.7$ (see text for discussion).

‡ Identification was suggested to us by Johansson (1975) based on his work or on the work of Dobbie (1938).

§ Identification was suggested to us by Kelly (1976).

of 1.5 if the Tousey *et al.* data are used. This difference is not significant because the pointing accuracy of the Skylab spectrograph was about $1''$ (Bartoe *et al.* 1974). In $1''$ the actual line intensities vary by at least a factor of 2 (see Fig. 2 and § IIIc).

b) The Spectrum Recorded at $+4''$ above the Limb

The lines observed in the quiet Sun spectrum recorded at $+4''$ above the limb are given in Table 1.

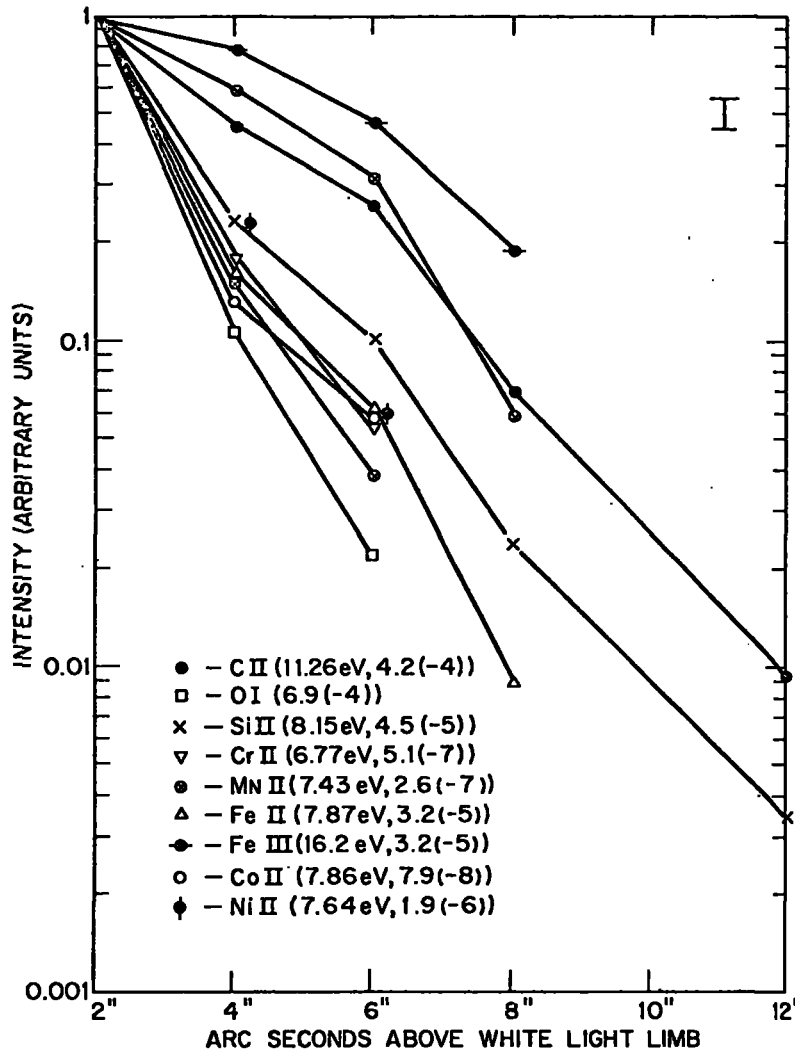


FIG. 2.—The intensity behavior of chromospheric ions above the limb. The data in parentheses are the ionization potential of the next lower stage of ionization (Kelly and Palumbo 1973) and the element abundance relative to hydrogen (Ross and Aller 1976). The Upper Mn II curve is derived from the $^7S-^7P$ lines (see text).

The solar wavelengths were obtained by a standard polynomial fitting procedure. The wavelength accuracy was found to be $\pm 0.04 \text{ \AA}$. The wavelength standards used to calibrate the spectra were lines of Fe II and Cr II. The laboratory wavelengths were obtained from the sources from which identifications were made. Most of the identifications were based on the compilations of Moore. These are the Ultraviolet Multiplet Tables (NBS Circular 488), the Selected Tables of Atomic Spectra (NSRDS-NBS 3), and A Multiplet Table of Astrophysical Interest (NBS Technical Note 36). A few identifications have been obtained from other unpublished sources. These are marked in the table. Moore's multiplet numbers are also given, as well as intensities derived as described above. In obtaining the line intensities, it was necessary to

perform the integration in equation (3). If a line is optically thin and has a Gaussian profile, I_τ in equation (3) is given by

$$I_\tau = \frac{1}{2} \left(\frac{\pi}{\ln 2} \right)^{1/2} \frac{I_0' W}{R_\lambda}, \quad (4)$$

where I_0' is the peak line intensity, R_λ is the instrumental response at line center, and W is the full width at half-maximum intensity. Most of the lines in Table 1 have some opacity, and therefore equation (4) does not strictly apply. However, at $+4''$ above the limb, the position for which we give intensities, the opacity of most of the lines is small and the line profiles are approximately Gaussian. We found empirically that $W = 9.4 \times 10^{-6} \lambda$ for most of the singly ionized

E.2.2 (FD) "The Emission Spectrum of a Hydrogen Balmer Series
Observed Above the Solar Limb from Skylab II. Active Regions,"
U. Feldman and G. A. Doschek. Submitted to Ap. j.

TABLE 1 (FD)

Active Regions Observed

Active Region	McMath Plage No.	Time (UT)
A (31 May 1973)	357	$16^{\text{h}}55.2^{\text{m}} - 18^{\text{h}}20.8^{\text{m}}$
B (11 Aug 1973)	474	$18^{\text{h}}43.5^{\text{m}} - 20^{\text{h}}16.4^{\text{m}}$
C (29 Aug 1973)	488	$20^{\text{h}}36.2^{\text{m}} - 22^{\text{h}}13.6^{\text{m}}$

TABLE 2 (FD)
PROPERTIES OF HYDROGEN BALMER LINES IN ACTIVE REGIONS ABOVE THE SOLAR LIMB

<i>m</i>	$\lambda(\text{\AA})$	ACTIVE REGION A						ACTIVE REGION B						ACTIVE REGION C					
		Int.*	+2" $\Delta\lambda(\text{\AA})$	+4" Int.	+4" $\Delta\lambda(\text{\AA})$	+6" Int.	+6" $\Delta\lambda(\text{\AA})$	Int.	+2" $\Delta\lambda(\text{\AA})$	+4" Int.	+4" $\Delta\lambda(\text{\AA})$	+6" Int.	+6" $\Delta\lambda(\text{\AA})$	Int.	+2" $\Delta\lambda(\text{\AA})$	+4" Int.	+4" $\Delta\lambda(\text{\AA})$	+6" Int.	+6" $\Delta\lambda(\text{\AA})$
9.....	3835.38	22.0	0.39	16.3	0.42	3.0	0.47	17.1	0.42	3.8	0.50
10.....	3797.90	15.0	0.39	11.0	0.41	2.0	0.47	12.6	0.42	2.7	0.46
11.....	3770.63	6.6	0.37	1.3	0.37	10.0	0.42	1.8	0.46
12.....	3750.15	8.6	0.41	5.5	0.36	1.0	0.39	7.5	0.39	1.5	0.44
13.....	3734.37	6.3	0.41	4.1	0.37	0.9	0.42	6.4	0.41	1.5	0.48
14.....	3721.94	5.2	0.42	3.7	0.42	5.2	0.41
15.....	3711.97	3.5	0.37	3.0	0.42	49.0	0.33	4.5	0.41
16.....	3703.85	35.7	0.39	2.4	0.34	22.6	0.30	1.8	0.37	37.8	0.36	3.1	0.37
17.....	3697.15	28.7	0.36	2.1	0.34	20.2	0.32	1.9	0.36	32.3	0.37	2.9	0.37
18.....	3691.55	24.7	0.36	2.1	0.39	16.2	0.29	2.0	0.47	27.7	0.41	3.4	0.50
19.....	3686.83	19.5	0.36	2.1	0.44	15.0	0.32	1.5	0.41	24.4	0.41	2.5	0.51
20.....	3682.81	16.3	0.32	1.6	0.46	12.0	0.33	1.2	0.37	20.7	0.41	1.8	0.37
21.....	3679.35	13.6	0.32	1.5	0.47	12.0	0.36	1.0	0.37	19.2	0.45	1.8	0.44
22.....	3676.36	12.2	0.37	10.3	0.44BL†	17.2	0.48
23.....	3673.76	9.9	0.34	7.9	0.39	14.5	0.50
24.....	3671.48	9.9	0.38BL	8.9	0.47BL	14.8	0.55BL
25.....	3669.46	8.1	0.37	6.7	0.43	11.9	0.50
26.....	3667.68	5.6	0.40	5.8	0.44	10.9	0.51
27.....	3666.10	5.5	0.42	5.3	0.46	8.4	0.53
28.....	3664.68	7.6	0.55
29.....	3663.40	4.9	0.52	5.2	0.55	8.3	0.64
30.....	3662.26
31.....	3661.22	4.2	0.56

* Intensity in units $10^3 \text{ ergs cm}^{-2} - \text{s}^{-1} - \text{sr}^{-1}$ at the Sun.

† $\Delta\lambda = \langle \text{FWHM} \rangle$ of the line after correcting for instrumental width.

‡ BL = blend.

E. 3 Forbidden Lines

E.3.1 (SBT) "Forbidden Lines of the Solar Corona and Transition Zone 975 Å - 3000 Å," G. D. Sandlin, G. E. Brueckner and R. Tousey. Submitted to Ap. J.

TABLE I (SPT)
FORBIDDEN LINES OF $5 \times 10^4 - 3 \times 10^6$ K PLASMA**

λ (Å)	σ	Class	Identification	Int.		FWHM		λ (Å)	σ	Class	Identification	Int.		FWHM	
				4"	40"	4"	40"					4"	40"	4"	40"
974.86	.05		Fe XVIII $2s^2 2p^5$ ($2P_{3/2} - 2P_{1/2}$)					1467.44	.03	P IV	$3s^2$ $1S_0 - 3s3p^3 P_1$				
997.1	.1		Ne VI $2s^2 2p$ ($2P_{1/2} - 2s2p^2$ $4P_{1/2}$)					1486.52	.02	N IV	$2s^2$ $1S_0 - 2s2p^3 P_1$	11.	0.12	.23	.19
999.2	.1		Ne VI $2P_{3/2} - 4P_{5/2}$					1489.04	.03	Cr X	$3s^2 3p^3$ ($4S_{3/2} - 2P_{3/2}$)			0.09	.20
1005.7	.1		Ne VI $2P_{3/2} - 4P_{3/2}$					1510.51	.03	>V				0.04	
1010.2	.1		Ne VI $2P_{3/2} - 4P_{1/2}$					1564.30	.02	>V	Cr X $3s^2 3p^3$ ($4S_{3/2} - 2P_{1/2}$)			0.05	
1118.07	.05		Fe XIX $2s^2 2p^4$ ($3P_2 - 3P_1$)					1574.9		III	Ne V $2s^2 2p^2$ ($3P_1 - 1S_0$)			0.05	
1136.51	.02	II	Ne V $2s^2 2p^2$ ($3P_1 - 2s2p^3$ $5S_2$)					1582.56	.04	>V	Ar XIII† $2s^2 2p^2$ ($3P_2 - 1D_2$)			0.36	.22
1145.61	.02	II	Ne V $3P_2 - 5S_2$					1601.5, .7		II	Ne IV $2s^2 2p^3$ ($4S_{3/2} - 2P_{3/2}, 2P_{1/2}$)				
1174.72#	.05	>IV	Ni XIV $3s^2 3p^3$ ($4S_{3/2} - 2P_{1/2}$)		0.24			1603.21	.01	IV	Fe X† $3p^4 3d$ ($4D_{7/2} - 2G_{7/2}$)	0.5	1.5	.34	
1189.82	.01	IV	Mg VII $2s^2 2p^2$ ($3P_1 - 1S_0$)	2.5	1.9	.18		1611.70	.05	V		0.4	0.26	.27	
1190.07	.01	III	Mg VI $2s^2 2p^3$ ($4S_{3/2} - 2P_{3/2}$)		3.8	.18		1614.51	.03	VI	S XI $2s^2 2p^2$ ($3P_1 - 1D_2$)	0.4	0.74	.26	
1191.62	.02	III	Mg VI $4S_{3/2} - 2P_{1/2}$		0.75	.18		1623.54	.04	IV-VI	O VII $1s2s$ $3S_1 - 1s2p^3 P_2$	0.4	0.25		
1196.24	.01	V	S X $2s^2 2p^3$ ($4S_{3/2} - 2D_{5/2}$)		0.45	.17		1639.78	.03	IV-VI	O VII $3S_1 - 3P_0$	1.0	0.68		
1199.18	.01	II	S V $3s^2$ $1S_0 - 3s3p^3 P_1$	18.	0.11	.24	.12	1640.65	.03				0.27		
1212.96	.01	V	S X $2s^2 2p^3$ ($4S_{3/2} - 2D_{3/2}$)	4.8	1.4	.26	.17	1660.81	.01	I	O III $2s^2 2p^2$ $3P_1 - 2s2p^3$ $5S_2$	16.		.21	
1213.90	.05	II+	O V† $2s^2$ $1S_0 - 2s2p^3 P_2$					1666.16	.01	I	O III $3P_2 - 5S_2$	41.		.21	
1216.43	.01	VI	Fe XIII $3s^2 3p^3$ ($3P_1 - 1S_0$)	6.0	5.8			1666.95	.01				0.08	.23	
1218.35	.02	II+	O V $2s^2$ $1S_0 - 2s2p^3 P_1$	36.	1.2	.22	.15	1696.26	.05				0.06		
1232.62	.02	V			0.29	.17		1715.44	.01	IV+	S IX $2s^2 2p^4$ ($3P_2 - 1D_2$)	1.2	0.50	.26	
1242.00	.01	VI-	Fe XII $3s^2 3p^3$ ($4S_{3/2} - 2P_{3/2}$)	10.0	10.0	.19	.17	1717.42	.02	V	Ni XI $3s^2 3p^5 3d$ ($3P_2 - 3D_2$)			0.15	.21
1271.62	.02	>V			0.03			1746.81	.02	I	N III $2s^2 2p$ $2P_{1/2} - 2s2p^2$ $4P_{3/2}$	10.		.23	
1277.23	.01	VI	Ni XIII $3s^2 3p^4$ ($3P_1 - 1S_0$)	0.51	0.12	.21	.18	1748.63	.02	I	N III $2P_{1/2} - 4P_{1/2}$	4.4			
1307.65	.02				0.02			1749.67	.01	I	N III $2P_{3/2} - 4P_{5/2}$	18.	0.02	.23	
1322.2 #			Mn XII $3s^2 3p^2$ ($3P_1 - 1S_0$)		0.01			1752.14	.01	I	N III $2P_{3/2} - 4P_{3/2}$	2.7			
1324.44	.01	III	Mg V $2s^2 2p^4$ ($3P_1 - 1S_0$)		0.09	.20		1753.98	.01	I	N III $2P_{3/2} - 4P_{1/2}$	5.4		.23	
1331.52	.03		Ar XIII† $2s^2 2p^2$ ($3P_1 - 1D_2$)					1756.82	.03	I-	P III $3s^2 3p$ $2P_{1/2} - 3s3p^2$ $4P_{1/2}$				
1349.40	.01	VI-	Fe XII $3s^2 3p^3$ ($4S_{3/2} - 2P_{1/2}$)	5.1	6.7	.19	.17	1757.64	.03	I-	P III $2P_{3/2} - 4P_{5/2}$				
1351.92	.01		F IV† $2s^2 2p^2$ $3P_1 - 2s2p^3$ $5S_2$					1805.94	.03		Mg VI $2s^2 2p^3$ ($4S_{3/2} - 2D_{3/2}$)			0.06	
1354.08	.05		Fe XXI $2s^2 2p^2$ ($3P_0 - 3P_1$)					1826.21	.02	VI	S XI $2s^2 2p^2$ ($3P_2 - 1D_2$)	2.8	0.28	.21	.28
1359.05	.01		F IV† $2s^2 2p^2$ $3P_2 - 2s2p^3$ $5S_2$					1841.57	.02	IV	Fe IX $3s^2 3p^5 3d$ ($3P_1 - 3D_2$)			0.23	.27
1359.57	.02	V	Mn XI $3s^2 3p^3$ ($4S_{3/2} - 2P_{3/2}$)		0.06	.19		1847.25	.02	VI		1.7	0.20	.29	
1368.83	.02	>V			0.04	.17		1866.75	.01	VI	Ni XIV $3s^2 3p^3$ ($4S_{3/2} - 2D_{5/2}$)	1.3	0.35	.29	
1370.52	.02	>V			0.04	.19		1892.03		I-	Si III $3s^2$ $1S_0 - 3s(2S)3p^3 P_1$	440.	2.1	.08	
1375.95	.03	VI	Ca XV† $2s^2 2p^2$ ($3P_2 - 1D_2$)		0.04			1908.73	.01	I-	C III $2s^2$ $1S_0 - 2s2p^3 P_1$	71.	0.67	.19	
1392.12	.01	VI	Ar XI $2s^2 2p^4$ ($3P_2 - 1D_2$)		0.10	.22		1917.21	.02	IV	Fe IX $3s^2 3p^5 3d$ ($3P_2 - 1F_3$)			0.48	.28
1397.22	.02	II	O IV $2s^2 2p$ $2P_{1/2} - 2s2p^2$ $4P_{3/2}$	2.0	0.02	.23		1918.25	.01	V-	Fe X† $3s^2 3p^4 3d$ ($4D_{7/2} - 2F_{7/2}$)	2.7	1.1	.24	
1399.78	.01	II	O IV $2P_{1/2} - 4P_{1/2}$	6.6	0.06	.23	.15	1984.88	.02	IV+	Si IX $2s^2 2p^2$ ($3P_1 - 1D_2$)	6.6		.38	
1401.17	.01	II	O IV $2P_{3/2} - 4P_{5/2}$	28.	0.44	.23	.15	2000.4 §			Ni XI $3s^2 3p^5 3d$ ($3F_4 - 1F_3$)				
1404.80	.02	II	O IV $2P_{3/2} - 4P_{3/2}$	13.	0.18	.23	.15	2042.35	.01	IV	Fe IX $3s^2 3p^5 3d$ ($3P_2 - 3D_2$)	12.		.38	
			S IV $3s^2 3p$ $2P_{1/2} - 3s3p^2$ $4P_{1/2}$					2085.51	.05	VI	Ni XV $3s^2 3p^2$ ($3P_1 - 1D_2$)	6.7		.40	
1406.08	.01	II	S IV $2P_{3/2} - 4P_{5/2}$	6.0	0.03	.23		2125.50	.02	VI-	Ni XIII $3s^2 3p^4$ ($3P_2 - 1D_2$)	12.		.35	
1407.39	.02	II	O IV $2P_{3/2} - 2s2p^2$ $4P_{1/2}$	6.8	0.05	.23		2146.64	.04	III	Si VII $2s^2 2p^4$ ($3P_2 - 1D_2$)	2.0		.35	
1408.65	.03	V		0.28	0.07	.17		2149.26	.05	IV+	Si IX $2s^2 2p^2$ ($3P_2 - 1D_2$)	11.		.43	
1409.45	.01	V+		0.37	0.19	.19		2169.08	.02	VI-	Fe XII $3s^2 3p^3$ ($4S_{3/2} - 2D_{5/2}$)	29.		.33	
1416.93	.01		S IV $3s^2 3p$ $2P_{3/2} - 3s3p^2$ $4P_{3/2}$	3.4	0.02			2184.28	.05	VI	Ni XIV $3s^2 3p^3$ ($4S_{3/2} - 2D_{3/2}$)	14.		.32	
1423.89	.01		S IV $3s^2 3p$ $2P_{3/2} - 3s3p^2$ $4P_{1/2}$	0.28				2405.68	.01	VI-	Fe XII $3s^2 3p^3$ ($4S_{3/2} - 2D_{3/2}$)	150.		.37	
1428.75	.01	>V		0.85	0.84	.21	.16	2497.5			Fe IX $3s^2 3p^5 3d$ ($3F_4 - 1F_3$)	~10.			
1440.01#	.02		Cr XI $3s^2 3p^3$ ($3P_1 - 1S_0$)		0.03			2565.93	.06	VI-	Fe XII $3s^2 3p^3$ ($2D_{3/2} - 2P_{3/2}$)	43.		.39	
1440.50	.01	IV	Si VIII $2s^2 2p^3$ ($4S_{3/2} - 2D_{5/2}$)		0.18	.22		2570.14	.02			28.		.38	
1445.75	.01	IV	Si VIII $2s^2 2p^3$ ($4S_{3/2} - 2D_{3/2}$)	1.1	3.70	.24	.22	2578.77	.01	VI	Fe XIII $3s^2 3p^2$ ($3P_1 - 1D_2$)	160.		.40	
1450.49	.05		Mn XI $3s^2 3p^3$ ($4S_{3/2} - 2P_{1/2}$)					2622.56	.05			19.		.42	
1463.49	.01	V-	Fe X† $3p^4 3d$ ($4F_{9/2} - 2F_{7/2}$)	2.3	0.72	.15	.17	2648.71	.02	V	Fe XI $3s^2 3p^4$ ($3P_2 - 1D_2$)	97.		.38	
1467.06	.01	V	Fe XI $3s^2 3p^4$ ($3P_1 - 1S_0$)	4.3	2.2	.17	.16								

Notes to Table I (537)

- * Observed in the NRL rocket spectrum of 1966 July 27.
- † Tentative identification.
- # Observed only in the 36-minute exposure of Figure 3.
- § Blended with Fe II 2000.3 Å. Wavelengths above 2000 Å are in air.
- ** Three flare lines of higher temperature are included for completeness.

Ionization Class	Log Te
I	4.7 - 5.0
II	5.0 - 5.3
III	5.3 - 5.6
IV	5.6 - 5.9
V	5.9 - 6.1
VI	6.1

The columns INT. and FWHM refer, respectively, to observations above AR 12114 at 4" above the limb, and above AR 12300 at 40" above the limb.

To be Typed